TECHNICAL REPORT HSM-R28-69

JULY 31, 1969

VOLUME ONE
THEORETICAL ANALYSES

Contract No. NAS8-21403

FINAL REPORT
COMPUTER PROGRAMS FOR
PREDICTION OF STRUCTURAL
VIBRATIONS DUE TO FLUCTUATING
PRESSURE ENVIRONMENTS

N70-27324

SPACE DIVISION **CHRYSLER CORPORATION**

HUNTSVILLE OPERATIONS

Technical Report HSM-R28-69
July 31, 1969

FINAL REPORT

COMPUTER PROGRAMS FOR PREDICTION OF STRUCTURAL,
VIBRATIONS DUE TO FLUCTUATING PRESSURE ENVIRONMENTS

VOLUME ONE

THEORETICAL ANALYSES

Contract No. NAS8-21403

Prepared for

GEORGE C. MARSHALL SPACE. FLIGHT CENTER
MARSHALL SPACE FLIGHT CENTER, ALABAMA 35812

By

Tsin N. Lee and Wayne L. Swanson

Vibration and Acoustics Group
Structural Engineering Branch

FOREWORD

The results presented in this report were the accomplishments of a research and development project performed for the Vibration and Acoustics Branch of the Goerge C. Marshall Space Flight Center, National Aeronautics and Space Administration under Contract No. NAS8-21403. This work has been accomplished by the Vibration and Acoustics Group, Structural Engineering Branch, Chrysler Corporation Space Division, Huntsville Operations from 1 July 1968 to 31 July 1969. Eleven Monthly Progress Reports have been submitted for the past months presenting derivations of equations and analyses of results. The final results of this project are presented in Two Volumes: This is Volume One, Theoretical Analyses, and Volume Two is a Users' Manual for Computer Program RANDOM.

ACKNOWLEDGMENT

ABSTRACT

Formulations were derived and computer programs were written to calculate the random vibrational responses of rectangular cylindrical panels cross-reinforced with ribs and stringers subjected to the fluctuating pressure enviornments. Three boundary conditions are considered: four edges simply supported; four edges clamped; two opposite edges simply supported and the other two clamped. Special cases of complete cylinders and flat panels are also included. The computer programs can be selected to run on any one or all three of the boundary conditions. Either the spectral density or the one-third –octave level of the excitation pressure may be input in any discrete frequencies. The computer programs will apply when either the complete panel or a portion of it is subjected to the excitation pressure. The frequency equations are incorporated in the computer programs. Input data include only the geometric dimensions and material properties of the panel. Formulations are according to the normal mode approach. The responses calculated are the acceleration, the displacement, and the stress spectral densities. Mean-square and root-mean-square values are calculated by numerical integration. All spectral densities are tabulated and plotted. New expressions for the joint acceptance of all mode combinations for different correlation functions are derived. Both the main and the cross terms are taken into account to obtain the responses. Up to 625 terms are summed to obtain the spectral density at one data point. More than 1000 data points are calculated for each spectrum. Both the local responses at any point and the average responses over the complete panel are calculated. The program can be used to investigate the contribution of main terms and cross terms. Comparison of calculated results with test data shows good agreement.

TABLE OF CONTENTS

TABLE OF CONTENTS (Concluded)

LIST OF FIGURES

LIST OF FIGURES (Continued)

LIST OF FIGURES (Continued)

I. INTRODUCTION

The purpose of this project was to develop computer programs to calculate the random vibrational responses of rectangular cylindrical shell panels cross-reinforced with ribs and stringers. The boundary conditions considered are four edges simply-supported, four edges clamped, and two opposite edges simply-supported while other two clamped. The special cases of complete cylinders and flat panels are also included.

A total of more than ten programs have been developed. The main program RANDOM contained the formulations for the three boundary conditions and will calculate the responses with a single loading of the input data. It can also be selected to calculate the responses for any one of the three boundary conditions. For accurate results, and large frequency range, programs were written for each boundary condition to perform special investigations.

The one-third octave spectrum of the excitation pressure is read in as input in a sequence of any discrete frequencies. Hence, any excitation pressure spectrum of any shape can be used as input. This improves the simulation of the excitation pressure field. The excitation spectrum is converted into pounds-per-square-inch squared per Hertz. Excitation pressure for each data point frequency is obtained by interpolation. The excitation pressure spectrum is plotted out both in decibel scale and in $(psi)^2$ per Hertz.

The formulations are according to the normal mode approach. Both Alan Powell's [1] joint acceptance and Y. K. Lin's [2] cross spectral density of the generalized force are used in the formulations. The relation of these two quantities is derived. The advantages and disadvantages of each are discussed. The analytical expressions of these two quantities for all mode combinations for two correlation functions are derived. These are believed to be new. One correlation function is exponentially decaying with separation distance and frequency while the other is a cosine function with exponentially decaying amplitude. Separate computer programs are written to study the joint acceptance and the cross spectral density of the generalized force. It is found that the curves of the joint acceptance and the cross spectral density of the generalized force are very regular for the exponentially decaying correlation function. The behavior of these quantities for the sinusoidal and exponentially decaying correlation function is very irregular.

Contributions of both the main terms and the cross terms are summed to obtain the responses. The one n-th octave bandwidth is used for frequency increment to save computer time and yield smooth spectral density plots of the responses. The frequency range for the spectrum is 5000 Hertz or more. Up to 625 terms are summed to give the response spectral density at each data point. More than 1000 data points can be calculated for each response spectral density plot. The responses are calculated as the displacement, the acceleration, and the stress spectral densities. Mean-square and root-mean-square values are calculated by numerically integrating the area under the spectral density curve. The response spectral densities are tabulated and plotted in graphical forms with the root-mean-square value printed at the top of the plot. The programs will apply when either the complete panel or a portion is exposed to the excitation

1

pressure. Both the local responses at any point and the average responses over the whole panel can be calculated by the programs.

In one of the programs, the acceleration spectral density is expressed in decibels referenced gravity acceleration and the vibro-acoustic transfer function is calculated as the acceleration spectral density minus the excitation. This is very useful for the investigation of the transfer function of aerospace vehicle structures.

Separate programs are written to investigate the contribution of the cross terms to the total response. It is found that although the cross terms do not contribute very much to the mean-square response, they do affect the shape of the response spectral density plot to a certain degree.

The natural frequencies of the panel are calculated in the programs. These frequency equations are newly derived or modification of those available in the literature. For panels of uniform thickness, these equations are the same as those in the literature. For cylindrical shell panels cross-reinforced with stiffeners, no frequency equations can be found in the literature that can be advantageously used in the programs. These newly derived equations though approximate in nature, yet yield reasonable results. The frequency equations account for the boundary conditions, the rigidity of the stiffeners, and the curvature of the shell. They are not very complicated so they can be incorporated into the computer programs without requiring a large amount of computer time.

A program is written to calculate the total number of natural frequencies up to a certain range and the modal density. This program is useful in the investigation of the dynamic characteristics of the structure.

By utilization of the developed computer programs, investigations on the effect of boundary conditions on the responses, on the contribution of each mode and the cross terms to the responses are performed. It is found that the more rigid the boundary condition, the less the displacement spectral density and the larger the acceleration spectral density at resonance. The root-mean-square displacements for the three boundary conditions are not very much different. Estimation of the responses are made by the spectral density at fundamental mode. It is found that the fundamental mode contributes up to 50% of the mean-square responses, and the second mode contributes more to the acceleration than the displacement responses.

By assuming that the continuous structure vibrates at its fundamental mode, simple formulas are derived to calculate the response spectral density and the mean-square responses. It is found that good approximation of the spectral density at fundamental mode and the mean-square responses can be obtained by intelligent use of these formulas.

Comparison of the computed results with experimental data from projects, the Chrysler Huntsville Operations is presently conducting for Marshall Space Flight Center, shows good agreement.

2

Since all the derivations of the equations used were reported in the Monthly Progress Reports, only the resulting equations are presented in this Final Report. For detail derivation, the reader will be referred to the applicable Monthly Progress Reports.

II. FORMULATIONS

2.1 Frequency Equations

2.1.1 Four Edges Simply-Supported Rectangular Cylindrical Shell Panels Cross-Reinforced With Stiffeners

The undamped natural frequencies of four-edges simply supported rectangular shell panels cross-reinforced with ribs and stringers may be expressed as

$$\omega_{jk} = (M)^{-1/2} \left\{ D_x \left(\frac{j\pi}{\ell} \right)^4 + 2H \left(\frac{j\pi}{\ell} \right)^2 \left(\frac{k\pi}{b} \right)^2 + D_y \left(\frac{k\pi}{b} \right)^4 \right.$$

$$\left. + \frac{Eh \left(\frac{j\pi}{\ell} \right)^4}{a^2 \left[\left(\frac{j\pi}{\ell} \right)^2 + \left(\frac{k\pi}{b} \right)^2 \right]^2} \right\}^{1/2}$$

(2.1-1)

2.1.2 Four Edges Clamped Rectangular Cylindrical Shell Panels Cross-Reinforced with Stiffeners

The frequency equations for cylindrical shell panels with edge conditions other than simply supported are involved and complicated. However, reasonable accurate expressions may be given as follows:

$$\omega_{11} = \frac{\pi^2}{\sqrt{M}} \left\{ D_x \left. \frac{1.5056}{\ell} \right)^4 + D_y \left(\frac{1.5056}{b} \right)^4 + 2H \left(\frac{1.2466}{b\ell} \right)^2 \right.$$

$$\left. + \frac{Eh}{a^2 \pi^4 \left[1 + \left(\frac{\ell}{b} \right)^2 \right]^2} \right\}^{1/2}$$

$$\omega_{1k} = \frac{\pi^2}{\sqrt{M}} \left\{ D_x \left(\frac{1.5056}{\ell} \right)^4 + D_y \left(\frac{k + 1/2}{b} \right)^4 \right.$$

$$+ 2H \frac{1.2466 \ (k + 1/2) [(k + 1/2) - 2/\pi]}{(b\ell)^2}$$

4

$$+ \frac{Eh}{a^2\pi^4\left[1 + \left(\frac{k + 1/2}{1.5056}\right)^2 \left(\frac{\ell}{b}\right)^2\right]^2}\Bigg\}^{1/2}$$

$$k = 2, 3, \ldots$$

$$\omega_{j1} = \frac{\pi^2}{\sqrt{M}} \Bigg\{ D_x\left(\frac{j + 1/2}{\ell}\right)^4 + D_y\left(\frac{1.5056}{b}\right)^4$$

$$+ 2H \frac{1.2466\ (j + 1/2)[(j + 1/2) - 2/\pi]}{(b\ell)^2}$$

$$+ \frac{Eh}{a^2\pi^4\left[1 + \left(\frac{1.5056}{j + 1/2}\right)^2 \left(\frac{\ell}{b}\right)^2\right]^2}\Bigg\}^{1/2}$$

$$j = 2, 3, \ldots$$

$$\omega_{jk} = \frac{\pi^2}{\sqrt{M}} \Bigg\{ D_x\ \frac{j + 1/2}{\ell}\Big)^4 + D_y\left(\frac{k + 1/2}{b}\right)^4$$

$$+ 2H \frac{(j + 1/2)(k + 1/2)[(j + 1/2) - 2/\pi][(k + 1/2) - 2/\pi]}{(b\ell)^2}$$

$$+ \frac{Eh}{a^2\pi^4\left[1 + \left(\frac{k + 1/2}{j + 1/2}\right)^2 \left(\frac{\ell}{b}\right)^2\right]^2}\Bigg\}^{1/2}$$

$$j, k = 2, 3, \ldots \tag{2.1-2}$$

2.1.3 Two Opposite Edges Simply-Supported and the Other Two Clamped
Rectangular Cylindrical Shell Panels Cross-Reinforced With
Stiffeners

The frequency equations for this case are as follows:

$$\omega_{11} = \frac{\pi^2}{\sqrt{M}} \Bigg\{ D_x\left(\frac{1}{\ell}\right)^4 + D_y\left(\frac{1.5056}{b}\right)^4 + 2H\left(\frac{1}{\ell}\right)^2\left(\frac{1.1165}{b}\right)^2$$

$$\frac{Eh}{a^2\pi^4\left[1 + \left(\frac{1}{1.5056}\right)^2\left(\frac{\ell}{b}\right)^2\right]^2}\Bigg\}^{1/2}$$

5

$$\omega_{1k} = \frac{\pi^2}{\sqrt{M}} \left\{ D_x \left(\frac{1}{\ell} \right)^4 + D_y \left(\frac{k + 1/2}{b} \right)^4 \right.$$

$$+ 2H \left(\frac{1}{\ell} \right)^2 \frac{(k + 1/2)[(k + 1/2) - 2/\pi]}{b^2}$$

$$\left. + \frac{Eh}{a^2 \pi^4 \left[1 + \left(\frac{1}{k + 1/2} \right)^2 \left(\frac{\ell}{b} \right)^2 \right]^2} \right\}^{1/2}$$

$$k = 2, 3, \ldots$$

$$\omega_{j1} = \frac{\pi^2}{\sqrt{M}} \left\{ D_x \left(\frac{j}{\ell} \right)^4 + D_y \left(\frac{1.5056}{b} \right)^4 \right.$$

$$2H \left(\frac{j}{\ell} \right)^2 \left(\frac{1.1165}{b} \right)^2$$

$$\left. + \frac{Eh}{a^2 \pi^4 \left[1 + \left(\frac{j}{1.5056} \right)^2 \left(\frac{\ell}{b} \right)^2 \right]^2} \right\}^{1/2}$$

$$j = 2, 3, \ldots$$

$$\omega_{jk} = \frac{\pi^2}{\sqrt{M}} \left\{ D_x \left(\frac{j}{\ell} \right)^4 + D_y \left(\frac{k + 1/2}{b} \right)^4 \right.$$

$$+ 2H \left(\frac{j}{\ell} \right)^2 \frac{(k + 1/2)[(k + 1/2) - 2/\pi]}{b^2}$$

$$\left. \frac{Eh}{a^2 \pi^4 \left[1 + \left(\frac{j}{k + 1/2} \right)^2 \left(\frac{\ell}{b} \right)^2 \right]^2} \right\}^{1/2}$$

$$j, k = 2, 3, \ldots \hspace{3cm} (2.1\text{-}3)$$

where

ω_{jk} = undamped natural frequency in radians per second

6

The rigidities are given by (refer to Figure 1 for geometric dimensions)

$$D_x = \frac{Eh^3}{12(1-\nu^2)} + \frac{E'I_1}{b_1}$$

$$D_y = \frac{Eh^3}{12(1-\nu^2)} + \frac{E'I_2}{a_1}$$

$$H = \frac{Eh}{12(1-\nu^2)} \qquad\qquad (2.1-4)$$

The smeared-out mass per unit area is

$$M = \rho h + \rho'h' \qquad\qquad (2.1-5)$$

E = Young's modulus of panel skin

E' = Young's modulus of stiffeners

h = Thickness of panel skin

h' = Smeared-out thickness of stiffeners

ν = Poisson's ration of panel skin

a = Radius of shell

a_1 = Spacing of width-direction stiffeners

b_1 = Spacing of length-direction stiffeners

b = Circumferential width of panel

ℓ = Axial length of panel

I_1 = Moment of inertia of one length-direction stiffener with respect to neutral axis

I_2 = Moment of inertia of one width direction stiffener with respect to neutral axis

ρ = Mass density of panel skin

ρ' = Mass density of stiffeners

7

2.1.4 Flat Panels

The flat panel is the limit of a cylindrical shell panel when the radius approaches infinite. All the frequency equations for the shell panels reduce to the corresponding equations of the flat panels, when the radius "a" approaches infinite.

2.1.5 Complete Thin-Walled Cylinders

It can be shown that the frequency equations of the two-side simply-supported and the other two clamped rectangular cylindrical shell panels reduces to those of complete thin-walled cylinders with both ends simply-supported when the circumferential width "b" is equal to πa. Similarly the frequency equations for complete thin-walled cylinders with both ends fixed are identical with those of four-side clamped rectangular cylindrical shell panels with circumferential width equal to πa. Hence, the upper limit of the circumferential width for the validity of the frequency equations is

$$b \leq \pi a$$

When b equal to πa, the difference between the complete cylinders and the shell panels lies in that the index k in the frequency equations gives the number of waves around the circumference of the complete cylinder but the number of half-waves in the shell panel. The index j gives the number of half-waves in both the complete cylinder and the shell panel.

2.1.6 Cylinders and Shell Panels of Uniform Thickness

When the moment of inertia of the stiffeners, [I_1 and I_2 in Equation (2.1-4)] approach zero or when the spacings of the stiffeners [a_1 and b_1] in Equation (2.1-4) approach infinite, the cylinders and the shell panels will be of uniform thickness. Equation (2.1-4) shows this is actually the case. Therefore all the frequency equations apply to both structures of uniform thickness as well as reinforced by ribs and stringers.

2.2 The Normal Modes

The normal mode shapes of rectangular cylindrical shell panels cross-reinforced with ribs and stringers subjected to different boundary conditions may be reasonably represented as

$$F_{jk}(\vec{r}) = X_j(x)Y_k(y) \tag{2.2-1}$$

The functions X_j and Y_k for each boundary condition are given in the following sections.

2.2.1 Four Edges Simply-Supported Rectangular Cylindrical Shell Panels Cross-Reinforced With Stiffeners

For the four edge simply-supported rectangular cylindrical shell panel cross-reinforced with ribs and stringers, the X_j and Y_k functions may be reasonably represented by the normal modes of four edges simply supported rectangular flat panel of uniform thickness, namely:

$$X_j = \sin \frac{j\pi x}{\ell} \tag{2.2-2a}$$

$$Y_k = \sin \frac{k\pi y}{b} \tag{2.2-2b}$$

2.2.2 Four Edges Clamped Rectangular Cylindrical Shell Panels Cross-Reinforced With Stiffeners

For the four edge clamped rectangular cylindrical shell panel cross-reinforced with ribs and stringers, the X_j and Y_k functions for the normal modes may be reasonably represented by

$$X_1 = X_1(x) = \cosh \frac{1.5056\pi x}{\ell} - \cos \frac{1.5056\pi x}{\ell} \tag{2.2-3a}$$

$$- 0.9825 \left(\sinh \frac{1.5056\pi x}{\ell} - \sin \frac{1.5056\pi x}{\ell} \right)$$

$$Y_1 = Y_1(y) = \cosh \frac{1.5056\pi y}{b} - \cos \frac{1.5056\pi y}{b} \tag{2.2-3b}$$

$$- 0.9825 \left(\sinh \frac{1.5056\pi y}{b} - \sin \frac{1.5056\pi y}{b} \right)$$

$$X_j = X_j(x) = \cosh \frac{(j + 1/2)\pi x}{\ell} - \cos \frac{(j + 1/2)\pi x}{\ell} \tag{2.2-3c}$$

$$- \sinh \frac{(j + 1/2)\pi x}{\ell} + \sin \frac{(j + 1/2)\pi x}{\ell}$$
$$j = 2, 3, \ldots$$

$$Y_k = Y_k(y) = \cosh \frac{(k + 1/2)\pi y}{b} - \cos \frac{(k + 1/2)\pi y}{b} \tag{2.2-3d}$$

$$- \sinh \frac{(k + 1/2)\pi y}{b} + \sin \frac{(k + 1/2)\pi y}{b}$$
$$k = 2, 3, \ldots$$

2.2.3   Two Opposite Edges Simply-Supported While Other Two Clamped
        Rectangular Cylindrical Shell Panels Cross-Reinforced With
        Stiffeners

For two opposite edges (perpendicular to x-axis) simply-supported and other two clamped rectangular cylindrical shell panels cross-reinforced with ribs and stringers, the X_j function is given by Equation (2.2-2a) while the Y_k functions is given by Equations (2.2-3b) and (2.2-3d).

2.3   Spatial Correlation of the Excitation Pressure Field

The spatial correlation coefficient of a time stationary excitation pressure field at any two points is defined as

$$\rho(\vec{r}_1, \vec{r}_2) = \frac{<p(\vec{r}_1)p(\vec{r}_2)>}{p_r^2} \tag{2.3-1}$$

where

$$p(\vec{r}_1), p(\vec{r}_2) = \text{pressure at the two points } \vec{r}_1 \text{ and } \vec{r}_2$$

$$<p(\vec{r}_1), p(\vec{r}_2)> = \text{temporal average of the pressure product}$$

$$p_r^2 = \sqrt{<p^2(r_1)> <p^2(r_2)>} = \text{reference mean-square pressure}$$

For space stationary excitation pressure fields, the spatial correlation coefficient will be a function of the separation distance

$$\rho(|\vec{\xi}|) = \frac{<p(\vec{r}_1)p(\vec{r}_2)>}{p_r^2} \tag{2.3-2}$$

where

$$\vec{\xi} = \vec{r}_1 - \vec{r}_2$$

For the stationary both in time and space pressure field, the mean-square pressure of the field will be used as the reference pressure.

For the fluctuating pressure field encountered in aerospace vehicle, both theory and experiments indicate the correlation coefficient may be reasonably represented by the following expressions

10

$$\rho_1(\xi) \quad = \quad \exp(-A_1 K\xi) \qquad\qquad (2.3\text{-}3)$$

$$\rho_2(\xi) \quad = \quad \exp(-A_2 K\xi) \cos(K\xi) \qquad\qquad (2.3\text{-}4)$$

where

$\xi \quad = \quad$ separation distance

$A_1, A_2 \quad = \quad$ decay constants

$K \quad = \quad \dfrac{\omega}{c} \quad = \quad$ wave number

$\omega \quad = \quad$ circular frequency

$c \quad = \quad$ speed of the pressure wave

Equation (2.3-3) expresses the correlation coefficient decreasing exponentially as the separation distance and wave number increase. This is appropriate to be used when the pressure field is a boundary layer field. Equation (2) expresses the correlation coefficient as a cosine function of the product of the wave number and separation distance with amplitude decreasing exponentially. This will apply to progressive pressure fields.

Typical curves for equation (2.3-3) are shown in Figures 43 and 44. In Figure 43:

$A_1 \quad = \quad 5$

$\omega \quad = \quad 100$ Hertz $= 200\pi$ radian/second

$c \quad = \quad 13500$ inches/second

In Figure 44:

$A_1 \quad = \quad 0.5$

$\omega \quad = \quad 100$ Hertz $= 200\pi$ rad/sec

$c \quad = \quad 13500$ in/sec

11

Typical curves for Equation (2.3-4) are shown in Figures 45 and 46. In Figure 45:

$$A_2 \quad = \quad 5$$

$$\omega \quad = \quad 100 \text{ Hertz} = 200\pi \text{ rad/sec}$$

$$c \quad = \quad 13500 \text{ in./sec.}$$

In Figure 46:

$$A_2 \quad = \quad 0.5$$

$$\omega \quad = \quad 100 \text{ Hertz} = 200\pi \text{ rad/sec}$$

$$c \quad = \quad 13500 \text{ in./sec.}$$

2.4   The Joint Acceptance and the Cross Spectral Density of the Generalized Force

New expressions for the joint acceptance squared and the cross spectral density of the generalized force of rectangular panels subjected to the excitation of fluctuating pressure environments are derived in the following. In this derivation, the analytical expression of the cross spectral density function of pressure field conforms quite accurately to the actual environments of the aerospace vehicles. Analytical expressions for the joint acceptance squared and the cross spectral density of the generalized force as a function of frequency are derived for all possible mode combinations. This is believed to be new.

2.4.1   Cross Spectral Density of Generalized Force, Sinusoidal Decaying Correlation

The cross spectral density of the generalized force of the pressure field is defined as [see Reference 2, Chapter 7, Section 7-2, Page 211, Equation (7-39)]:

$$I_{jkmn} \quad = \quad \int \int \phi_{pp}(\vec{r}_1, \vec{r}_2, \omega) \, F_{jk}(\vec{r}_1) \, F_{mn}(\vec{r}_2) \, d\vec{r}_1 \, d\vec{r}_2 \qquad (2.4-1)$$

$$F_{jk}, F_{mn} \quad = \quad \text{normal modes of the structure}$$

For space homogeneous pressure field, the cross spectral density is equal to the product of the homogeneous spectral density and the correlation coefficient function:

$$\phi_{pp}(\vec{r}_1, \vec{r}_2, \omega) \quad = \quad \Phi_{pp}(\omega)\rho(\vec{r}_1, \vec{r}_2) \qquad (2.4-2)$$

When the correlation coefficient function is represented by Equation (2-3-4) in Section 2-3, the cross spectral density function of the excitation pressure will be:

$$\phi_{pp}(\vec{r}_1, \vec{r}_2, \omega) = \Phi_{pp}(\omega) \; [\exp(-A_1 K\xi) \cos K\xi] \; [\exp(-A_2 K\eta) \cos K\eta]$$

$$(2.4-3)$$

where

$\Phi_{pp}(\omega)$ = the homogeneous spectral density of the excitation pressure

ξ = $|x_1 - x_2|$ = separation distance along x-axis

η = $|y_1 - y_2|$ = separation distance along y-axis

$(x_1, y_1), (x_2, y_2)$ = coordinates of $\vec{r}_1$ and $\vec{r}_2$

A_1, A_2 = correlation decay constants

2.4.1.1 Four Edges Simply-Supported Rectangular Panels

For four-side simply supported panels, the normal mode is:

$$F_{jk} = \sin\frac{j\pi x}{\ell} \sin\frac{k\pi y}{b}$$

$$(2.4-4)$$

Substitution of Equations (2.4-3) and (2.4-4) into Equation (2.4-1) gives the cross spectral density of the generalized force:

$$I_{jkmn} = \phi_{pp}(\omega) \int_0^\ell \int_0^\ell e \exp(-A_1 K\xi) \cos K\xi \, \sin\frac{j\pi x_1}{\ell} \sin\frac{m\pi x_2}{\ell} \, dx_1 dx_2$$

$$\cdot \int_0^b \int_0^b e \exp(-A_2 K\eta) \cos K\eta \, \sin\frac{k\pi y_1}{b} \sin\frac{n\pi y_2}{b} \, dy_1 dy_2$$

$$= \Phi_{pp}(\omega) \; I_x I_y$$

$$(2.4-5)$$

where I_x and I_y represent the two double integrals respectively.

13

These integrals can be carried out by using the following identify:

$$I_x = \int_0^\ell \int_0^\ell e \exp(-A_1 K\xi) \cos K\xi \sin \frac{j\pi x_1}{\ell} \sin \frac{m\pi x_2}{\ell} dx_1 dx_2$$

$$= \int_0^\ell \int_0^{x_1} \exp[-A_1 K(x_1 - x_2)] \cos K(x_1 - x_2) \sin \frac{j\pi x_1}{\ell} \sin \frac{m\pi x_2}{\ell} dx_2 dx_1$$

$$+ \int_0^\ell \int_0^{x_2} \exp[-A K(x_2 - x_1)] \cos K(x_2 - x_1) \sin \frac{j\pi x_1}{\ell} \sin \frac{m\pi x_2}{\ell} dx_1 dx_2$$

$$= I_1 + I_2 \qquad\qquad (2.4-6)$$

where I_1 and I_2 represent the two integrals respectively in the above expression.

The identity of the above expression can best be seen from the following figure. If the variable x_1 and x_2 are represented on rectangular coordinates ox_1 and ox_2, then the region of integration of the left-hand side of Equation (2.4-6) is the square OABC. This square is divided by the diagonal OB into two isosceles right triangles. Inside triangle OAB, $x_1 > x_2$, while inside triangle OBC, $x_2 > x_1$. On the diagonal OB, $x_1 = x_2$. It is easily seen that integral I_1 represents the integration over the triangle OAB, and integral I_2 represents the integration over the triangle OBC. Therefore the sum of I_1 and I_2 is the integration over the square OABC.
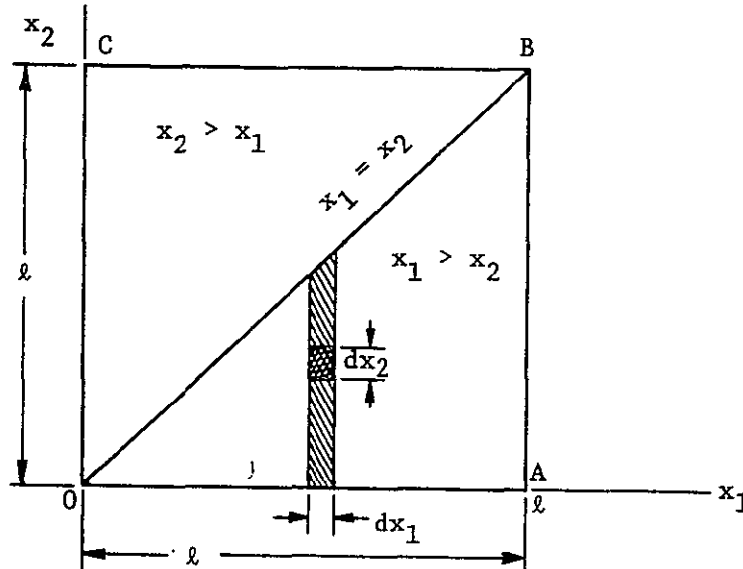
Carefully carrying out the integrations in eq. (2-4-6) yields

$$\tilde{I}_x = \frac{I_x}{\ell^2} = \tilde{I}_{x11} + \tilde{I}_{x12} + \tilde{I}_{x13} + \tilde{I}_{x14}$$

$$+ \quad \tilde{I}_{x21} + \tilde{I}_{x22} + \tilde{I}_{x23} + \tilde{I}_{x24} \qquad (2.4\text{-}7)$$

Similar calculation gives

$$\tilde{I}_y = \frac{I_y}{b^2} = \tilde{I}_{y11} + \tilde{I}_{y12} + \tilde{I}_{y13} + \tilde{I}_{y14}$$

$$+ \quad \tilde{I}_{y21} + \tilde{I}_{y22} + \tilde{I}_{y23} + \tilde{I}_{y24} \qquad (2.4\text{-}7a)$$

Substitution of eqs. (2.4-7) into eq. (2.4-6) yield the normalized cross spectral density of the generalized force as:

$$\tilde{I}_{jkmn} = \frac{I_{jkmn}}{(b\ell)^2 \, \Phi_{pp}} = \tilde{I}_{x11} + \tilde{I}_{x12} + \tilde{I}_{x13} + \tilde{I}_{x14} + \tilde{I}_{x21} + \tilde{I}_{x22}$$

$$+ \tilde{I}_{x23} + \tilde{I}_{x24} + \tilde{I}_{y11} + \tilde{I}_{y12} + \tilde{I}_{y13} + \tilde{I}_{y14} + \tilde{I}_{y21}$$

$$+ \tilde{I}_{y22} + \tilde{I}_{y23} + \tilde{I}_{y24} \qquad (2.4\text{-}8)$$

where

$$\tilde{I}_{x11} = \frac{1}{8\left[\alpha_1^2 + (m\pi + \lambda_1)^2\right]}$$

$$\times \left[I_{x111} - (m\pi + \lambda_1) \, I_{x112} + 2(-1)^{j+1} \, (m\pi + \lambda_1) \, e^{-\alpha_1} \, I_{x113} \right]$$

$$\tilde{I}_{x12} = \frac{1}{8\left[\alpha_1^2 + (m\pi - \lambda_1)^2\right]}$$

$$\times \left[I_{x121} - (m\pi - \lambda_1) \, I_{x122} + 2(-1)^{j+1} \, (m\pi - \lambda_1) \, e^{-\alpha_1} \, I_{x123} \right]$$

$$\tilde{I}_{x13} = \frac{1}{8\left[\alpha_1^2 + (m\pi - \lambda_1)^2\right]} \left[I_{x131} + (m\pi - \lambda_1) \, I_{x132} - 2\alpha_1 \, I_{x133} \right]$$

15

$$\tilde{I}_{x14} = \frac{1}{8\left[\alpha_1^2 + (m\pi + \lambda_1)^2\right]} \left[I_{x141} - (m\pi + \lambda_1)\, I_{x142} - 2\alpha_1\, I_{x143}\right]$$

$$\tilde{I}_{x21} = \frac{1}{8\left[\alpha_1^2 + (j\pi + \lambda_1)^2\right]}$$

$$\times \left[I_{x211} - (j\pi + \lambda_1)\, I_{x212} + 2(-1)^{m+1}\, (j\pi + \lambda_1)e^{-\alpha_1}\, I_{x213}\right]$$

$$\tilde{I}_{x22} = \frac{1}{8\left[\alpha_1^2 + (j\pi - \lambda_1)^2\right]}$$

$$\times \left[I_{x221} - (j\pi + \lambda_1)\, I_{x222} + 2(-1)^{m+1}\, (j\pi - \lambda_1)e^{-\alpha_1}\, I_{x223}\right]$$

$$\tilde{I}_{x23} = \frac{1}{8\left[\alpha_1^2 + (j\pi - \lambda_1)^2\right]} \left[I_{x231} + (j\pi - \lambda_1)\, I_{x232} - 2\alpha_1\, I_{x233}\right]$$

$$\tilde{I}_{x24} = \frac{1}{8\left[\alpha_1^2 + (j\pi + \lambda_1)^2\right]} \left[I_{x241} - (j\pi + \lambda_1)\, I_{x242} - 2\alpha_1\, I_{x243}\right] \qquad (2.4\text{-}9)$$

$$\tilde{I}_{y11} = \frac{1}{8\left[\alpha_2^2 + (n\pi + \lambda_2)^2\right]}$$

$$\times \left[I_{y111} - (n\pi + \lambda_2)\, I_{y112} + 2(-1)^{k+1}\, (n\pi + \lambda_2)e^{-\alpha_2}\, I_{y113}\right]$$

$$\tilde{I}_{y12} = \frac{1}{8\left[\alpha_2^2 + (n\pi - \lambda_2)^2\right]}$$

$$\times \left[I_{y121} - (n\pi - \lambda_2)\, I_{y122} + 2(-1)^{k+1}\, (n\pi - \lambda_2)e^{-\alpha_2}\, I_{y123}\right]$$

$$\tilde{I}_{y13} = \frac{1}{8\left[\alpha_2^2 + (n\pi - \lambda_2)^2\right]} \left[I_{y131} + (n\pi - \lambda_2)\, I_{y132} - 2\alpha_2\, I_{y133}\right]$$

$$\tilde{I}_{y14} = \frac{1}{8\left[\alpha_2^2 + (n\pi + \lambda_2)^2\right]} \left[I_{y141} - (n\pi + \lambda_2)\, I_{y142} - 2\alpha_2\, I_{y143}\right]$$

$$\tilde{I}_{y21} = \frac{1}{8\left[\alpha_2^2 + (k\pi + \lambda_2)^2\right]}$$

$$\times \left[I_{y211} - (k\pi + \lambda_2)\, I_{y212} + 2(-1)^{n+1}\, (k\pi + \lambda_2)e^{-\alpha_2}\, I_{y213}\right]$$

$$\tilde{I}_{y22} = \frac{1}{8\left[\alpha_2^2 + (k\pi - \lambda_2)^2\right]}$$

$$\times \left[I_{y221} - (k\pi - \lambda_2)\, I_{y222} + 2(-1)^{n+1}\, (k\pi - \lambda_2)e^{-\alpha_2}\, I_{y223}\right]$$

$$\tilde{I}_{y23} = \frac{1}{8\left[\alpha_2^2 + (k\pi - \lambda_2)^2\right]} \left[I_{y231} + (k\pi - \lambda_2)\, I_{y232} - 2\alpha_2\, I_{y233}\right]$$

$$\tilde{I}_{y24} = \frac{1}{8\left[\alpha_2^2 + (k\pi + \lambda_2)^2\right]} \left[I_{y241} - (k\pi + \lambda_2)\, I_{y242} - 2\alpha_2\, I_{y243}\right] \qquad (2.4\text{-}10)$$

$$I_{x111} = (-1)^{m+j}\, \alpha_1 \left[\frac{1}{(m+j)\pi + 2\lambda_1} + \frac{1}{(m-j)\pi + 2\lambda_1}\right] \sin 2\lambda_1$$

$$I_{x112} = \frac{1 - (-1)^{j+m}}{(j+m)\pi} + \frac{1 - (-1)^{j-m}}{(j-m)\pi} + \frac{1 - (-1)^{m+j}\cos 2\lambda_1}{(m+j)\pi + 2\lambda_1}$$

$$+ \frac{-1 + (-1)^{m-j}\cos 2\lambda_1}{(m-j)\pi + 2\lambda_1}$$

$$I_{x113} = \frac{\alpha_1 \sin\lambda_1 + (j\pi + \lambda_1)\cos\lambda_1}{\alpha_1^2 + (j\pi + \lambda_1)^2} + \frac{-\alpha_1 \sin\lambda_1 + (j\pi - \lambda_1)\cos\lambda_1}{\alpha_1^2 + (j\pi - \lambda_1)^2} \qquad (2.4\text{-}11a)$$

$$I_{x121} = (-1)^{j+m}\, \alpha_1 \left[\frac{1}{(j+m)\pi - 2\lambda_1} + \frac{1}{(j-m)\pi + 2\lambda_1}\right] \sin 2\lambda_1$$

$$I_{x122} = \frac{1 - (-1)^{m+j}}{(m+j)\pi} + \frac{-1 + (-1)^{m-j}}{(m-j)\pi} + \frac{1 - (-1)^{j+m}\cos 2\lambda_1}{(j+m)\pi - 2\lambda_1}$$

$$+ \frac{1 - (-1)^{j-m}\cos 2\lambda_1}{(j-m)\pi + 2\lambda_1}$$

$$I_{x123} = \frac{\alpha_1 \sin\lambda_1 + (j\pi + \lambda_1)\cos\lambda_1}{\alpha_1^2 + (j\pi + \lambda_1)^2}$$

$$+ \frac{-\alpha_1 \sin\lambda_1 + (j\pi - \lambda_1)\cos\lambda_1}{\alpha_1^2 + (j\pi + \lambda_1)^2} \tag{2.4-11b}$$

$$I_{x131} = (-1)^{j+m} \alpha_1 \left[\frac{1}{(j+m)\pi - 2\lambda_1} + \frac{1}{(j-m)\pi + 2\lambda_1} \right] \sin 2\lambda_1$$

$$I_{x132} = \frac{-1 + (-1)^{m+j}}{(m+j)\pi} + \frac{1 - (-1)^{m-j}}{(m-j)\pi} + \frac{1 - (-1)^{j+m}\cos 2\lambda_1}{(j+m)\pi - 2\lambda_1}$$

$$+ \frac{1 - (-1)^{j-m}\cos 2\lambda_1}{(j-m)\pi + 2\lambda_1}$$

$$I_{x133} = \frac{(1)^{j+1}\left[-\alpha_1 \cos\lambda_1 + (j\pi + \lambda_1)\sin\lambda_1\right]e^{-\alpha_1} - \alpha_1}{\alpha_1^2 + (j\pi + \lambda_1)^2}$$

$$+ \frac{(-1)^{j+1}\left[\alpha_1 \cos\lambda_1 + (j\pi - \lambda_1)\sin\lambda_1\right]e^{-\alpha_1} + \alpha_1}{\alpha_1^2 + (j\pi - \lambda_1)^2} \tag{2.4-11c}$$

$$I_{x141} = (-1)^{m+j} \alpha_1 \left[\frac{1}{(m+j)\pi + 2\lambda_1} + \frac{1}{(m-j)\pi + 2\lambda_1} \right] \sin 2\lambda_1$$

$$I_{x142} = \frac{-1 + (-1)^{j+m}}{(j+m)\pi} + \frac{-1 + (-1)^{j-m}}{(j-m)\pi} + \frac{1 - (-1)^{m+j}\cos 2\lambda_1}{(m+j)\pi + 2\lambda_1}$$

$$+ \frac{-1 + (-1)^{m-j}\cos 2\lambda_1}{(m-j)\pi + 2\lambda_1}$$

18

$$I_{x143} = \frac{(-1)^{j+1} \left[- \alpha_1 \cos \lambda_1 + (j\pi + \lambda_1) \sin \lambda_1\right] e^{-\alpha_1} - \alpha_1}{\alpha_1^2 + (j\pi + \lambda_1)^2}$$

$$+ \frac{(-1)^{j+1} \left[\alpha_1 \cos \lambda_1 + (j\pi - \lambda_1) \sin \lambda_1\right] e^{-\alpha_1} + \alpha_1}{\alpha_1^2 + (j\pi - \lambda_1)^2} \qquad (2.4\text{-}11\text{d})$$

$$I_{x211} = (-1)^{j+m} \alpha_1 \left[\frac{1}{(j+m)\pi + 2\lambda_1} + \frac{1}{(j-m)\pi + 2\lambda_1}\right] \sin 2\lambda_1$$

$$I_{x212} = \frac{1 - (-1)^{m+j}}{(m+j)\pi} + \frac{1 - (-1)^{m-j}}{(m-j)\pi} + \frac{1 - (-1)^{j+m} \cos 2\lambda_1}{(j+m)\pi + 2\lambda_1}$$

$$+ \frac{-1 + (-1)^{j-m} \cos 2\lambda_1}{(j-m)\pi + 2\lambda_1}$$

$$I_{x213} = \frac{\alpha_1 \sin \lambda_1 + (m\pi + \lambda_1) \cos \lambda_1}{\alpha_1^2 + (m\pi + \lambda_1)^2}$$

$$+ \frac{-\alpha_1 \sin \lambda_1 + (m\pi - \lambda_1) \cos \lambda_1}{\alpha_1^2 + (m\pi - \lambda_1)^2} \qquad (2.4\text{-}11\text{e})$$

$$I_{x221} = (-1)^{m+j} \alpha_1 \left[\frac{1}{(m+j)\pi - 2\lambda_1} + \frac{1}{(m-j)\pi + 2\lambda_1}\right] \sin 2\lambda_1$$

$$I_{x222} = \frac{1 - (-1)^{j+m}}{(j+m)\pi\pi} + \frac{-1 + (-1)^{j-m}}{(j-m)\pi} + \frac{1 - (-1)^{m+j} \cos 2\lambda_1}{(m+j)\pi - 2\lambda_1}$$

$$+ \frac{1 - (-1)^{m-j} \cos 2\lambda_1}{(m-j)\pi + 2\lambda_1}$$

$$I_{x223} = \frac{\alpha_1 \sin \lambda_1 + (m\pi + \lambda_1) \cos \lambda_1}{\alpha_1^2 + (m\pi + \lambda_1)^2}$$

$$+ \frac{-\alpha_1 \sin \lambda_1 + (m\pi - \lambda_1) \cos \lambda_1}{\alpha_1^2 + (m\pi - \lambda_1)^2} \qquad (2.4\text{-}11f)$$

$$I_{x231} = (-1)^{m+j} \alpha_1 \left[\frac{1}{(m+j)\pi - 2\lambda_1} + \frac{1}{(m-j)\pi + 2\lambda_1} \right] \sin 2\lambda_1$$

$$I_{x232} = \frac{-1 + (-1)^{j+m}}{(j+m)\pi} + \frac{1 - (-1)^{j-m}}{(j-m)\pi} + \frac{1 - (-1)^{m+j} \cos 2\lambda_1}{(m+j)\pi - 2\lambda_1}$$

$$+ \frac{1 - (-1)^{m-j} \cos 2\lambda_1}{(m-j)\pi + 2\lambda_1}$$

$$I_{x233} = \frac{(-1)^{m+1} \left[- \alpha_1 \cos \lambda_1 + (m\pi + \lambda_1) \sin \lambda_1 \right] e^{-\alpha_1} - \alpha_1}{\alpha_1^2 + (m\pi + \lambda_1)^2}$$

$$+ \frac{(-1)^{m+1} \left[\alpha_1 \cos \lambda_1 + (m\pi - \lambda_1) \sin \lambda_1 \right] e^{-\alpha_1} + \alpha_1}{\alpha_1^2 + (m\pi - \lambda_1)^2} \qquad (2.4\text{-}11g)$$

$$I_{x241} = (-1)^{m-j} \alpha_1 \left[\frac{1}{(j+m)\pi + 2\lambda_1} + \frac{1}{(j-m)\pi + 2\lambda_1} \right] \sin 2\lambda_1$$

$$I_{x242} = \frac{-1 + (-1)^{m+j}}{(m+j)\pi} + \frac{-1 + (-1)^{m-j}}{(m-j)\pi} + \frac{1 - (-1)^{j+m} \cos 2\lambda_1}{(j+m)\pi + 2\lambda_1}$$

$$+ \frac{-1 + (-1)^{j-m} \cos 2\lambda_1}{(j-m)\pi + 2\lambda_1}$$

$$I_{x243} = \frac{(-1)^{m+1}\left[-\alpha_1 \cos \lambda_1 + (m\pi + \lambda_1) \sin \lambda_1\right]e^{-\alpha_1} - \alpha_1}{\alpha_1^2 + (m\pi + \lambda_1)^2}$$

$$+ \frac{(-1)^{m+1}\left[\alpha_1 \cos \alpha_1 + (m\pi - \lambda_1)\sin \lambda_1\right]e^{-\alpha_1} + \alpha_1}{\alpha_1^2 + (m\pi - \lambda_1)^2} \qquad (2.4\text{-}11h)$$

$$I_{y111} = (-1)^{n+k} \alpha_2 \left[\frac{1}{(n+k)\pi + 2\lambda_2} + \frac{1}{(n-k)\pi + 2\lambda_2}\right]\sin 2\lambda_2$$

$$I_{y112} = \frac{1 - (-1)^{k+n}}{(k+n)\pi} + \frac{1 - (-1)^{k-n}}{(k-n)\pi} + \frac{1 - (-1)^{n+k} \cos 2\lambda_2}{(n+k)\pi + 2\lambda_2}$$

$$+ \frac{-1 + (-1)^{n-k} \cos 2\lambda_2}{(n-k)\pi + 2\lambda_2}$$

$$I_{y113} = \frac{\alpha_2 \sin \lambda_2 + (k\pi + \lambda_2) \cos \lambda_2}{\alpha_2^2 + (k\pi + \lambda_2)^2}$$

$$+ \frac{-\alpha_2 \sin \lambda_2 + (k\pi - \lambda_2) \cos \lambda_2}{\alpha_2^2 + (k\pi - \lambda_2)^2} \qquad (2.4\text{-}12a)$$

$$I_{y121} = (-1)^{k+n} \alpha_2 \left[\frac{1}{(k+n)\pi - 2\lambda_2} + \frac{1}{(k-n)\pi + 2\lambda_2}\right] \sin 2\lambda_2$$

$$I_{y122} = \frac{1 - (-1)^{n+k}}{(n+k)\pi} + \frac{-1 + (-1)^{n-k}}{(n-k)\pi} + \frac{1 - (-1)^{k+n} \cos 2\lambda_2}{(k+n)\pi - 2\lambda_2}$$

$$+ \frac{1 - (-1)^{k-n} \cos 2\lambda_2}{(k-n)\pi + 2\lambda_2}$$

21

$$I_{y123} = \frac{\alpha_2 \sin \lambda_2 + (k\pi + \lambda_2) \cos \lambda_2}{\alpha_2^2 + (k\pi + \lambda_2)^2}$$

$$+ \frac{-\alpha_2 \sin \lambda_2 + (k\pi - \lambda_2) \cos \lambda_2}{\alpha_2^2 + (k\pi - \lambda_2)^2} \tag{2.4-12b}$$

$$I_{y131} = (-1)^{k+n} \alpha_2 \left[\frac{1}{(k+n)\pi - 2\lambda_2} + \frac{1}{(k-n)\pi + 2\lambda_2} \right] \sin 2\lambda_2$$

$$I_{y132} = \frac{-1 + (-1)^{k+n}}{(k+n)\pi} + \frac{1 - (-1)^{k-n}}{(k-n)\pi} + \frac{1 - (-1)^{n+k} \cos 2\lambda_2}{(n+k)\pi - 2\lambda_2}$$

$$+ \frac{1 - (-1)^{n-k} \cos 2\lambda_2}{(n-k)\pi + 2\lambda_2}$$

$$I_{y133} = \frac{(-1)^{k+1} \left[-\alpha_2 \cos \lambda_2 + (k\pi + \lambda_2) \sin \lambda_2 \right] e^{-\alpha_2} - \alpha_2}{\alpha_2^2 + (k\pi + \lambda_2)^2}$$

$$+ \frac{(-1)^{k+1} \left[\alpha_2 \cos \lambda_2 + (k\pi - \lambda_2) \sin \lambda_2 \right] e^{-\alpha_2} - \alpha_2}{\alpha_2^2 + (k\pi - \lambda_2)^2} \tag{2.4-12c}$$

$$I_{y141} = (-1)^{n+k} \alpha_2 \left[\frac{1}{(n+k)\pi + 2\lambda_2} + \frac{1}{(n-k)\pi + 2\lambda_2} \right] \sin 2\lambda_2$$

$$I_{y142} = \frac{-1 + (-1)^{k+n}}{(k+n)\pi} + \frac{-1 + (-1)^{k-n}}{(k-n)\pi} + \frac{1 - (-1)^{n+k} \cos 2\lambda_2}{(n+k)\pi + 2\lambda_2}$$

$$+ \frac{-1 + (-1)^{n-k} \cos 2\lambda_2}{(n-k)\pi + 2\lambda_2}$$

22

$$I_{y143} = \frac{(-1)^{k+1} \left[-\alpha_2 \cos \lambda_2 + (k\pi + \lambda_2) \sin \lambda_2 \right] e^{-\alpha_2} - \alpha_2}{\alpha_2^2 + (k\pi + \lambda_2)^2}$$

$$+ \frac{(-1)^{k+1} \left[\alpha_2 \cos \lambda_2 + (k\pi - \lambda_2) \sin \lambda_2 \right] e^{-\alpha_2} - \alpha_2}{\alpha_2^2 + (k\pi - \lambda_2)^2} \qquad (2.4\text{-}12\text{d})$$

$$I_{y211} = (-1)^{k+n} \alpha_2 \left[\frac{1}{(k+n)\pi + 2\lambda_2} + \frac{1}{(k-n)\pi + 2\lambda_2} \right] \sin 2\lambda_2$$

$$I_{y212} = \frac{1 - (-1)^{n+k}}{(n+k)\pi} + \frac{1 - (-1)^{n-k}}{(n-k)\pi} + \frac{1 - (-1)^{k+n} \cos 2\lambda_2}{(k+n)\pi + 2\lambda_2}$$

$$+ \frac{-1 + (-1)^{k-n} \cos 2\lambda_2}{(k-n)\pi + 2\lambda_2}$$

$$I_{y213} = \frac{\alpha_2 \sin \lambda_2 + (n\pi + \lambda_2) \cos \lambda_2}{\alpha_2^2 + (n\pi + \lambda_2)^2}$$

$$+ \frac{-\alpha_2 \sin \lambda_2 + (n\pi - \lambda_2) \cos \lambda_2}{\alpha_2^2 + (n\pi - \lambda_2)^2} \qquad (2.4\text{-}12\text{e})$$

$$I_{y221} = (-1)^{n+k} \alpha_2 \left[\frac{1}{(n+k)\pi - 2\lambda_2} + \frac{1}{(n-k)\pi + 2\lambda_2} \right] \sin 2\lambda_2$$

$$I_{y222} = \frac{1 - (-1)^{k+n}}{(k+n)\pi} + \frac{-1 + (-1)^{k-n}}{(k-n)\pi} + \frac{1 - (-1)^{n+k} \cos 2\lambda_2}{(n+k)\pi - 2\lambda_2}$$

$$+ \frac{1 - (-1)^{n-k} \cos 2\lambda_2}{(n-k)\pi + 2\lambda_2}$$

23

$$I_{y223} = \frac{\alpha_2 \sin \lambda_2 + (n\pi + \lambda_2) \cos \lambda_2}{\alpha_2^2 + (n\pi + \lambda_2)^2}$$

$$+ \frac{-\alpha_2 \sin \lambda_2 + (n\pi - \lambda_2) \cos \lambda_2}{\alpha_2^2 + (n\pi - \lambda_2)^2} \qquad (2.4\text{-}12f)$$

$$I_{y231} = (-1)^{n+k} \alpha_2 \left[\frac{1}{(n+k)\pi - 2\lambda_2} + \frac{1}{(n-k)\pi + 2\lambda_2} \right] \sin 2\lambda_2$$

$$I_{y232} = \frac{-1 + (-1)^{k+n}}{(k+n)\pi} + \frac{1 - (-1)^{k-n}}{(k-n)\pi} + \frac{1 - (-1)^{n+k} \cos 2\lambda_2}{(n+k)\pi - 2\lambda_2}$$

$$+ \frac{1 - (-1)^{n-k} \cos 2\lambda_2}{(n-k)\pi + 2\lambda_2}$$

$$I_{y233} = \frac{(-1)^{n+1} \left[-\alpha_2 \cos \lambda_2 + (n\pi + \lambda_2) \sin \lambda_2 \right] e^{-\alpha_2} - \alpha_2}{\alpha_2^2 + (n\pi + \lambda_2)^2}$$

$$+ \frac{(-1)^{n+1} \left[\alpha_2 \cos \lambda_2 + (n\pi - \lambda_2) \sin \lambda_2 \right] e^{-\alpha_2} + \alpha_2}{\alpha_2^2 + (n\pi - \lambda_2)^2} \qquad (2.4\text{-}12g)$$

$$I_{y241} = (-1)^{k+n} \alpha_2 \left[\frac{1}{(k+n)\pi + 2\lambda_2} + \frac{1}{(k-n)\pi + 2\lambda_2} \right] \sin 2\lambda_2$$

$$I_{y242} = \frac{-1 + (-1)^{n+k}}{(n+k)\pi} + \frac{-1 + (-1)^{n-k}}{(n-k)\pi} + \frac{1 - (-1)^{k+n} \cos 2\lambda_2}{(k+n)\pi + 2\lambda_2}$$

$$+ \frac{-1 + (-1)^{k-n} \cos 2\lambda_2}{(k-n)\pi + 2\lambda_2}$$

24

$$I_{y243} \quad + \quad \frac{(-1)^{n+1}\left[-\alpha_2 \cos \lambda_2 + (n\pi + \lambda_2) \sin \lambda_2\right]e^{-\alpha_2} - \alpha_2}{\alpha_2^2 + (n\pi + \lambda_2)^2}$$

$$+ \quad \frac{(-1)^{n+1}\left[\alpha_2 \cos \lambda_2 + (n\pi - \lambda_2) \sin \lambda_2\right]e^{-\alpha_2} + \alpha_2}{\alpha_2^2 + (n\pi - \lambda_2)^2} \qquad (2.4\text{-}12h)$$

Note: When j=m or k=n, the indeterminate terms $\left(\frac{0}{0}\right)$ in the above expressions for the I should be set equal to zero.

$$\alpha_1 \quad = \quad A_1 K \ell$$

$$\alpha_2 \quad = \quad A_2 K b$$

$$\lambda_1 \quad = \quad K \ell$$

$$\lambda_2 \quad = \quad K b$$

$$K \quad = \quad \frac{\omega}{c} \qquad\qquad (2.4\text{-}13)$$

2.4.1.2   Four Edges Clamped Rectangular Panels

For the four edge clamped rectangular panel, the normal mode is:

$$F_{jk} \quad = \quad X_j (x) \; Y_k (y)$$

where

$$X_1(x) \quad = \quad \cosh \tilde{x}_1 - \cos \tilde{x}_1$$

$$- 0.9825 \, (\sinh \tilde{x}_1 - \sin \tilde{x}_1)$$

$$Y_1(y) \quad = \quad \cosh \tilde{y}_1 - \cos \tilde{y}_1$$

$$- 0.9825 \, (\sinh \tilde{y}_1 - \sin \tilde{y}_1)$$

$$X_j(x) \quad = \quad \cosh \tilde{x}_j - \cos \tilde{x}_j - (\sinh \tilde{x}_j - \sin \tilde{x}_j)$$

$$j = 2, 3 \ldots$$

25

$$Y_k(y) = \cosh \tilde{y}_k - \cos \tilde{y}_k - (\sinh \tilde{y}_k - \sin \tilde{y}_k)$$

$$k = 2, 3 \ldots$$

$$\tilde{x}_1 = \frac{1.5056 \, \pi x}{\ell}$$

$$\tilde{y}_1 = \frac{1.5056 \, \pi y}{b}$$

$$\tilde{x}_j = \frac{(j + 1/2)\pi x}{\ell} \qquad j = 2, 3 \ldots$$

$$\tilde{y}_k = \frac{(k + 1/2)\pi y}{b} \qquad k = 2, 3 \ldots \qquad (2.4\text{-}15)$$

For this case the carrying out of the integration in Equation (2.4-1) is too complicated and is not practical. Therefore the calculation for the I_{jkmn} has to be done by numerical integration. Substitution of Equation (2.4-15) into Equation (2.4-1) and representing the double integration by double summation yields

$$\frac{I_{jkmn}(\omega)}{\Phi_{pp}(\omega)} = \int_0^\ell \int_0^\ell \exp(-A_1 K\xi) \cos(K\xi) X_j(x_1) \, X_m(x_2) \, dx_1 dx_2$$

$$\cdot \int_0^b \int_0^b \exp(-A_2 K\eta) \cos(K\eta) Y_k(y_1) \, Y_n(y_2) \, dy_1 dy_2$$

$$= \sum_p \sum_q \exp(-A_1 K\xi) \cos(K\xi) X_j(x_p) \, X_m(x_q) \, \Delta x_1 \, \Delta x_2$$

$$\cdot \sum_{p'} \sum_{q'} \exp(-A_2 K\eta) \cos(K\eta) Y_k(y_{p'}) \, Y_n(y_{q'}) \, \Delta y_1 \, \Delta y_2$$

When the length ℓ and width b are divided into s and s' equal divisions respectively, simple calculation gives

$$\Delta x_1 = \Delta x_2 = \frac{\ell}{s}$$

$$\Delta y_1 = \Delta y_2 = \frac{b}{s'}$$

26

$$\xi \;=\; \frac{\ell}{s}\,|p - q|$$

$$\eta \;=\; \frac{b}{s}\,|p'- q'|$$

$$x_p \;=\; \left(p - \tfrac{1}{2}\right)\frac{\ell}{s}$$

$$x_q \;=\; \left(q - \tfrac{1}{2}\right)\frac{\ell}{s}$$

$$y_{p'} \;=\; \left(p' - \tfrac{1}{2}\right)\frac{b}{s'}$$

$$y_{q'} \;=\; \left(q' - \tfrac{1}{2}\right)\frac{b}{s'}$$

$$\tilde{x}_1 \;=\; \frac{1.5056\,\pi}{\ell}\,x_p \;=\; \frac{1.5056\,\pi\,(p - 1/2)}{s}$$

$$\tilde{y}_1 \;=\; \frac{1.5056\,\pi}{b}\,y_p \;=\; \frac{1.5056\,\pi\,(p' - 1/2)}{s'}$$

$$\tilde{x}_j \;=\; \frac{(j + 1/2)\,\pi\,(p - 1/2)}{s} \qquad j = 2,\,3\,\ldots$$

$$\tilde{y}_k \;=\; \frac{(k + 1/2)\,\pi\,(p' - 1/2)}{s'} \qquad k = 2,\,3\,\ldots \tag{2.4-17}$$

Substitution of Equation (2.4-17) into Equation (2.4-16) yields the normalized cross spectral density of the generalized force as

$$
\tilde{I}_{jkmn}(\omega) \;=\; \frac{I_{jkmn}(\omega)}{b^2\ell^2\,\Phi_{pp}(\omega)}
$$

$$
\;=\; \frac{1}{(ss')^2}\sum_{p=1}^{s}\sum_{q=1}^{s}\sum_{p'=1}^{s'}\sum_{q'=1}^{s'}\exp\left[-\frac{A_1 K\ell}{s}\,|p - q|\right]
$$

27

$$\cdot \cos\left[\frac{K\ell}{s}(p-q)\right]X_j\ X_m$$

$$\cdot \exp\left[-\frac{A_2Kb}{s}\ |p'-q'|\right]\cos\left[\frac{Kb}{s'}(p'-q')\right]Y_k\ Y_n \qquad (2.4\text{-}18)$$

where the X and Y functions are given by Equation (2.4-15) with the $\tilde{x}$ and $\tilde{y}$ arguments given by Equation (2.4-17).

The numerical method described above can be applied to any correlation function and any mode shape.

2.4.2 Cross Spectral Density of Generalized Force, Exponentially Decaying Correlation

When the correlation coefficient is represented by Equation (2.3-3) in Section 2.3, the cross spectral density function of the excitation pressure becomes

$$\phi_{pp}(r_1,r_2,\omega) = \Phi_{pp}(\omega)\ \exp(-A_1K\xi)\ \exp(-A_2K\eta) \qquad (2.4\text{-}19)$$

Substitution of Equations (2.4-19) and (2.4-4) into Equation (2.4-1) yields

$$I_{jkmn} = \Phi_{pp}(\omega)\int_0^\ell\int_0^\ell \exp(-A_1K\xi)\ \sin\frac{j\pi x_1}{\ell}\ \sin\frac{m\pi x_2}{\ell}\ dx_1dx_2$$

$$\cdot \int_0^b\int_0^b \exp(-A_2K\eta)\ \sin\frac{k\pi y_1}{b}\ \sin\frac{n\pi y_2}{b}\ dy_1\ dy_2 \qquad (2.4\text{-}20)$$

The above integration can be carried out by the following identity:

$$\int_0^\ell\int_0^\ell \exp(-A_1K\xi)\ \sin\frac{j\pi x_1}{\ell}\ \sin\frac{m\pi x_2}{\ell}\ dx_1dx_2$$

$$= \int_0^\ell dx_1\int_0^{x_1} \exp[A_1K(x_1-x_2)]\sin\frac{j\pi x_1}{\ell}\ \sin\frac{m\pi x_2}{\ell}\ dx_2$$

28

$$+ \int_0^\ell dx_2 \int_0^{x_2} \exp\,[-A_2 K(x_2 - x_1)]\sin\frac{j\pi x_1}{\ell}\sin\frac{m\pi x_2}{\ell}\,dx_1$$

$$= \quad I_1 + I_2 \qquad\qquad\qquad\qquad\qquad (2.4\text{-}21)$$

Carrying out the integrals I_1 and I_2 yields

$$I_{jm} \quad = \quad \frac{1}{\ell^2}\int_0^\ell\int_0^\ell \exp\,(-A_1 K\xi)\,\sin\frac{j\pi x_1}{\ell}\sin\frac{m\pi x_2}{\ell}\,dx_1 dx_2$$

$$= \quad \frac{\alpha_1}{2}\left[\frac{1}{\alpha_1^2 + (j\pi)^2} + \frac{1}{\alpha_1^2 + (m\pi)^2}\right]$$

$$+ \quad (j\pi)(m\pi)\frac{2 + [(-1)^{j+1} + (-1)^{m+1}]\,\exp\,(-\alpha_1)}{\left[\alpha_1^2 + (j\pi)^2\right]\left[\alpha_1^2 + (m\pi)^2\right]}\quad \text{for } j = m$$

$$\qquad\qquad\qquad\qquad\qquad (2.4\text{-}22)$$

$$I_{jm}' \quad = \quad \frac{1}{\ell^2}\int_0^\ell\int_0^\ell \exp\,(-A_1 K\eta)\,\sin\frac{j\pi x_1}{\ell}\sin\frac{m\pi x_2}{\ell}\,dx_1 dx_2$$

$$= \quad (j\pi)(m\pi)\,\frac{2 + [\,(-1)^{j+1} + (-1)^{m+1}]\,\exp\,(-\alpha_1)}{[\,\alpha_1^2 + (j\pi)^2]\,[\,\alpha_1^2 + (m\pi)^2]}$$

$$+ \quad \frac{j}{\alpha_1^2 + (j\pi)^2}\left[\frac{(-1)^{m-j} - 1}{2\,(m-j)} + \frac{(-1)^{m+j} - 1}{2\,(m+j)}\right]$$

$$+ \quad \frac{m}{\alpha_1^2 + (m\pi)^2}\left[\frac{(-1)^{j-m} - 1}{2\,(j-m)} + \frac{(-1)^{j+m} - 1}{2\,(j+m)}\right]\quad \text{for } j \neq m$$

$$\qquad\qquad\qquad\qquad\qquad (2.4\text{-}23)$$

Similarly the double integration on y_1 and y_2 in Equation (24-20) can be carried out to give

$$I_{kn} = \frac{1}{b^2} \int_o^b \int_o^b \exp(-A_2 K\eta) \sin\frac{k\pi y_1}{b} \sin\frac{n\pi y_2}{b} \, dy_1 dy_2$$

$$= \frac{\alpha_2^2}{2} \left[\frac{1}{\alpha_2^2 + (k\pi)^2} + \frac{1}{\alpha_2^2 + (n\pi)^2} \right]$$

$$+ (k\pi)(n\pi) \frac{2 + [(-1)^{k+1} + (-1)^{n+1}] \exp(-\alpha_2)}{\left[\alpha_2^2 + (k\pi)^2\right]\left[\alpha_2^2 + (n\pi)^2\right]} \quad \text{for } k = n$$

$$(2.4\text{-}24)$$

$$I'_{kn} = \frac{1}{b^2} \int_o^b \int_o^b \exp(-A_2 K\eta) \sin\frac{k\pi y_1}{b} \sin\frac{n\pi y_2}{b} \, dy_1 dy_2$$

$$= (k\pi)(n\pi) \frac{2 + [(-1)^{k+1} + (-1)^{n+1}] \exp(-\alpha_2)}{\left[\alpha_2^2 + (k\pi)^2\right]\left[\alpha_2^2 + (n\pi)^2\right]}$$

$$+ \frac{k}{\alpha_2^2 + (k\pi)^2} \left[\frac{(-1)^{n-k}-1}{2(n-k)} + \frac{(-1)^{n+k}-1}{2(n+k)} \right]$$

$$+ \frac{n}{\alpha_2^2 + (n\pi)^2} \left[\frac{(-1)^{k-n}-1}{2(k-n)} + \frac{(-1)^{k+n}-1}{2(k+n)} \right] \quad \text{for } k \neq n$$

$$(2.4\text{-}25)$$

Substitution of Equations (2.4-22), (2.4-23), (2.4-24), and (2.4-25) into Equation (2.4-20) yields the cross spectral density of the generalized force of the excitation as:

$$I_{jkmn} = (b\ell)^2 \, \Phi_{pp}(\omega) \, I_{jm}I_{kn} \quad \text{for } j = m, \; k = n$$

$$= (b\ell)^2 \, \Phi_{pp}(\omega) \, I_{jm}I'_{kn} \quad \text{for } j = m, \; k \neq n$$

$$= (b\ell)^2 \, \Phi_{pp}(\omega) \, I'_{jm}I_{km} \quad \text{for } j \neq m, \; k = n$$

30

$$= (b\ell)^2 \, \Phi_{pp}(\omega) \, I'_{jm} \, I'_{kn} \qquad \text{for } j \neq m, \, k \neq n \qquad (2.4\text{-}26)$$

2.4.3 Joint Acceptance and Normalized Cross Spectral Density of Generalized Force

The normalized cross spectral density of the generalized force of the excitation is defined as

$$\tilde{I}_{jkmn} = \frac{I_{jkmn}}{S^2 \, \Phi_{pp}(\omega)} \qquad (2.4\text{-}27)$$

where

$$S = b\ell = \text{area of the panel}$$

The relation between the joint acceptance squared and the normalized cross spectral density of the generalized force is given by [see Reference 3, Chapter VI, Section 6.2, Page 24, Equation (6-25) and Reference 2, Chapter 7, Section 7.2, Page 212].

$$J^2_{jkmn} = \tilde{I}_{jkmn} \cos \, \omega \, (\tau_{jk} - \tau_{mn}) \qquad (2.4\text{-}28)$$

$$\omega(\tau_{jk} - \tau_{mn}) = \text{phase difference of the jk and mn modes}$$

$$A_{jkmn} = \left[1 - (\omega/\omega_{jk})^2 \right] \left[1 - (\omega/\omega_{mn})^2 \right] + 4\zeta_{jk}\zeta_{mn} \, \omega^2 / (\omega_{jk}\omega_{mn})$$

$$C^2_{jkmn} = A^2_{jkmn} + B^2_{jkmn}$$

$$B_{jkmn} = 2 \left\{ \left[1 - (\omega/\omega_{jk})^2 \right] \zeta_{mn}\omega/\omega_{mn} - \left[1 - (\omega/\omega_{mn})^2 \right] \zeta_{jk}\omega/\omega_{jk} \right\}$$

$$\cos \, \omega(\tau_{jk} - \tau_{mn}) = \frac{A_{jkmn}}{C_{jkmn}} \qquad (2.4\text{-}29)$$

31

2.5   The Displacement Response

The displacement response spectral density at any point $\vec{r}(x,y)$ is given by [see Reference 3, Section VI, Equation 6-24, Page 24].

$$\Phi_{ww}(\vec{r},\omega) \quad = \quad S'^2 \Phi_{pp}(\omega) \sum_{j,k,m,n} F_{jk}F_{mn}|H_{jk}|\ |H_{mn}^*|J_{jkmn}^2$$

(2.5-1)

where

$$\Phi_{ww}(\vec{r},\omega) \quad = \quad \text{displacement spectral density in } \frac{(\text{inch})^2}{\text{rad./sec.}}$$

$$S' = b'\ell' \quad = \quad \text{area of panel subjected to excitation in } (\text{inch})^2$$

$$b' \quad = \quad \text{width of panel subjected to excitation in inches}$$

$$\ell' \quad = \quad \text{length of panel subjected to excitation in inches}$$

$$F_{jk}, F_{mn} \quad = \quad \text{normal modes}$$

$$\Phi_{pp}(\omega) \quad = \quad \text{spectral density of the spatial homogeneous excitation pressure in } (\text{psi})^2/\text{radian per second}$$

The magnitudes of the complex frequency response functions and their complex conjugates are given by

$$|H_{jk}| \quad = \quad M_{jk}^{-1}\left[(\omega_{jk}^2 - \omega^2)^2 \ + \ (2\zeta_{jk}\omega_{jk}\omega)^2\right]^{-1/2}$$

$$|H_{mn}^*| \quad = \quad M_{mn}^{-1}\left[(\omega_{mn}^2 - \omega^2)^2 \ + \ (2\zeta_{mn}\omega_{mn}\omega)^2\right]^{-1/2}$$

(2.5-2)

where

$$\omega \quad = \quad \text{frequency in radians per second}$$

$$= \quad 2\pi f$$

$$f \quad = \quad \text{frequency in Hertz}$$

The modal masses are

$$M_{jk} = M_{mn} = \int MF^2_{jk}\, dr = \frac{M\ell b}{4} \tag{2.5-3}$$

with

$$M = \rho h + \rho'h' = \text{mass distribution per unit area}$$

The joint acceptance squared for different mode combinations are given by Equation (2.4-28), in Section 2.4.

The displacement response spectral density in $inch^2$/Hertz is given by

$$S_{ww}(\vec{r},f) = 2\pi\Phi_{ww}(\vec{r},\omega) \tag{2.5-4}$$

The mean-square displacement response in $inch^2$ is given by

$$w^2(\vec{r}) = \int S_{ww}(\vec{r},f)\, df \tag{2.5-5}$$

The root-mean-square displacement in inches is given by

$$w(\vec{r}) = [w^2(\vec{r})]^{1/2} \tag{2.5-6}$$

2.6   The Excitation Pressure Data

For derivation of the formulas, see Reference 4, Section 6.1. The excitation spectral density in $\dfrac{(psi)^2}{\text{radian/sec.}}$ is given by

$$\Phi_{pp}(\omega) = \frac{1}{2\pi} [10]^{\frac{S_{pp}(f) - 170.576}{10}} \tag{2.6-1}$$

The excitation spectral density in decibels/Hertz is given by

$$S_{pp}(f) = S_{3rd}(f) - 10 \log_{10}(0.23157f) \tag{2.6-2}$$

33

where

$$S_{3rd}(f) = \text{one-third octave excitation pressure level} \\ \text{in decibels (input)}$$

The excitation spectral density in $(psi)^2$/Hertz is given by

$$S'_{pp}(f) = 2\pi\Phi_{pp}(\omega) \tag{2.6-3}$$

The relations between the overall mean-square pressure and the overall pressure level of the excitation are:

$$p_a^2 = 8.75526 \times 10^{-18} [10]^{L_a/10} \tag{2.6-4}$$

and

$$L_a = 170.576 + 10 \log_{10} (p_a^2) \tag{2.6-5}$$

where

$$p_a^2 = \text{mean-square pressure in } (psi)^2$$

$$L_a = \text{excitation overall pressure level in decibels} \\ \text{referenced } 0.00002 \text{ Newton/meter}^2$$

2.7 The Acceleration Response

The acceleration response spectral density at any point $\vec{r}(x,y)$ in $\left(\dfrac{\text{inch}}{\text{sec}^2}\right)^2 \dfrac{1}{\text{rad/sec}}$ is given by

$$\Phi_{\overset{....}{ww}}(\vec{r},\omega) = \omega^4 \Phi_{ww}(\vec{r},\omega) \tag{2.7-1}$$

where the displacement response $\Phi_{ww}(\vec{r},\omega)$ is given by equation (2.5-1) in Section 2.5.

The acceleration response spectral density in g^2/Hertz is given by [see Reference 4, Section 6.1, Page 18].

$$S_{\overset{....}{ww}}(\vec{r},f) = 4.215093 \times 10^{-5} \Phi_{\overset{....}{ww}}(\vec{r},\omega) \tag{2.7-2a}$$

The acceleration spectral density in decibels referenced "g" is

$$S_{\overset{..}{wg}}(\vec{r},f) = 10 \log_{10} [S_{\overset{....}{ww}}(\vec{r},f)] \tag{2.7-2b}$$

34

The mean-square acceleration response in "g^2" is given by

$$G^2(\vec{r}) \quad = \quad \int S_{\dddot{w}\dddot{w}}(\vec{r},f)df \qquad \qquad (2.7\text{-}3)$$

The root-mean square acceleration in "g" is given by

$$G(\vec{r}) \quad = \quad [G^2(r)]^{1/2} \qquad \qquad (2.7\text{-}4)$$

2.8 The Stress Response

For derivation of the formulas, see Reference 3, Section 6.1. The stress response spectral density in $(psi)^2$/radian per sec. is given by

$$\Phi_{\sigma\sigma}(\vec{r},\omega) \quad = \quad \gamma^2(\vec{r})\Phi_{ww}(\vec{r},\omega) \qquad \qquad (2.8\text{-}1)$$

where the displacement response spectral density $\Phi_{ww}(\vec{r},\omega)$ is given by Equation (2.5-1). The factor to convert the displacement response into stress response is given by

$$\gamma^2(\vec{r}) \quad = \quad \frac{(Eh_1)^2}{4(1-\nu^2)} \cdot \frac{Q^2_x + Q^2_y}{Q^2_w} \qquad \qquad (2.8\text{-}2)$$

$$h_1 \quad = \quad h + h_2$$

$$h_2 \quad = \quad \text{largest height of stiffeners at } \vec{r} \text{ (See Figure 1)}$$

$$Q_x \quad = \quad \sum_{\substack{m,n \\ =1,3 \ldots}}^{\infty} \frac{\pi^2}{mn}\left[\left(\frac{m}{\ell}\right)^2 + \nu\left(\frac{n}{b}\right)^2\right] \frac{\sin\frac{m\pi x}{\ell}\sin\frac{n\pi y}{b}}{D_x\left(\frac{m}{\ell}\right)^4 + 2H\left(\frac{mn}{\ell b}\right)^2 + D_y\left(\frac{n}{b}\right)^4}$$

$$(2.8\text{-}3)$$

$$Q_y \quad = \quad \sum_{\substack{m,n \\ = 1,3,\ldots}}^{\infty} \frac{\pi^2}{mn}\left[\left(\frac{n}{b}\right)^2 + \nu\left(\frac{m}{\ell}\right)^2\right] \frac{\sin\frac{m\pi x}{\ell}\sin\frac{n\pi y}{b}}{D_x\left(\frac{m}{\ell}\right)^4 + 2H\left(\frac{mn}{\ell b}\right)^2 + D_y\left(\frac{n}{b}\right)^4}$$

$$(2.8\text{-}4)$$

35

$$Q_w = \sum_{\substack{m,n \\ = 1,3,\ldots}}^{\infty} \frac{\sin \frac{m\pi x}{\ell} \sin \frac{n\pi y}{b}}{mn \left[D_x \left(\frac{m}{\ell} \right)^4 + 2H \left(\frac{mn}{\ell b} \right)^2 + D_y \left(\frac{n}{b} \right)^4 \right]}$$

(2.8-5)

The stress response spectral density in $(psi)^2$/Hertz is given by

$$S_{\sigma\sigma}(\vec{r},f) = 2\pi\Phi_{\sigma\sigma}(r,\omega)$$

(2.8-6)

The mean-square stress response in $(psi)^2$ is given by

$$\sigma^2(\vec{r}) = \int S_{\sigma\sigma}(\vec{r},f)df$$

(2.8-7)

The root-mean-square stress response in pounds/inch^2 is given by

$$\sigma(\vec{r}) = [\sigma^2(\vec{r})]^{1/2}$$

(2.8-8)

2.9 Average Responses Over the Whole Structure

The average response over the whole structure is obtained by integrating and dividing the result with the area of the structure. Detail derivation of the formulas is given in Reference 5, Section 2.5. The final results are summarized as follows: The average displacement spectral density in inch^2/rad./sec. is

$$\Phi_{ww}(\omega) = S'^2 \Phi_{pp}(\omega) \sum_{j,k} I_x I_y |H_{jk}|^2 J^2_{jkjk}$$

(2.9-1)

where the expressions for I_x and I_y for different boundary conditions are as follows:

2.9-1 Four Edges Simply-Supported Panels

$$I_x = I_y = \frac{1}{2}$$

(2.9-2)

2.9.2 Four Edges Clamped Panels

$$I_x(1) = I_y(1) = \frac{1}{1.5056\pi} \left[(1.5056)\pi - 1 + \frac{1}{2} \sinh 2(1.5056\pi) \right.$$

$$\left. -\sinh^2 (1.5056\pi) - 2 \exp (-1.5056\pi) \right]$$

(2.9-3a)

36

$$I_x = I_x(j) = \frac{1}{(j + \frac{1}{2})\pi}\left[(j + \frac{1}{2})\pi - 1 + \frac{1}{2} \sinh 2 \ (j + \frac{1}{2})\pi \right.$$

$$\left. -\sinh^2 \ (j + \frac{1}{2})\pi - 2(-1)^{j+1} \exp \ [-(j + \frac{1}{2})\pi] \right]$$

$$j = 2, \ 3, \ \ldots \qquad\qquad\qquad (2.9\text{-}3b)$$

$$I_y = I_y(k) = \frac{1}{(k + \frac{1}{2})\pi}\left[(k + \frac{1}{2})\pi - 1 + \frac{1}{2} \sinh 2 \ (k + \frac{1}{2})\pi \right.$$

$$\left. -\sinh^2 \ (k + \frac{1}{2}) - 2(-1)^{k+1} \exp \ [-(k + \frac{1}{2}) \ ] \right]$$

$$k = 2, \ 3, \ \ldots \qquad\qquad\qquad (2.9\text{-}3c)$$

2.9-3 Two opposite edges simply-supported while other two clamped panels

$$I_x = \frac{1}{2} \qquad\qquad\qquad (2.9\text{-}4)$$

$I_y(k)$ is given by Equations (2.9-3a) and (2.9-3c)

2.10 One-nth Octave Frequency Increment and Number of Data Points

In the calculation of the response spectrum as a function of frequency, uniform frequency increment is not convenient, because when the spectrum is plotted with the frequency in logarithmic scale, the points will be too close in high frequency and too separated in low frequency. In order to obtain good plots and save computer time, it is the most convenient to use one-nth octave frequency increment in the calculation.

The interval from frequency f_1 to f_2 will be one-nth octave if

$$\left(\frac{f_2}{f_1} \right)^n = 2 \qquad\qquad\qquad (2.10\text{-}1a)$$

or $\qquad f_2 = 2^{1/n} f_1 \qquad\qquad\qquad (2.10\text{-}1b)$

The bandwidth of the one-nth octave band expressed in terms of the lower limit f_1 is:

$$\Delta f = f_2 - f_1 = (2^{1/n} - 1) \ f_1 = D_n' f_1 \qquad\qquad\qquad (2.10\text{-}1c)$$

where

$$D_n' = 2^{\frac{1}{n}} - 1 \tag{2.10-1d}$$

The geometric mean frequency of f_1 and f_2 is

$$f = (f_1 f_2)^{1/2} \tag{2.10-2}$$

Solving equations (2.10-1a) and (2.10-1b) gives the lower and the upper limits of the one-nth octave band in terms of the geometric mean frequency:

$$f_1 = (2)^{-\frac{1}{2n}} f$$

$$f_2 = (2)^{\frac{1}{2n}} f \tag{2.10-3b}$$

Therefore the band-width of the one n-th octave band is

$$\Delta f = f_2 - f_1 = D_n f \tag{2.10-3c}$$

where the one n-th octave band width constant is given by

$$D_n = 2^{\frac{1}{2n}} - 2^{-\frac{1}{2n}} \tag{2.10-3d}$$

The values of D_n' and D_n for n from 1 through 50 are as follows. Note that when n equals to 1, 2, and 3, the values of D_n' and D_n are the corresponding one-octave, one-half-octave and one-third-octave band width constants.

Value of n	Value of $D' = 2^{1/n} - 1$	Value of $D = 2^{1/2n} - 2^{-1/2n}$
1	1.	0.707107
2	0.41421	0.348311
3	0.25992	0.231563
4	0.18920	0.173504
5	0.14869	0.138740
6	0.12246	0.115588
7	0.10409	0.0990615
8	0.09050	0.0866705
9	0.08006	0.0770354
10	0.07177	0.0693286
11	0.06504	0.0630238
12	0.05946	0.0577703
13	0.05476	0.0533253
14	0.05075	0.0495156
15	0.04729	0.0462139
16	0.04427	0.0433251
17	0.04161	0.0407762
18	0.03925	0.0285106
19	0.03715	0.0364835
20	0.03526	0.0346591
21	0.03355	0.0330085
22	0.03200	0.0315080
23	0.03059	0.0301380
24	0.02930	0.0288821
25	0.02811	0.0277268
26	0.02701	0.0266603
27	0.02600	0.0256728
28	0.02506	0.0247559
29	0.02419	0.0239022
30	0.02337	0.0231054
31	0.02261	0.0223601
32	0.02189	0.0216613
33	0.02122	0.0210048
34	0.02059	0.0203870
35	0.02000	0.0198045
36	0.01944	0.0192544
37	0.01891	0.0187340
38	0.01840	0.0182410
39	0.01793	0.0177732
40	0.01748	0.0173289
41	0.01705	0.0169062
42	0.01664	0.0165037
43	0.01625	0.0161199
44	0.01587	0.0157535
45	0.01552	0.0154034
46	0.01518	0.0150686
47	0.01485	0.0147479
48	0.01454	0.0144407
49	0.01424	0.0141460
50	0.01395	0.0138631

When the one nth octave bandwidth is used for frequency increments, the expression for the number of data points can be derived as follows.

By definition of the one-nth octave band, the number of band between frequencies f and 2f is n. Hence for the geometric series

$$f_o = f_o$$

$$f_1 = 2f_o$$

$$f_2 = 2^2 f_o \qquad (2.10\text{-}4a)$$

$$\text{-----------}$$

$$f_j = 2^j f_o$$

between each consecutive pair of frequencies, there are n bands. Therefore the total number of data points is

$$i = nj + 1 \qquad (2.10\text{-}4b)$$

But

$$2^j = \frac{f_i}{f_o}$$

or

$$j = \frac{\log \dfrac{f_i}{f_o}}{\log 2}$$

Substituting into Equation (2.10-4b) gives

$$i = n \frac{\log \dfrac{f_j}{f_o}}{\log 2} \qquad (2.10\text{-}4c)$$

When the result of Equation (2.10-4c) is not an integer, it should be increased to the next integer. Equation (2.10-4c) is very convenient for hand calculation to determine the number of data points. For example

$$n = 33$$

$$f_o = 5$$

$$f_j = 5000$$

Substituting into Equation (2.10-4c) gives the number of data points

$$i = 33 \frac{\log \frac{5000}{5}}{\log 2} + 1 = 331$$

III. ANALYSES OF THE RESULTS

3.1 Effect of Boundary Conditions

For a typical run (Run No. 8010) of the Program RANDOM with input data described in Section 5.7, the frequency of the fundamental mode, the displacement, the stress and the acceleration spectral densities at fundamental mode, the root-mean-square displacement, stress, and acceleration at the center of the panel for the three boundary conditions are as follows:

Boundary Condition	Fundamental Mode Frequency in Hertz	Displacement Spectral Density at Fundamental Mode in in.^{2}/Hertz	Stress Spectral Density at Fundamental Mode in (psi)^2/Hertz	Acceleration Spectral Density at Fundamental Mode in g^2/Hertz
SSSS	148.0	0.48339292E-05	7304.0415	24.259805
CCCC	215.2	0.37594843E-05	5680.5610	84.278543
SCSC	206.4	0.18984536E-05	2868.5533	36.038467

Here

SSSS = Four edges simply-Supported

CCCC = Four edges clamped

SCSC = Two opposite edges simply-supported while other two clamped

Boundary Condition	RMS Displacement in inch	RMS Stress in psi	RMS Acceleration in g	RMS Excitation psi
SSSS	0.010248574	398.37757	23.549822	0.22680647
CCCC	0.011197214	435.25270	49.516272	0.22680647
SCSC	0.0078521891	305.22652	34.075105	0.22680647

It is interesting to note the following results from the effect of the boundary conditions:

(1) The more rigid the boundary condition, the higher the natural frequency. Hence, the four edges clamped panel has the highest frequency, the SCSC panel next and the four edges simply-supported panel has the lowest frequency.

(2) The more rigid the boundary condition, the less the displacement and the stress spectral densities at resonance. The panel with four edges clamped has the least displacement and stress spectral densities at the fundamental mode, the SCSC panel next, and the panel with four edges simply-supported has the largest. This conforms to common sense reasoning.

42

(3)   The four edges clamped panel has the largest acceleration spectral
density at the fundamental mode and the largest root-mean-square acceleration,
the SCSC panel has the second largest, while the four edges simply-supported
panel has the lowest. This is because that acceleration is proportional to the
square of the frequency, and acceleration spectral density to the fourth power
of the frequency.

(4)   The root-mean-square displacements and stresses for all three cases
are not much different. The four edges clamped panel is 10% higher than the four
edges simply-supported panel. The SCSC panel is 20% lower than the four edges simply-
supported panel.

The plots of the response spectral densities are shown in Figures 2 through
10.

3.2   Contribution of Each Mode

The contribution of each mode to the responses can be estimated from the
response spectral density at each mode and the half-power bandwidth at each fre-
quency. The contributions of each mode to the mean-square displacement and
acceleration are given respectively by

$$w_i^2 \quad = \quad B_i S_{ww} \tag{3.2-1a}$$

$$G_i^2 \quad = \quad B_i S_{\ddddot{w}\ddddot{w}}$$

where

$w_i^2 \quad = \quad$ contribution of the ith mode to the mean-square
displacement

$G_i^2 \quad = \quad$ contribution of the ith mode to the mean-square
acceleration

$S_{ww} \quad = \quad$ displacement spectral density at the ith mode

$S_{\ddddot{w}\ddddot{w}} \quad = \quad$ acceleration spectral density at the ith mode

The half-power bandwidth of the ith mode is given by

$$B_i \quad = \quad 2\zeta_i f_i \tag{3.2-2}$$

where

$\zeta_i \quad = \quad$ damping ratio at the ith mode

$f_i \quad = \quad$ frequency of the ith mode

Here in the typical test run described in Sections 3.1 and 5.7, the damping
ratio for all modes is

$$\zeta \quad = \quad 0.04$$

43

The contributions of the fundamental mode to the mean-square displacement and acceleration are calculated as follows:

Boundary Condition	Bandwidth At Fundamental Mode in Hertz	Fundamental Mode Contribution to M.S. Displacement in $inch^2$	Fundamental Mode Contribution to M. S. Acceleration in g^2	% of M.S. Displacement Contributed by Fundamental Mode	% of M.S. Acceleration Contributed by Fundamental Mode
SSSS	11.85	$57.\ 2 \times 10^{-6}$	288.5	54.5	52
CCCC	17.22	$64.\ 7 \times 10^{-6}$	1453	51.8	59
SCSC	16.55	$31.\ 41 \times 10^{-6}$	597	51.0	49

From the above results, it is seen that the contribution of the fundamental mode to the mean-square response amounts to approximately 50% of the total mean-square value for both the displacement and the acceleration.

It is to be noted that when the mean-square value contributed by the fundamental mode is used to estimate the root-mean-square response, the result will amount to

$$(0.50)^{1/2} = 0.706 = 70.6\%$$

of the actual root-mean-square response for both the displacement and the acceleration. The detail values for each boundary condition are tabulated as follows:

Boundary Condition	RMS Displacement Estimated from Fundamental Mode in inch	RMS Acceleration Estimated from Fundamental Mode in g	Estimate Amounts to % of Total rms Displacement	Estimate Amounts to % of Total rms Acceleration
SSSS	0.00757	16.95	73.8	72
CCCC	0.00804	38.1	71.8	76.8
SCSC	0.0056	24.4	71.3	70

It is seen that the estimation of the root-mean-square response by the principal mode yields a result approximately 28% lower both in displacement and acceleration.

The contributions of the (3,1) mode to the mean-square displacement and acceleration are estimated as follows:

Boundary Condition	(3,1) Mode Frequency in Hertz	Displacement Spectral Density At (3,1) Mode in in^2/Hz	Acceleration Spectral Density at (3,1) Mode in g^2/Hz
SSSS	571.6	9.848×10^{-10}	1.099
CCCC	764.7	5.254×10^{-10}	1.879
SCSC	548.4	3.528×10^{-10}	3.335

Boundary Condition	Bandwidth at (3.1) Mode in Hertz	(3,1) Mode Contribution to M.S. Displacement in inch^2	(3,1) Mode Contribution to M.S. Acceleration in g^2	% of M.S Displacement Contributed by (3,1) Mode	% of M.S. Acceleration Contributed by (3,1) Mode
SSSS	45.7	45×10^{-9}	50.2	0.0428	9
CCCC	61.2	32.3×10^{-9}	115	0.0289	4.67
SCSC	43.9	156×10^{-9}	146	0.252	12.6

It is seen that the higher mode contributes more to the acceleration than to the displacement response.

3.3 Contribution of the Cross-Terms

In the expression for the displacement spectral density, the summation may be separated into two groups of terms - the main terms and the cross terms as follows:

$$\Phi_{ww}(\vec{r},\omega) = S'^2 \Phi_{pp}(\omega) \sum_{\substack{j,k,m,n \\ j=m,k=n}} F_{jk}(\vec{r}) \, F_{mn}(\vec{r}) \, |H_{jk}| \, |H_{mn}| J^2_{jkmn}(\omega)$$

$$+ \, S' \Phi_{pp}(\omega) \sum_{\substack{j,k,m,n \\ j \neq m \\ k \neq n}} F_{jk}(\vec{r}) \, F_{mn}(\vec{r}) \, |H_{jk}| \, |H_{mn}| J^2_{jkmn}(\omega) \qquad (3.3-1)$$

where

$\Phi_{ww}(\vec{r},\omega)$ = displacement spectral density at any point $\vec{r}$ as function of frequency ω

S'^2 = area of structure subjected to excitation

45

$\Phi_{pp}(\omega)$ = Homogeneous spectral density of the excitation pressure

F_{jk}, F_{mn} = normal modes

$|H_{jk}|, |H_{mn}|$ = magnitudes of the frequency response function

J^2_{jkmn} = joint acceptance of the jk and mn modes combination as function of frequency

It is generally true that the cross terms contribute only a small portion of the total displacement. This is because $|H_{jk}||H_{mn}|$ is much smaller than $|H_{jk}|^2$. As to how small the summation of the cross-terms is and how it affects the spectrum of the response, there is limited information available in the literature.

Program RSRPC3 is a modification of Program RSRPC1 designed to study the contribution of the cross-terms and their effect on the response spectrum. Typical results of this program are given in the following. The input data for these results are the same as those of Section 5.7 except the radius of curvature is 70 inches instead of 100 inches. The fundamental mode frequency is 216.92 Hertz. Data in item 1 are the results of summation of all the terms while data in item 2 are the results of the summation of the main terms only. The range of the index j,k,m,n is from 1, 2,... to 5. That is $5^4 = 625$ terms are summed for each frequency to obtain the spectral density. The plots of the displacement and acceleration responses for four locations are shown in Figures 11 to 34. It is seen that the cross-terms contribute not very much to the response but affect the response spectrum to some degree. It is to be noticed that the cross-terms sums up to positive values in some locations and negative in other locations.

a. Location: Center of Panel $x = \dfrac{\ell}{2} = 23.75$ inches

$y = \dfrac{b}{2} = 29.187$ inches

Run No. 4220 Frequency Increment n = 33

Item	Displacement Spectral Density at Fundamental Mode in inch^2/Hertz	Stress Spectral Density at Fundamental Mode in (psi)^2/Hertz	Acceleration Spectral Density at Fundamental Mode in g^2/Hertz	Excitation Spectral Density at Fundamental Mode in (psi)^2/rad. per sec.
1	0.22309226E-05	3072.8148	50.011887	0.14171840E-04
2	0.22350181E-05	3078.4558	50.103698	0.14171840E-04

46

Item	RMS Displacement in inch	RMS Stress in psi	RMS Acceleration in g	RMS Excitation in psi
1	0.86932536E-02	322.63266	39.575629	0.090482687
2	0.87852818E-02	326.04810	39.582969	0.090482687

b.   Location $x = \dfrac{\ell}{4} = 11.87$ Inches

$y = \dfrac{b}{4} = 14.594$ Inches

Run No.   4519   Frequency Increment   n = 33

Item	Displacement Spectral Density at Fundamental Mode in $inch^2$/Hertz	Stress Spectral Density at Fundamental Mode in $(psi)^2$ Hertz	Acceleration Spectral Density at Fundamental Mode in g^2/Hertz	Excitation Spectral Density at Fundamental Mode in $(psi)^2$/rad per sec.
1	0.56087514E-06	938.52039	125.73464	0.14171840E-04
2	0.55967865E-06	936.51828	125.46641	0.14171840E-04

Item	RMS Displacement in inch	RMS Stress in psi	RMS Acceleration in g	RMS Excitation in psi
1	0.0045961768	188.01195	25.549804	0.090482687
2	0.00453378169	185.62468	25.572445	0.090482687

Note: For frequency increment n = 33, the peak of the response spectrum occurs at 215.2 Hertz.

c.   Location $x = \dfrac{\ell}{2} = 23.75$ Inches

$y = \dfrac{b}{4} = 14.595$ Inches

Run No.   6520   Frequency Increment   n = 50

Item	Displacement Spectral Density at Fundamental Mode in $inch^2$/Hertz	Stress Spectral Density at Fundamental Mode in $(psi)^2$/Hertz	Acceleration Spectral Density at Fundamental Mode in g^2/Hertz	Excitation Spectral Density at Fundamental Mode in $(psi)^2$/rad per sec
1	0.11141607E-05	1644.1638	26.010334	0.14039524E-04
2	0.11142897E-05	1644.3542	26.013345	0.14039524E-04

Item	RMS Displacement in inch	RMS Stress in psi	RMS Acceleration in g	RMS Excitation in psi
1	0.0062653206	240.68110	28.105585	0.090482687
2	0.0062120453	238.63453	28.061311	0.090482687

d.   Location: $x = \dfrac{\ell}{4} = 11.87$ Inches

$y = \dfrac{b}{2} = 29.187$ Inches

Run No.   7412   Frequency Increment n = 50

Item	Displacement Spectral Density at Fundamental Mode in $inch^2$/Hertz	Stress Spectral Density At Fundamental Mode in $(psi)^2$/Hertz	Acceleration Spectral Density at Fundamental Mode in g^2/Hertz	Excitation Spectral Density at Fundamental Mode in $(psi)^2$/rad per sec.
1	0.11158915E-05	1670.4033	26.050740	0.14039524E-04
2	0.11161287E-05	1670.7584	26.056278	0.14039524E-04

Item	RMS Displacement in inch	RMS Stress in psi	RMS Acceleration in g	RMS Excitation in psi
1	0.0063428457	245.40528	36.238683	0.090482687
2	0.0064173551	248.28806	36.224862	0.090482687

Note: For frequency increment n = 50, the peak of the response spectrum
         ocurrs at 217.4 Hertz

48

3.4   Average Responses Over the Whole Structure

The formulations for the average responses over the whole structure are given in Section 2.9. The 4-series programs, RSRPC4, RFRPC4, and RSFRP4, are written to calculate the average responses over the complete structure as well as those at any local point. The input data for these programs are the same as those for the 1-series program and Program RANDOM (see Section 5.7). Following are the results of typical runs of Program RSRPC4 with input data described in Section 5.7. Data in item 1 are the local response at local point of the panel and those in item 2 are the average responses over the whole panel. Typical plots of average response spectral densities are shown in Figures 35 through 46, with plots of responses at a local point for comparison.

a.   Local point: $x = \dfrac{\ell}{2} = 23.75$ Inches

$\qquad\qquad\qquad y = \dfrac{b}{2} = 29.187$ Inches

Run No.   8009   Frequency Increment $n = 33$

Radius of curvature $a = 100$ Inches

Fundamental mode Frequency   167.7 Hertz

Item	Displacement Spectral Density at Fundamental Mode in $inch^2$/Hertz	Stress Spectral Density at Fundamental Mode in $(psi)^2$/Hertz	Acceleration Spectral Density at Fundamental Mode in g^2/Hertz	Excitation Spectral Density at Fundamental Mode in $(psi)^2$/rad. per sec.
1	0.93176196E-05	12833.847	77.012151	0.16478916E-04
2	0.23318242E-05	3211.794	19.27303	0.16478916E-04
Ratio of Item 2 to 1	0.25	0.25	0.25	

Item	RMS Displacement in inch	RMS Stress in psi	RMS Acceleration in g	RMS Excitation in psi
1	0.15389093E-01	571.13519	43.193045	0.090482687
2	0.78098409E-02	289.84652	25.131164	0.090482687
Ratio of Item 2 to 1	0.507	0.507	0.58	

49

For this particular case, it is seen that the root-mean-square responses at the center of the panel are approximately twice the average responses over the whole panel.

b. Local Point: $x = \frac{\ell}{2} = 23.75$ inches

$y = \frac{b}{4} = 14.595$ inches

Run No. 6072   Frequency Increment n = 33

Radius of curvature a = 70 Inches

Fundamental Mode Frequency : 215.2 Hertz

Item	Displacement Spectral Density at Fundamental Mode in inch^2/Hertz	Stress Spectral Density at Fundamental Mode in $(\text{psi})^2$/Hertz	Acceleration Spectral Density at Fundamental Mode in g^2/Hertz	Excitation Spectral Density at Fundamental Mode in $(\text{psi})^2$/rad.per sec.
1	0.11195455E-05	1652.1102	25.097502	0.14171840E-04
2	0.55951962E-06	825.23883	12.536351	0.14171840E-04
Ratio	0.501	0.501	0.501	

Item	RMS Displacement in inch	RMS Stress in psi	RMS Acceleration in g	RMS Excitation in psi
1	0.62654106E-02	240.68455	28.105819	0.090482687
2	0.44660961E-02	171.56422	23.146045	0.090482687
Ratio	0.712	0.712	0.822	

c. Local Point: $x = \frac{\ell}{4} = 11.87$ inches

$y = \frac{b}{2} = 29.187$ inches

Run No. 6654   Frequency Increment n = 33

Radius of Curvature a = 70 inches

Fundamental Mode Frequency: 215.2 Hertz

Item	Displacement Spectral Density at Fundamental Mode in $inch^2$/Hertz	Stress Spectral Density at Fundamental Mode in $(psi)^2$/Hertz	Acceleration Spectral Density at Fundamental Mode in g^2/Hertz	Excitation Spectral Density at Fundamental Mode in $(psi)^2$/rad. per sec.
1	0.11169505E-05	1671.9886	25.039328	0.14171840E-04
2	0.55961962E-06	837.10857	12.536351	0.14171840E-04
Ratio	0.501	0.501	0.501	

Item	RMS Displacement in inch	RMS Stress in psi	RMS Acceleration in g	RMS Excitation in psi
1	0.63429322E-02	245.40861	36.238836	0.090482687
2	0.4460961E-02	172.79365	23.146045	0.090482687
Ratio	0.704	0.704	0.639	

Comparisons of the average responses over the whole panel and the responses at several local points for several panel configurations and subjected to different spectra of excitation pressure have been investigated. The results can be summarized as follows:

- The ratio of the average response over the whole panel to the local response at a certain point is affected by many factors — the panel configuration and properties, the excitation spectrum and the position of the local point, etc.

- Because of the relations in the formulations, the ratios of the average response spectral densities to the local ones at a certain point for any frequency should be equal. This can serve as a check for the computation.

- The ratio of the average displacement and stress overall root-mean-square responses to the local ones at a certain point are approximately equal to the square root of the ratio of the average displacement and stress spectral densities at fundamental mode to the local ones. This is an indication that the fundamental mode dominates the overall responses.

- Because of the assumption of linear structure, the ratios of the average displacement and stress to the local ones at a certain point are always the same.

51

3.5 Estimation By Formulas of Single Degree of Freedom

3.5.1 Derivation of Formulas

Since the fundamental mode contributes the most of the response, the responses of a continuous structure subjected to random loading may be estimated by assuming the structure as a single-degree-of-freedom system vibrating at its fundamental frequency. For a single degree of freedom system, it is well known that the following relation holds for the spectral densities of the displacement response and the excitation force:

$$\Phi_{ww}(\omega) = \Phi_{pp}(\omega) |H(\omega)|^2 \qquad (3.5-1)$$

where

$$\Phi_{ww}(\omega) = \text{displacement spectral density}$$

$$\Phi_{pp}(\omega) = \text{excitation spectral density}$$

The square of the magnitude of the frequency response function is given by

$$|H(\omega)|^2 = \frac{1}{m^2[(\omega_o^2 - \omega^2)^2 + (2\zeta\omega_o\omega)^2]} \qquad (3.5-2)$$

where

$$m = \text{mass of the system}$$

$$\omega_o = \text{frequency of the system}$$

$$\omega = \text{independent frequency variable}$$

$$\zeta = \text{damping ratio of the system}$$

By definition, the mean-square displacement is given by

$$w^2 = \int_o^\infty \Phi_{ww}(\omega) d\omega$$

$$= \int_o^\infty \Phi_{pp}(\omega) |H(\omega)|^2 d\omega \qquad (3.5-3)$$

52

When the excitation spectral density is constant for all frequency, the integration in Equation (3.5-3) can be carried to yield the mean-square displacement as

$$w^2 = \frac{\pi \Phi_{pp}}{4 \zeta \omega_o^3 \, m^2} \qquad (3.5\text{-}4)$$

When the excitation spectral density is not constant, Equation (5.3-4) still gives very good approximation of the mean-square displacements.

The half-power bandwidth at the fundamental mode is

$$B_o = 2 \zeta \omega_o \qquad (3.5\text{-}5)$$

The displacement spectral density at resonance can be obtained by setting $\omega = \omega_o$ in Equation (3.5-2) and substituting the result into Equation (3.5-1) as

$$\Phi_{ww}(\omega_o) = \frac{\Phi_{pp}(\omega_o)}{(2 \zeta \omega_o^2 m)^2} \qquad (3.5\text{-}6)$$

The mean-square displacement may also be approximated by the product of the displacement spectral density and the bandwidth at resonant frequency:

$$w^2 = B_o \Phi_{ww}(\omega_o) \qquad (3.5\text{-}7)$$

The acceleration spectral density of the single degree of freedom system will be given by

$$\Phi_{\ddot{w}\ddot{w}}(\omega) = \omega^4 \Phi_{ww}(\omega) = \omega^4 \Phi_{pp}(\omega) |H(\omega)|^2 \qquad (3.5\text{-}8)$$

where

$\Phi_{ww}(\omega)$ is given by Equation (3.5-1).

The acceleration spectral density at resonance can be obtained by setting $\omega = \omega_o$ in Equation (3.5-8):

$$\Phi_{\ddot{w}\ddot{w}}(\omega_o) = \omega_o^4 \, \Phi_{ww}(\omega_o) = \frac{\Phi_{pp}(\omega_o)}{(2 \zeta m)^2} \qquad (3.5\text{-}9)$$

The mean-square acceleration is given by

$$G^2 = \int \Phi_{\ddot{w}\ddot{w}}(\omega)d\omega \tag{3.5-10}$$

In general, the excitation spectral density $\Phi_{pp}(\omega)$ can not be expressed in an analytical form. Hence, the integration in Equation (3.5-10) has to be evaluated numerically. However, approximation to the mean-square acceleration can be obtained by miltiplying the spectral density at resonance with the half-power bandwidth at resonance frequency:

$$G^2 = B_o \Phi_{\ddot{w}\ddot{w}}(\omega)$$

$$= \omega_o \frac{\Phi_{pp}(\omega_o)}{2\zeta m^2}$$

$$= \omega_o^4 w^2 \tag{3.5-11}$$

When these equations are used to estimate the responses of a continuous structure, the fundamental frequency will be used for ω_o, the spectral density of the excitation pressure will be used for Φ_{pp}, the mass per unit area of the structure will be used for m, and the damping ratio for the fundamental mode will be used for ζ.

If only a portion of the structure is subjected to the excitation, the square of the ratio of the area under excitation to the total area may be used to multiply the results to give the responses:

$$\Phi_{ww}(\omega) = \left(\frac{S'}{S}\right)^2 \Phi_{pp}(\omega)|H(\omega)|^2 \tag{3.5-12}$$

$$w^2 = \left(\frac{S'}{S}\right)^2 \int_o^\infty \Phi_{pp}(\omega)|H(\omega)|^2 d\omega \tag{3.5-13}$$

$$w^2 = \left(\frac{S'}{S}\right)^2 \frac{\pi\Phi_{pp}}{4\zeta\omega_o^3 m^2} \tag{3.5-14}$$

$$\Phi_{ww}(\omega_o) = \left(\frac{S'}{S}\right)^2 \frac{\Phi_{pp}(\omega_o)}{(2\zeta\omega_o^2 m)^2} \tag{3.5-15}$$

$$\Phi_{ww}(\omega) = \left(\frac{S'}{S} \right)^2 \frac{\Phi_{pp}(\omega_o)}{(2\zeta m)^2} = \left(\frac{S'}{S} \right)^2 \omega_o^4 \, \Phi_{ww}(\omega_o) \qquad (3.5\text{-}16)$$

$$G^2 = \left(\frac{S'}{S} \right)^2 \frac{\omega_o \Phi_{pp}(\omega_o)}{2\zeta m^2} = \left(\frac{S'}{S} \right)^2 \omega_o^4 \, w^2 \qquad (3.5\text{-}17)$$

3.5.2 Example

As an example to illustrate the application, the above formulas are used to estimate the responses of the panel described in Section 3.4. In this case:

The spectral density of the excitation pressure corresponding to the fundamental frequency is

$$\Phi_{pp} = 1.648 \times 10^{-5} \quad (psi)^2/rad. \text{ per sec.}$$

The fundamental frequency is

$$\omega_o = 167.7 \text{ Hertz} = 1055 \text{ rad/sec.}$$

The damping ratio is

$$\zeta = 0.04$$

The smeared-out mass per square inch is

$$m = \rho h + \rho' h' = 2.51 \times 10^{-4} \times 0.05 + 2.60 \times 10^{-4} \times 0.05$$

$$= 2.555 \times 10^{-5} \quad lbf\text{-}sec^2/in^3$$

The area of the panel is

$$S = b\ell = 58.375 \times 47.5 = 2871 \text{ inch}^2$$

The area of the panel exposed to the excitation pressure is

$$S' = b'\ell' = 50 \times 45 = 2250 \text{ inch}^2$$

55

Substitution of the above values into Equation (3.5-14) gives the mean-square displacement as

$$w^2 = \frac{\pi(1.648 \times 10^{-5})}{4(0.04)(1054)^3(2.555 \times 10^{-5})^2} \cdot \left(\frac{2250}{2871}\right)^2$$

$$= 2.6 \times 10^{-4} \ \text{inch}^2$$

or the root-mean-square displacement is

$$w = (2.6 \times 10^{-4})^{1/2} = 0.0161 \ \text{inch}$$

This agrees very closely with the actual root-mean-square displacement at the center of the panel calculated by Program RSRPC4 which is

$$w = 0.01539 \ \text{inch}$$

Substitution of the above values into Equation (3.5-6) gives the displacement spectral density at the fundamental frequency as

$$\Phi_{ww}(\omega_o) = \frac{1.648 \times 10^{-5}}{(2 \times 0.04 \times 1055^2 \times 2.555 \times 10^{-5})^2} \cdot \left(\frac{-4250}{4571}\right)^2$$

$$= 1.96 \times 10^{-6} \ \text{in.}^2/\text{rad. per sec.} = 12.3 \ \text{in.}^2/\text{Hertz}$$

The actual displacement spectral density at the fundamental frequency calculated by Program RSRPC4 is

$$\Phi_{ww}(\omega_o) = 9.3176 \ \text{in.}^2/\text{Hertz}$$

From Equation (3.5-5) the bandwidth of the fundamental frequency is

$$B_o = 2 \times 0.04 \times 1055 = 84.4 \ \text{rad./sec.}$$

Substituting these values into Equation (3.5-7) gives mean-square displacement as

$$w^2 = 84.4 \times 1.96 \times 10^{-6}$$

$$= 1.655 \times 10^{-4} \text{ inch}^2$$

Hence, the root-mean-square displacement is

$$w = (1.655 \times 10^{-4})^{1/2}$$

$$= 0.01286 \text{ inch}$$

From Equation (3.5-9), the acceleration spectral density at the fundamental frequency is

$$\Phi_{\ddot{w}\ddot{w}}(\omega_o) = 1054^4 (1.96 \times 10^{-6}) = 16.3 \text{ g}^2/\text{rad. per sec.}$$

From Equation (3.5-11), the mean-square acceleration is

$$G^2 = 84.4 \times 16.3 = 1377 \text{ g}^2$$

Hence, the root-mean-square acceleration is

$$G = 37.05 \text{ g}$$

The actual root-mean-square acceleration calculated with Program RSRPC4 is 43.193 g.

3.6   Number of Modes and Modal Density

Analytical expressions for the total number of modes and the modal density are involved. Only approximate solutions to simple cases can be found in the literature. When the natural frequency of a structure have been calculated from the frequency equations, the total number of modes and modal density can be solved easily with the computer.

Let f_{jk} be the frequency of a two dimensional structure as solved from the frequency equations or some other method. Arrange f_{jk} in the ascending order in a single array.

$$f_n \qquad n = 1, 2, \ldots$$

The curve of n versus f_n will give the total number of modes up to any frequency range.

The slope of the n-f curve will yield the modal density as a function of frequency. In the calculation, the slope of the curve is approximated by

$$\frac{dn}{df}\bigg|_{f = f_j} = \frac{\Delta n_j}{\Delta f_j} \qquad (3.6\text{-}1)$$

where

$$\Delta n_j = n_{j+1} - n_j = 1$$

$$\Delta f_j = f_{j+1} - f_j \qquad (3.6\text{-}2)$$

$$j = 1, 2, 3 \ldots$$

The plot of $\Delta n_j / \Delta f_j$ versus f_j gives the variation of modal density as a function of frequency.

Program NFUOP1 is written to investigate the total number of modes and the modal density. Figures 41 and 42 are typical plots of the total number of modes and the modal density. These curves are very useful in the analysis of the dynamic characteristics of the structure. It is seen that the plot of the total number of mode is a rather smooth curve while the modal density curve is not. The peaks in the modal density plot indicate where two frequencies are very close together. Sudden change in plot of the number of modes will imply some peculiar dynamic characteristics of the structure.

3.7 Joint Acceptance and Correlation Coefficients

Because of their influence on the responses and the complexity of the analytical expressions for the joint acceptance and the cross spectral density of the generalized force, Program JAESR1 is specially written to investigate the behavior of these two quantities as a function of the frequency with mode indices as parameter for both correlation functions described in Section 2.3. This program also computes and plots the curves of the correlation coefficient as a function of separation distance with the frequency as parameter. Figures 43 and 44 are typical curves of the exponentially decaying correlation coefficient (Equation 2.3-3). Representative curves of the sinusoidal decaying correlation coefficient (Equation 2.3-4) are shown in Figures 45 and 46. Figures 47 through 52 are typical curves of these quantities for the exponentially decaying correlation. Typical plots of the two quantities for the sinusoidal decaying correlation are shown in Figures 53 through 58. It is noted that J^2_{jkjk} is identical with I_{jkjk}. The curves of these two quantities are more regular for the exponentially decaying correlation than for the sinusoidal decaying correlation.

3.8 Vibro-Acoustic Transfer Function

The vibro-acoustic transfer function at any point of a structure is defined as the ratio of the response to the excitation. When the response and the excitation are expressed in decibel scale, the vibro-acoustic transfer function in decibel scale at any point $\vec{r}$ will be the excitation in decibels minus the response in decibels:

$$T_{\ddot{w}}(\vec{r},f) \quad = \quad S_{\ddot{w}g}(\vec{r},f) - S'_{pp}(f) \qquad\qquad (3.8-1)$$

where

$$T_{\ddot{w}}(\vec{r},f) \quad = \quad$$ Vibro-acoustic transfer function in decibels with excitation pressure referenced 0.00002 Newton/meter^2 and acceleration response referenced g

$$S_{\ddot{w}g}(\vec{r},f) \quad = \quad$$ Acceleration spectral density in decibels referenced g given by Equation (2.7-2b) in Section 2.7

$$S'_{pp}(f) \quad = \quad$$ The spatial homogeneous excitation spectral density in (psi)^2/Hertz given by Equation (2.6-3) in Section 2.6.

Program RSRPC2 is written to investigate the vibro-acoustic transfer function of four edges simply-supported rectangular cylindrical shell panels cross reinforced with ribs and stringers. Typical plots of this program are shown in Figures 59 and 60.

59

IV. COMPARISON OF COMPUTED RESULTS WITH TEST DATA

The developed computer programs have been used in the research project which Chrysler Huntsville Operations was currently conducting for Marshall Space Flight Center under Contract No. NAS8-21425. The object of this project is to develop comparative analysis of acoustic testing techniques and to determine the time for acoustic qualification test at level other than specified levels. Comparison of the computed results with test data shows good agreement.

One of the test specimens in Project NAS8-21425 was a 4 in. x 13 in., 0.2 in. thick aluminum flat plate. The plate is knife-edges supported on four sides and is subjected to high level acoustic pressure until fatigue failure occurs. The input spectrum of the acoustic pressure is shown in Figure 61. The following input data are used in Program RFRPC1 to calculate the responses at six locations of the plate. Figure 62 shows the calculated acceleration spectral density compared with test data at location number 9, the coordinates of which are x = 6.5 inches and y = 1 inch.

Notation In Formulas	Fortran Notation	Definition and Description	Data Used In Test Run
E	E	Young's modulus of panel skin	10×10^6 lbf/in.^{2}
E'	EP	Young's modulus of stiffeners	0
ν	VIP	Poisson's ratio of panel skin	0.3
ρ	RHO	Mass density of panel skin	2.58×10^{-4} lbf-sec^2/in.^{4}
ρ'	RHOP	Mass density of stiffeners	0
ζ_{jk}	CI	Damping ratio of panel	0.065
a	RAD	Radius of panel	∞ inches
ℓ	PL	Axial length of panel	13 inches
b	B	Width of panel	4 inches
ℓ'	PLP	Length of panel subjected to excitation	13 inches
b'	BP	Width of panel subjected to excitation	4 inches
a_1	AL1	Spacing of width-direction stiffeners	∞ inches

Notation In Formulas	Fortran Notation	Definition and Description	Data Used In Test Run
b_1	BL1	Spacing of length-direction stiffeners	∞ inches
h	HS	Thickness of panel skin	0.2 inch
h'	HP	Smeared-out thickness of stiffeners	0 inch
h_2	H2	Largest height of stiffeners at point investigated	0
I_1	AI1	Moment of inertia of one length-direction stiffener with respect to neutral axis	0 inch^4
I_2	AI2	Moment of inertia of one width-direction stiffener with respect to neutral axis	0 inch^4
x	X	Coordinate of $\vec{r}$	6.5 inches
y	Y	Coordinate of $\vec{r}$	1 inch
A_1	A1	Correlation decay constant in axial length-direction	10
A_2	A2	Correlation decay constant in circumferential width-direction	0
c	C	Speed of sound in air	13500 in./sec.
$S_{3r}(f)$	S3RD	One-third octave pressure level spectrum of excitation	See Figure 61
n	FINN	One-nth octave increment	33

V. DESCRIPTION OF THE COMPUTER PROGRAMS

5.1 Program RANDOM

Program RANDOM is a combination of the three main programs RSRPC1, RFRPC1, and RSFRP1 described in the following sections. With this program a single loading of the input data will be sufficient to obtain the responses of a rectangular cylindrical shell panel cross-reinforced with stiffeners and subjected to three different boundary conditions : all edges simply-supported, all edges clamped, and two opposite edges simply-supported with other two clamped. Controls are also provided to run any one of the three boundary conditions.

The input data for this program are (a) the material constants, the geometric dimensions and properties of the shell panel and stiffeners, (b) the one-third octave spectrum of the excitation pressure, (c) the x and y coordinates of the point of interest and, (d) some control constants. (see Section 5.7).

The output data of this program include:

a.   All the input data with nomenclature.

b.   The input one-third octave spectrum of the excitation pressure, this excitation spectrum is also converted into spectral density both in decibel/Hertz and $(psi)^2$/Hertz, tabulated and plotted in graphical forms.

c.   The natural frequencies of the panel both in Hertz and radians/second.

d.   The spectral densities of displacement in $(inch)^2$/Hertz, of stress response in $(psi)^2$/Hertz, of acceleration response in g^2/Hertz and the excitation spectral density in $(psi)2$/rad. per sec. In addition to tabulation, all three response spectral densities are plotted out in graphical forms.

e.   The mean-square and the root-mean-square values of the responses and excitation.

f.   The constants Q_x, Q_y, and Q_w (QX, QY and QW) and the constant γ^2 (GAMMA2) to convert the displacement spectral density into stress spectral density.

g.   Some values of the joint acceptance squared of all combination of modes for the beginning frequency.

5.2 Programs RSRPC1, RSRPC2, RSRPC3 and RSRPC4

These four programs are writen and designed to calculate the responses of the simply-supported cylindrical shell rectangular panel cross-reinforced with ribs and stringers for various specific purposes. The input data for these programs are the same as for Program RANDOM described in Section 5.7. The output data for these four programs are the same as Program RANDOM but with

62

extra output for each individual program.

Program RSRPC1 calculates the spectral densities of the displacement response in (inch)^2/Hertz, the stress response in (psi)^2/Hertz, and the acceleration response in g^2/Hertz. Therefore the output data are identical with Program RANDOM run in the case of all edges simply-supported.

In addition to those as in Program RSRPC1, the output data of Program RSRPC2 include the acceleration spectral density in decibels referenced gravity acceleration (g) and the vibro-acoustic transfer function as a function of frequency. Both the transfer function and the decibel scale acceleration spectral density are also plotted out in graphical forms.

Program RSRPC3 is designed to investigate the contribution of the cross terms to the vibrational responses. Both the responses of all terms summation and cross terms neglected are tabulated and plotted for comparison. Formulations for responses with all terms summation and cross terms neglected and analysis of the results are given in Section 3.3. Typical plots of this program are shown in Figures 11 through 34.

Program RSRPC4 is a modification of Program RSRPC1 and is written to calculate responses at any point of the structure and the average responses over the whole structure. Formulations for the average displacement response over the panel are derived in Section 2.9. Analysis of the results is given in Section 3.4. Typical plots of this program are shown in Figures 35 through 40.

5.3 Program RFRPC1 and RFRPC4

These programs are written to calculate the vibrational responses of the four edges clamped cylindrical shell rectangular panel cross-reinforced with ribs and stringers. The input data for these programs are the same as those for Program RANDOM described in Section 5.7. The output data for these programs are essentially the same as Program RANDOM except Program RFRPC4 also gives the average responses over the whole panel.

Program RFRPC1 calculates and plots the spectral densities of the displacement response in (inch)^2/Hertz, the stress response in (psi)^2/Hertz, and the acceleration response in g^2/Hertz. Therefore, the output data are identical with Program RANDOM run in the case of all edge clamped, except the frequency range can be higher and the frequency increment can be smaller.

Program RFRPC4 is a modification of Program RFRPC1. In addition to the output of Program RFRPC1, Program RFRPC4 calculates the average responses over the whole structure. Formulations for the average responses over the whole panel are derived in Section 2.9.

63

5.4   Programs RSFRP1 and RSFRP4

These programs are written to calculate the vibrational response of the
two opposite edges simply-supported while other two clamped rectangular cylin-
drical shell panel cross-reinforced with ribs and stringers. The input data
for these programs are the same as Program RANDOM described in Section 5.7. The
output data for these programs are the same as Program RANDOM except that Program
RSFRP4 also calculates the average responses over the whole panel.

Program RSFRP1 calculates and plots the spectral densities of the displace-
ment response in (inch)^2/Hertz, the stress response in (psi)^2/Hertz, and the
acceleration response in g^2/Hertz. Therefore, the output data are identical
with Program RANDOM run in the case of two opposite edges simply-supported while
other two clamped, except with higher frequency range and smaller frequency
increment.

Program RSFRP4 is a modification of RSFRP1. In addition to calculating the
local responses at any point of the structure, Program RSFRP4 also calculates and
plots the average responses over the whole panel. Formulations for the average
responses over the whole panel are derived in Section 2.9.

5.5   Program JARSR1

This is a computer program written to study the correlation coefficient as
a function of separation distance, the joint acceptance and the normalized cross
spectral density of the generalized force as a function of frequency for various
correlation functions. The correlation functions investigated and the derivation
of the expressions for the joint acceptance and -the normalized cross spectral
density of the generalized force are given in Sections 2.3 and 2.4. Typical
plots of the correlation coefficients, the joint acceptance and the normalized
cross spectral density of the generalized force are shown in Figures 43 through
58.

5.6   Program NFUOP1

Program NFUOP1 is to calculate the total number of modes and the modal
density. The input data to this program are the material constants, the geo-
metric dimensions and properties of the structure required in the frequency
equations. The output data of this program are the tabulated and plotted number
of modes and the modal density as a function of frequency. Formulations of this
program are given in Section 3.6. Sample results are given in Figures 41 and
42. The analysis of the number of modes and modal density is very useful
in the evaluation of the frequency equations. It enables the structures engineer
to determine the accuracy and the behavior of the frequency equations. This
program can be modified to apply to any structure.

64

5.7 The Input Data

The input data for these programs include: (a) the material constants, the geometric dimensions and properties of the shell panel and the stiffeners, (b) the one-third octave pressure level spectrum and the spatial correlation properties of the excitation pressure field, (c) the coordinates of the point concerned, and (d) some control constants. These are listed as follows:

Notation In Formulas	Fortran Notation	Definition And Descritption	Typical Data Used In Test Run
E	E	Young's modulus of panel skin	10×10^6 lbf/in.^{2}
E'	EP	Young's modulus of stiffeners	12×10^6 lbf/in.^{2}
ν	VIP	Poisson's ratio of panel skin	0.3
ρ	RHO	Mass density of panel skin	2.51×10^{-4} lbf-sec^2/in.^{4}
ρ'	RHOP	Mass density of stiffeners	2.60×10^{-4} lbf-sec^2/in.^{4}
ζ_{jk}	CI	Damping ratio of panel	0.04
a	RAD	Radius of panel	100 inches
ℓ	PL	Axial length of panel (along x-axis)	47.5 inches
b	B	Width of panel (along y-axis)	58.375 inches
ℓ'	PLP	Length of panel subjected to excitation	45 inches
b'	BP	Width of panel subjected to excitation	50 inches
a_1	AL1	Spacing of width-direction stiffeners	11.9 inches
b_1	BL1	Spacing of length-direction stiffeners	14.6 inches
h	HS	Thickness of panel skin	0.1 inch
h'	HP	Smeared-out thickness of stiffeners	0.08 inch
h_2	H2	Largest height of stiffeners at point investigated	1.0 inch

65

Notation In Formulas	Fortran Notation	Definition and Description	Data Used In Test Run
I_1	AI1	Moment of inertia of one length-direction stiffener with respect to neutral axis	0.5 $inch^4$
I_2	AI2	Moment of inertia of one width-direction stiffener with respect to neutral axis.	0.6 $inch^4$
x	X	Coordinate of $\vec{r}$	23.75 inches
y	Y	Coordinate of $\vec{r}$	28.1875 inches
A_1	A1	Correlation decay constant in axial length-direction	10
A_2	A2	Correlation decay constant in circumferential width-direction	0
c	C	Speed of sound in air	13500 in./sec
$S_{3r}(f)$	S3RD	One-third octave pressure level spectrum of excitation	See Figures 63 and 64 and the following table
f	F3RD	Input spectrum frequencies	
n	FINN	One-nth octave increment	33

Note: Refer to Figure 1 for identification of geometrical dimensions.

The one-thrid octave level spectrum of the excitation pressure input data in a typical test run is as follows:

One-3RD Octave Mean Frequency F3RD	One-3RD Octave Level In Decibels S3rd
5.000	129.000
6.300	131.000
8.000	133.000
10.000	135.000
12.500	136.000
16.000	138.000
20.000	139.000
25.000	140.500
31.500	142.000
40.000	143.000
50.000	144.000
63.000	145.000
80.000	145.500
100.00	145.000
125.000	146.500
160.000	146.500
200.000	147.000
250.000	147.000
315.000	146.000
400.000	145.500
500.000	145.500
630.000	144.000
800.000	142.500
1000.000	141.000
1250.000	139.500
1600.000	137.500
2000.000	136.000
2500.000	134.500
3150.000	133.000
4000.000	131.000
5000.000	129.500

Note: Point frequencies can be any discrete frequencies with any increment.

The above spectrum is the preliminary acoustic test specification for components of Saturn IB vehicle in Subzone 7-1 for static firing, (See reference 6, Page 64).

The input data spectrum of the excitation pressure is converted into spectral density in decibels/Hertz, $(psi)^2$/Hertz and $(psi)^2$/rad./sec. by the computer and plotted as in Figures 63 and 64 .

Frequency In Hertz	Spectral Density In Decibels/Hertz SPPF	Spectral Density In PSI SQ/RAD/SEC FIPW
5	128.365	0.95653E-05
6.3	129.361	0.12032E-04
8	130.324	0.15017E-04
10	131.354	0.19040E-04
12.5	131.885	0.21516E-04
16	132.313	0.23744E-04
20	132.344	0.23913E-04
25	132.875	0.27023E-04
31	133.371	0.30294E-04
40	133.334	0.30034E-04
50	133.365	0.30248E-04
63	133.361	0.30222E-04
80	132.824	0.26704E-04
100	132.354	0.23970E-04
125	131.885	0.21516E-04
160	130.813	0.16809E-04
200	130.344	0.15088E-04
250	129.375	0.12071E-04
315	127.371	0.76095E-05
400	125.834	0.53408E-05
500	124.865	0.42727E-05
630	122.361	0.24006E-05
800	119.824	0.13384E-05
1000	117.354	0.75800E-06
1250	114.885	0.42930E-06
1600	111.813	0.21162E-06
2000	109.344	0.11985E-06
2500	106.875	0.67878E-07
3150	104.371	0.38138E-07
4000	101.334	0.18950E-07
5000	98.865	0.10732E-07

68

5.8   The Output Data

The output data of the programs for the responses are as follows:

a.   All the input data.

b.   The excitation spectrum expressed in one-third octave level in decibels, in spectral density in decibels per Hertz, and in $(psi)^2$ per radian per second.

c.   The natural frequencies of the structure both in Hertz and radians per second.

d.   The displacement, the stress, the acceleration and the excitation pressure spectral densities both in tabulations and plots.

e.   The mean-square and the root-mean-square values of the responses and the excitation.

f.   Some values of the joint acceptance.

g.   Other special output and plots for each individual program.

VI. CONCLUSIONS AND RECOMMENDATIONS

6.1 Conclusions

6.1.1 In the calculation of the random structural vibrational responses due to the fluctuating pressure environments by the normal mode approach, the important factors that have to be determined are:

    a. The normal modes

    b. The natural frequencies

    c. The joint acceptance or the cross spectral density of the generalized force which in turn depends on:

        (1) The normal modes

        (2) The correlation properties of the pressure field.

        (3) The spectral density of the excitation pressure.

6.1.2 For simple structures, the determination of the mode shapes and frequencies can be obtained to a certain degree of accuracy. For complex structures, the mode shapes and frequencies are difficult to determine in general.

6.1.3 Except for simple pressure fields, the correlation properties are not easy to determine. Some experiments have been done in this field, but scattering of the test data is tremendous.

6.1.4 Any discrepancy of the factors mentioned in 6.1.1 will affect the accuracy of the computed results.

6.1.5 To develop computer programs for the calculation of this kind of random vibrations, the important tasks are to search or develop the necessary frequency equations, the normal modes, the analytical expressions for the correlation properties and the joint acceptance. The degree of accuracy of the expressions for these quantities must be consistent. When these quantities are incorporated in the formulations of the programs, the requirement of computer time should be moderate as to make them practical for use. Such tasks have been done in this project.

6.1.6 One of the important features of the computer programs developed here is that any shape of the spectrum of the excitation pressure can be input into the programs. Thus, the simulation of the excitation will be as accurate as the spectral analysis of the random pressure.

6.1.7 The discrepancy in the determination of the natural frequencies will affect the response spectrum to some degree while it will not affect the overall mean-square response very much.

6.1.8 It is well known that the determination of the damping properties
of structures is very difficult. By utilization of the developed computer
programs and the results of test data, the damping properties of structures
can be determined. This is another application of these programs.

6.1.9 In the design stage of structures of aerospace vehicles, desk
calculation to estimate the responses is very important. The developed
computer programs are good guides for the designer as to the degree of approxi-
mation that can be obtained by assuming the structure vibrating at its funda-
mental mode and estimating the responses by intelligent use of simple formulas.

6.2   Recommendations for Further Investigation

A study of the random vibration of structures is a very complicated pro-
ject. There are many additional areas not studied in detail during the per-
formance of this project that represent opportunities to extend the field. It
is believed the following recommendations are worthy of further investigations.

6.2.1 When a shell structure is reinforced by ribs and stringers, in
addition to the vibrations of the complete structure as a system, there are
local vibrations of the portions between the stiffeners. Thus the resultant
vibration of any point should be the superposition of the system vibrations
and the local vibrations. The computer programs developed in this project
can be easily modified to account for the local vibrations. When this is done,
the prediction of the structural vibrations will be significantly improved.

6.2.2 In the development of the computer programs, it is found that the
analytical expressions for the joint acceptance are the most complicated to
incorporate into the programs. Further study can be made to derive more
analytical expressions of the joint acceptance for some of the available
correlation functions and structure mode shapes. For the cases analytical
expressions are not practical, numerical integration should be incorporated.

6.2.3 For complex structures, only finite element methods will be
effective for the determination of the mode shapes and frequencies. Tremendous
progress has been made in the stress analysis of structures with the finite
element method. However, little has been done in structural random vibration
with this method. It is believed that application of the finite element method
to random vibrations of structures provides a promising field of research. The
program developed in this project can be adapted to the finite element method
without difficulty.

6.2.4 The vibro-acoustic transfer function is as important to random
vibrations as the impedance to harmonic vibrations. Experimental determination
of the vibro-acoustic transfer functions is expensive. The development of the
2-series programs to calculate the transfer functions at any point of the
structure subjected to any excitation pressure is promising. Further development
in this respect is recommended.

71

6.2.5 In practical applications, it may happen that the average responses over the whole structure are of interest. Formulations for the average responses have been derived for different boundary conditions. Further study in the programs is necessary.

Notation	Description
A_1	Decay constant along x-axis
A_2	Decay constant along y-axis
A_{jkmn}	See equation (2.4-29)
B_i	Half-power bandwidth of ith mode
B_{jkmn}	See equation (2.4-29)
C_{jkmn}	See equation (2.4-29)
$D_n = 2^{1/2n} - 2^{-1/2n}$	One-nth octave bandwidth constant referred to geometric mean frequency
$D'_n = 2^{1/n} - 1$	One-nth octave bandwidth constant referred to lower limit
D_x	Rigidity, equation (2.1-4)
D_y	Rigidity, equation (2.1-4)
E	Young's modulus of panel skin
E'	Young's modulus of stiffeners
$F_{jk}(\vec{r})$	Normal mode
$G(\vec{r})$	Root-mean-square acceleration in g
$G^2(\vec{r})$	Mean-square acceleration in g^2
G_i^2	Mean-square acceleration contributed by the ith mode
H	Rigidity, equation (2.1-4)
H_{jk}	Frequency response function
H_{mn}^*	Conjugate of H_{mn}
I_1	Moment of inertia of one length-direction stiffener with respect to neutral axis
I_2	Moment of inertia of one width-direction stiffener with respect to neutral axis

73

Notation	Description
I_1, I_2	Integrals, equation (2.4-6)
I_x, I_y	Integrals, equation (2.4-5); also different use in equation (2.9-1)
$\tilde{I}_x$, $\tilde{I}_y$	See equations (2.4-7) and (2.4-7a)
I_{jm}	See equation (2.4-22)
I'_{jm}	See equation (2.4-23)
I_{kn}	See equation (2.4-24)
I'_{kn}	See equation (2.4-25)
$\tilde{I}_{xij}$, $\tilde{I}_{yij}$	See equation (2.4-8)
I_{xijk}	See equation (2.4-9)
I_{yijk}	See equation (2.4-10)
I_{jkmn}	Cross spectral density of generalized force
$\tilde{I}_{jkmn}$	Normalized Cross Spectral Density of generalized Force
J^2_{jkmn}	Joint acceptance squared
$K = \dfrac{\omega}{c}$	Wave number
L_a	Excitation overall pressure level in decibels
M	Smeared-out mass per unit area
M_{jk}	Modal mass
Q_x	See equation (2.8-3)
Q_y	See equation (2.8-4)

Notation	Description
Q_W	See equation (2.8-5)
S	Area of panel
S'	Area of panel subjected to excitation
$S_{pp}(f)$	Excitation spectral density in decibels/Hertz
$S'_{pp}(f)$	Excitation spectral density in $(psi)^2$/Hertz
$S_{\ddot{w}g}(\vec{r},f)$	Acceleration spectral density in decibels referenced g
$S_{ww}(\vec{r},f)$	Displacement spectral density in $inch^2$/Hertz
$S_{\ddot{w}\ddot{w}}(\vec{r},f)$	Acceleration spectral density in g^2/Hertz
$S_{\sigma\sigma}(\vec{r},f)$	Stress spectral density in $(psi)^2$/Hertz
$S_{3rd}(f)$	One-third octave excitation pressure level in decibels
$T_{\ddot{w}}(\vec{r},f)$	Vibro-acoustic transfer function in decibels
$X_j(x)$	See equation (2.2-1)
$Y_k(y)$	See equation (2.2-1)
a	Radius of shell
a_1	Spacing of width-direction stiffeners
b	Circumferential width of panel
b'	Width of panel subjected to excitation
b_1	Spacing of length-direction stiffeners
c	Speed of sound in medium
e	Base of natural logarithm
f	Frequency in Hertz

Notation	Description
g	Gravity acceleration
h	Thickness of panel skin
h'	Smeared-out thickness of stiffeners
$h_1 = h + h_2$	Height
h_2	Largest height of stiffeners at $\vec{r}$ (see figure 1)
i	$\sqrt{-1}$; also index
j,k,m,n	Mode indices
ℓ	Axial length of panel
ℓ'	Length of panel subjected to excitation
n	One-nth octave increment
$p(\vec{r})$	Pressure at $\vec{r}$
p_r	Referenced pressure
p_a^2	Overall mean-square pressure in $(psi)^2$
$\vec{r}$	Position vector
$s,\ s'$	Number of divisions
$w(\vec{r})$	Root-mean-square displacement
$w^2(\vec{r})$	Mean-square displacement
x,y	Cartesian coordinates of $\vec{r}$
$\tilde{x}_j,\ \tilde{y}_k$	See equation (2.4-15)
$\phi_{pp}(\vec{r}_1,\vec{r}_2,\omega)$	Cross spectral density
$\Phi_{pp}(\omega)$	Excitation spectral density in $(psi)^2/rad.$ per sec.

Notation	Description
$\Phi_{ww}(\vec{r},\omega)$	Displacement spectral density in $inch^2$/rad. per sec.
$\Phi_{ww}(\omega)$	Average displacement spectral density in $inch^2$/rad. per sec.
$\Phi_{\ddddot{w}\ddddot{w}}(\vec{r},\omega)$	Acceleration spectral density in $(inch/sec^2)^2$/rad. per sec.
$\Phi_{\sigma\sigma}(\vec{r},\omega)$	Stress spectral density in $(psi)^2$/rad. per sec.
$\alpha_1 = A_1 K\ell$	See equation (2.4-13)
$\alpha_2 = A_2 Kb$	See equation (2.4-13)
$\gamma^2(\vec{r})$	Constant to convert displacement spectral density into stress
ζ_{jk}	damping ratio
η	Separation distance along y-axis
$\lambda_1 = K\ell$	See equation (2.4-13)
$\lambda_2 = Kb$	See equation (2.4-13)
ν	Poisson's ratio
ξ	Separation distance along x-axis
ρ	Mass density of panel skin
ρ'	Mass density of stiffeners
$\rho(\vec{r}_1,\vec{r}_2)$	Correlation coefficient
$\sigma(\vec{r})$	Root-mean-square stress in psi
$\sigma^2(\vec{r})$	mean-square stress in $(psi)^2$
ω	frequency in rad/sec.
ω_{jk}	Natural frequency in rad/sec.

VIII. REFERENCES

1.   Powell, Alan, "On the Fatigue Failure of Structure Due to Vibrations
      Excited by Random Pressure Fields", Journal of Acoustical Society of
      America, Volume 30, No. 12, December 1958, Pages 1130-1135.

2.   Lin, Y. K., "Probabilistic Theory of Structural Dynamics", McGraw-
      Hill, 1967.

3.   Lee, T. N., "Computer Program for Prediction of Structural Vibrations
      to Fluctuating Pressure Environments," Monthly Progress Report No. 4,
      Contract No. NAS8-21403, Chrysler Corporation Space Division, Huntsville
      Operations, October 1968.

4.   Lee, T. N., "Computer Program For Prediction of Structural
      Vibrations to Fluctuating Pressure Environments," Monthly Progress
      Report No. 3, Contract No. NAS8-21403. Chrysler Corporation Space
      Division, Huntsville Operations, September 1968.

5.   Lee, T. N., "Computer Program For Prediction of Structural Vibrations
      To Fluctuating Pressure Environments," Monthly Progress Report No. 11,
      Contract No. NAS8-21403, Chrysler Corporation Space Division, Huntsville
      Operations, May 1969.

6.   Sailors, C. W. and Lehner, F.A., "Preliminary Acoustic Test Specifications
      For Components on Saturn IB Vehicle", Technical Report HSM-N02-68,
      Chrysler Space Division, 2 June 1968.

IX. APPENDIX

9.1 Figures
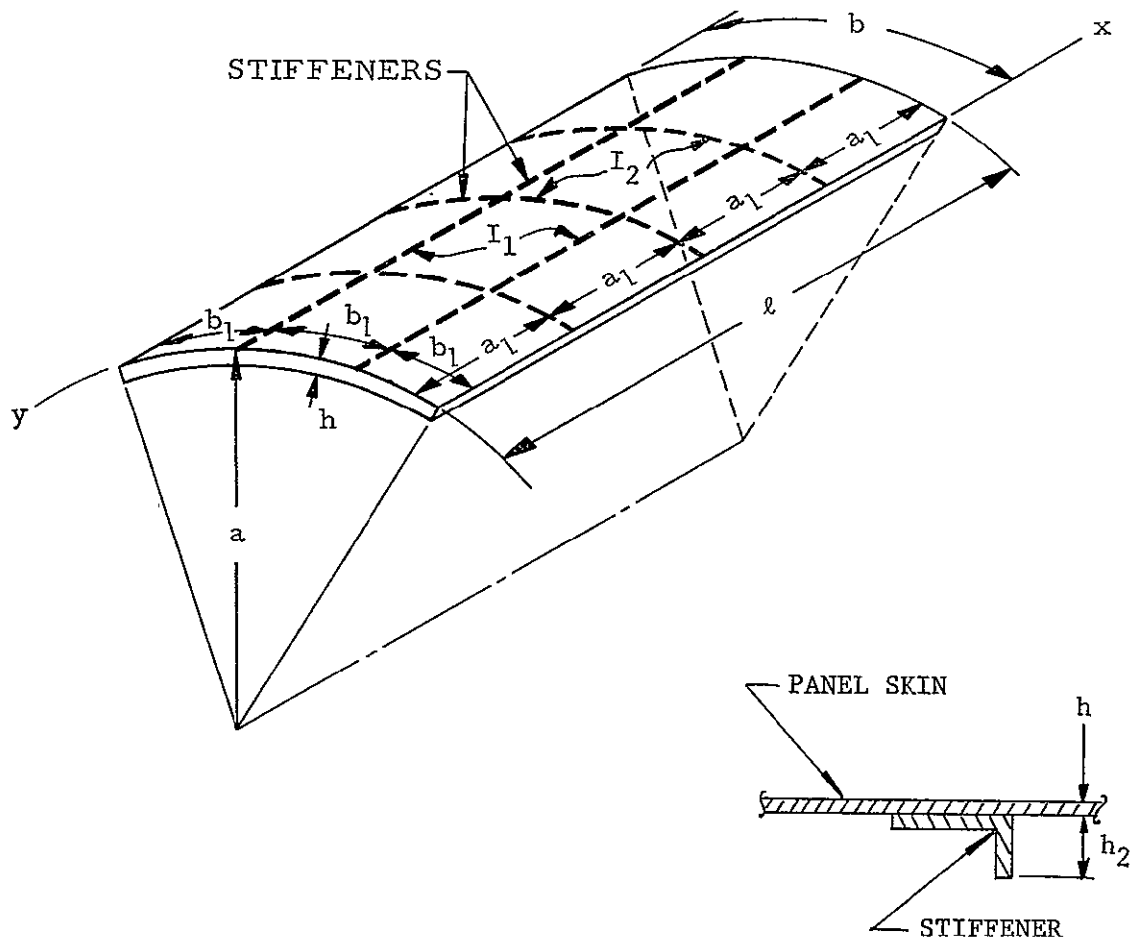
FIGURE 1.   GEOMETRY OF RECTANGULAR CYLINDRICAL SHELL PANEL
            CROSS-REINFORCED WITH STIFFENERS
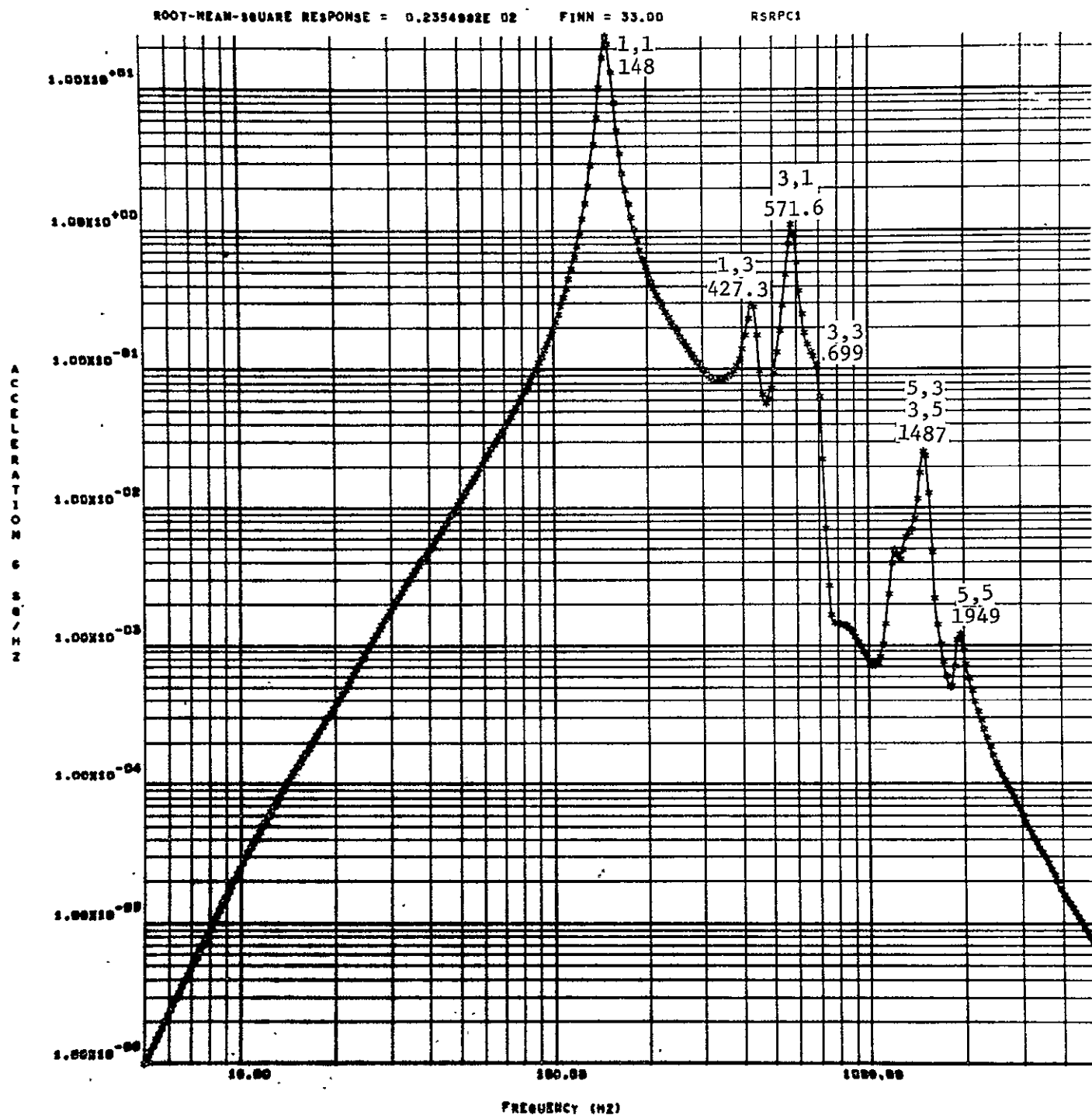
Note: Numbers in parenthesis indicate mode indices and frequencies

FIGURE 2   ACCELERATION SPECTRAL DENSITY AT CENTER OF FOUR EDGES SIMPLY-
SUPPORTED CURVED RECTANGULAR PANEL CROSS-REINFORCED WITH
STIFFENERS

81
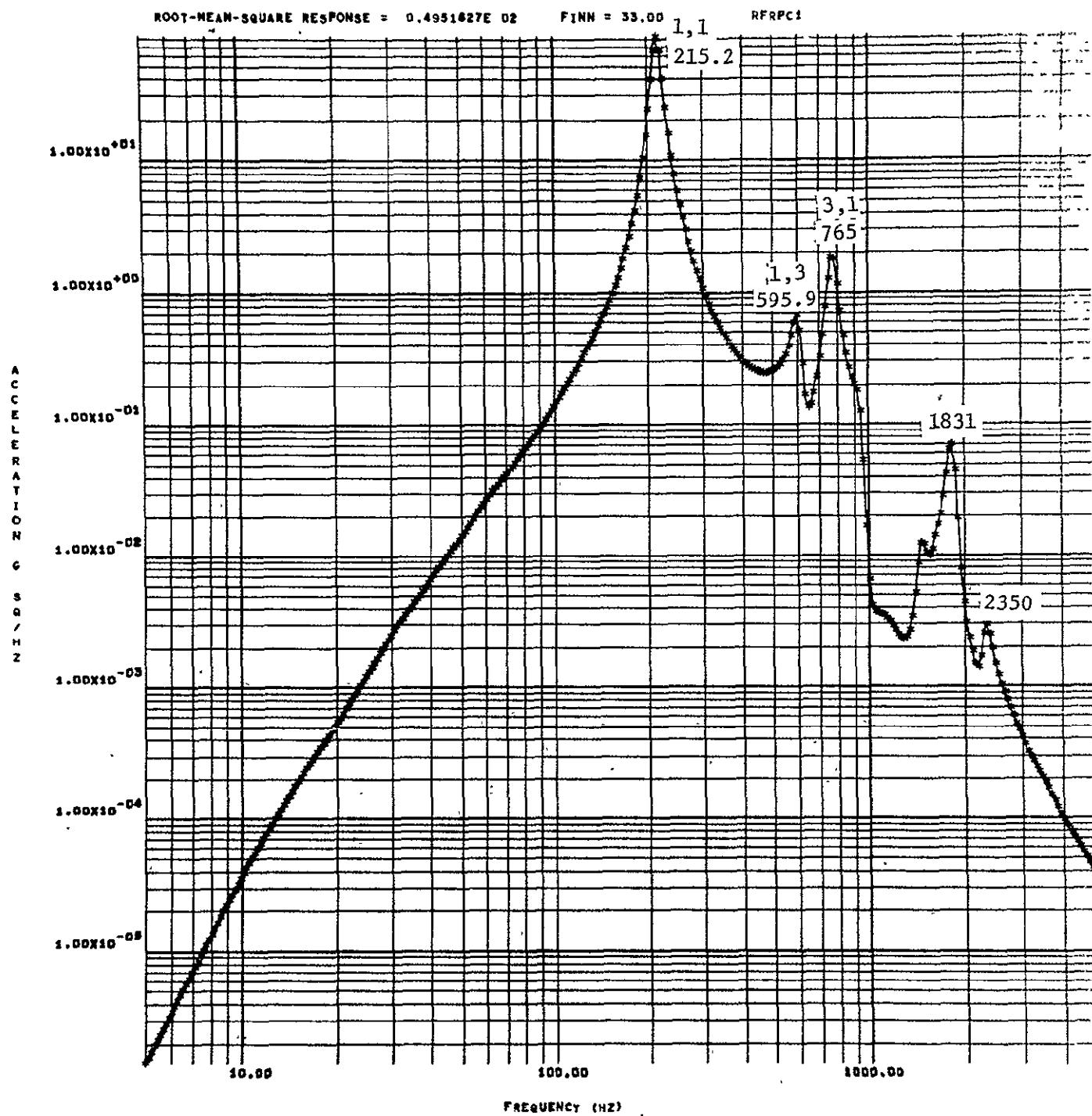
Note: Numbers in parenthesis indicate mode indices and frequencies.

FIGURE 3 ACCELERATION SPECTRAL DENSITY AT CENTER OF FOUR-EDGES CLAMPED
CURVED RECTANGULAR PANEL CROSS-REINFORCED WITH STIFFENER

82

ROOT-MEAN-SQUARE RESPONSE = 0.3407511E 02   FINN = 33.00   RSFRP1

Note: Numbers in parenthesis indicate mode indices and frequencies.

FIUGRE 4   ACCELERATION SPECTRAL DENSITY AT CENTER OF TWO OPPOSITE
EDGES SIMPLY-SUPPORTED AND OTHER TWO CLAMPED CURVED
RECTANGULAR PANEL CROSS-REINFORCED WITH STIFFENERS

ROOT-MEAN-SQUARE RESPONSE = 0.1024857E-01   FINN = 33.00   RSRPC1
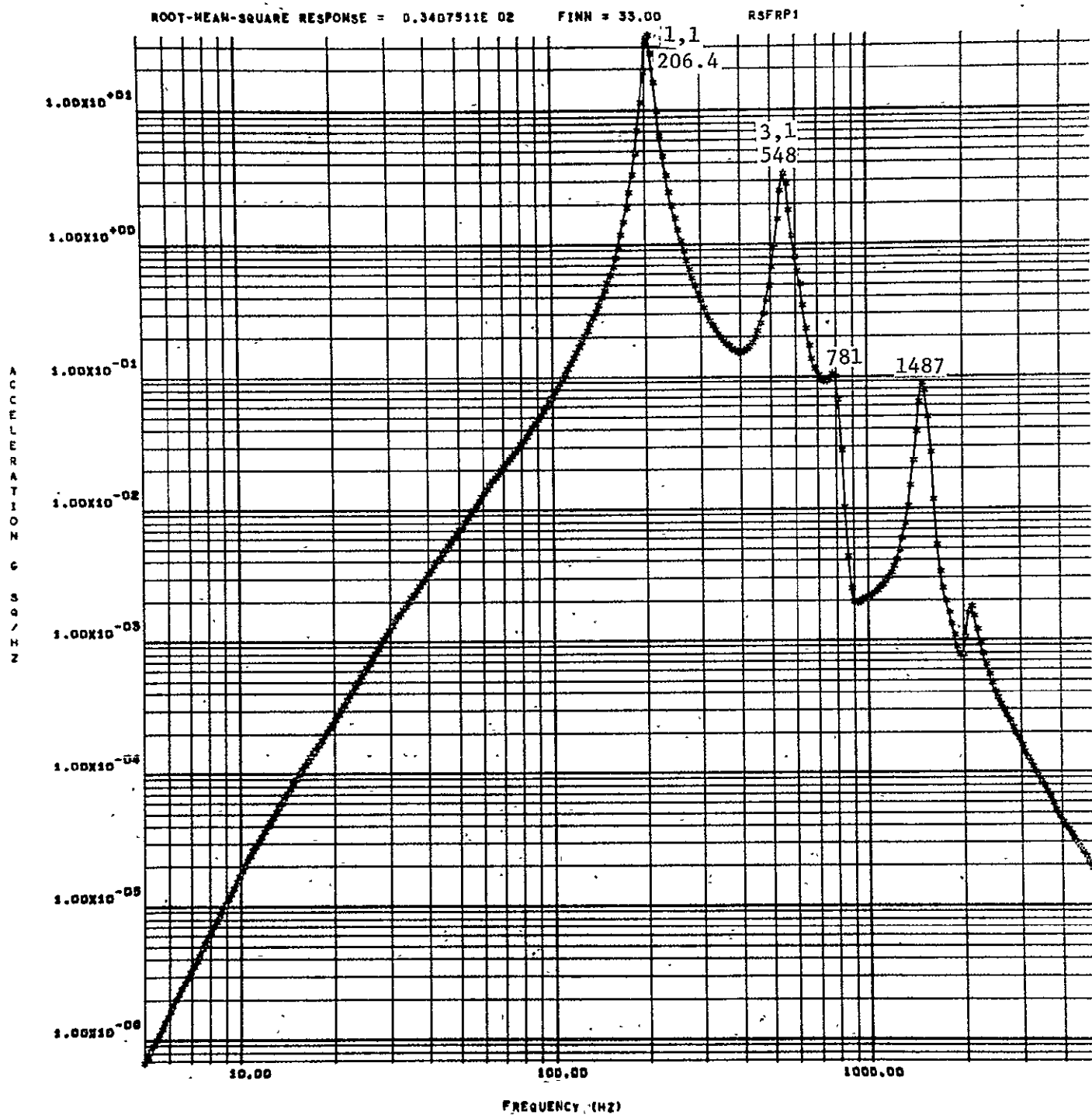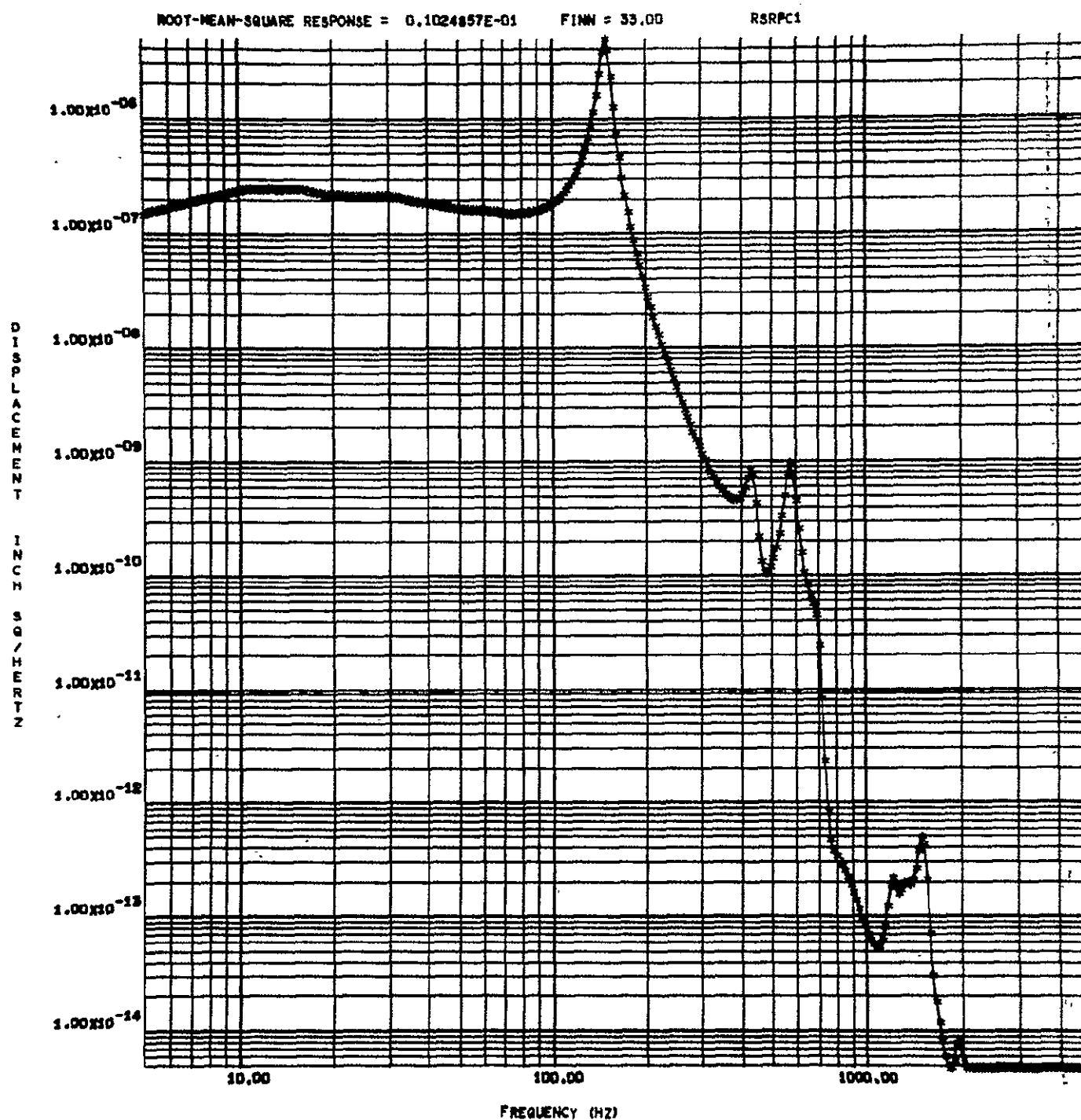
FIGURE 5   DISPLACEMENT SPECTRAL DENSITY AT CENTER OF FOUR
EDGES SIMPLY-SUPPORTED CURVED RECTANGULAR PANEL
CROSS-REINFORCED WITH STIFFENERS
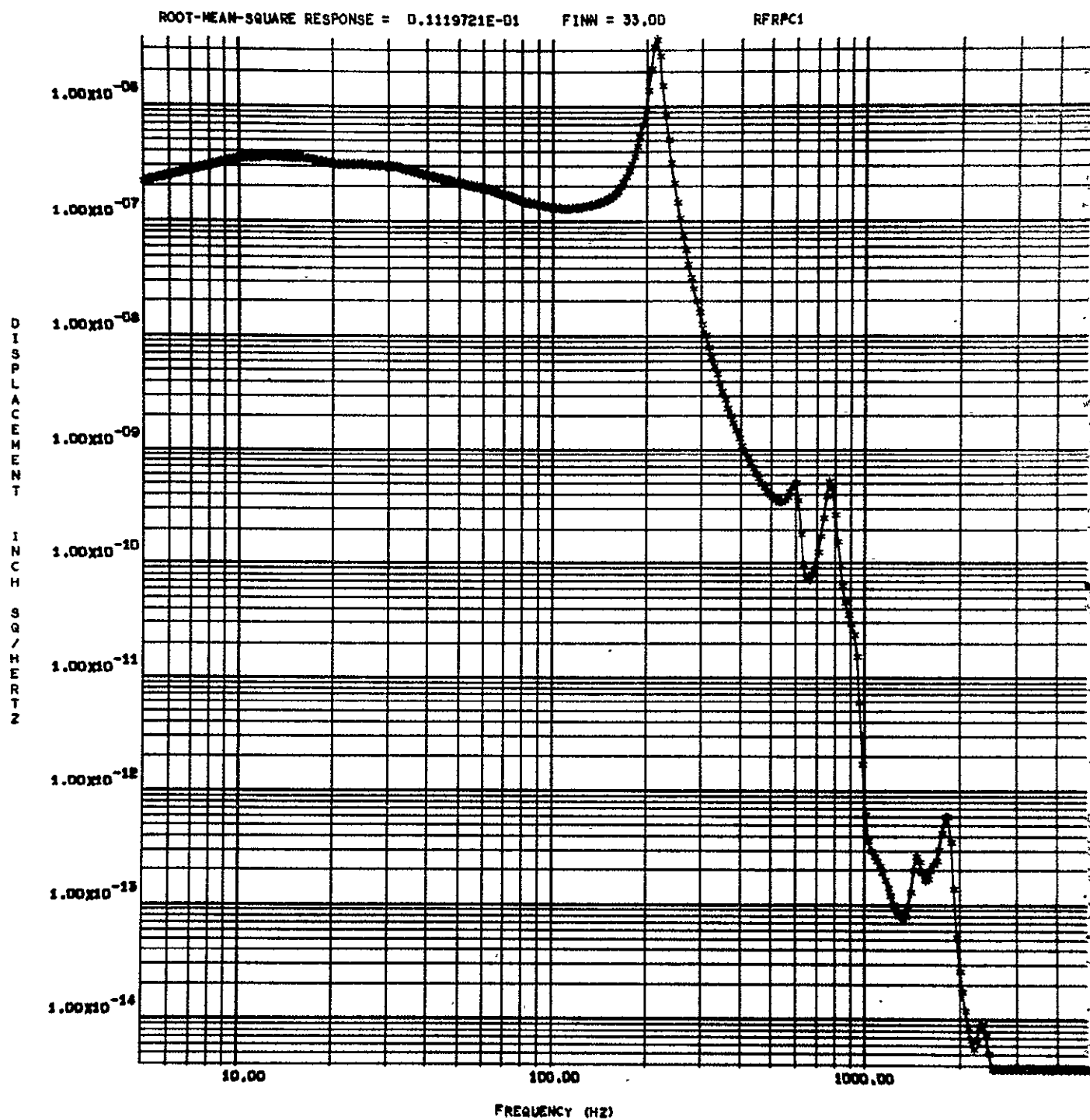
FIGURE 6   DISPLACEMENT SPECTRAL DENSITY AT CENTER OF FOUR EDGES
CLAMPED CURVED RECTANGULAR PANEL CROSS-REINFORCED
WITH STIFFENERS

85

ROOT-MEAN-SQUARE RESPONSE = 0.3052265E 03   FINN = 33.00   RSFRP1
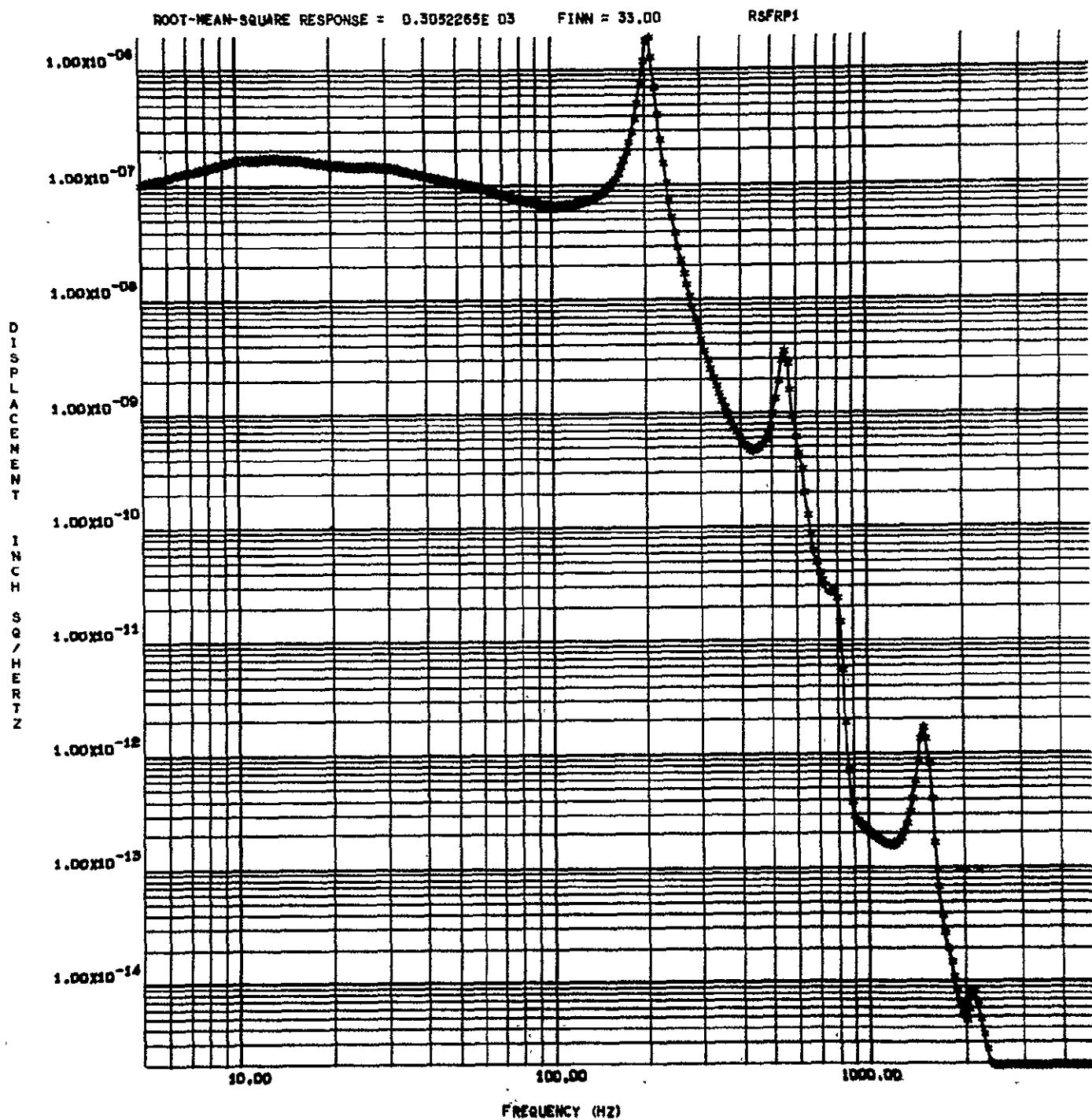
FIGURE 7   DISPLACEMENT SPECTRAL DENSITY AT CENTER OF TWO OPPOSITE
EDGES SIMPLY-SUPPORTED AND OTHER TWO CLAMPED CURVED
RECTANGULAR PANEL CROSS-REINFORCED WITH STIFFENERS
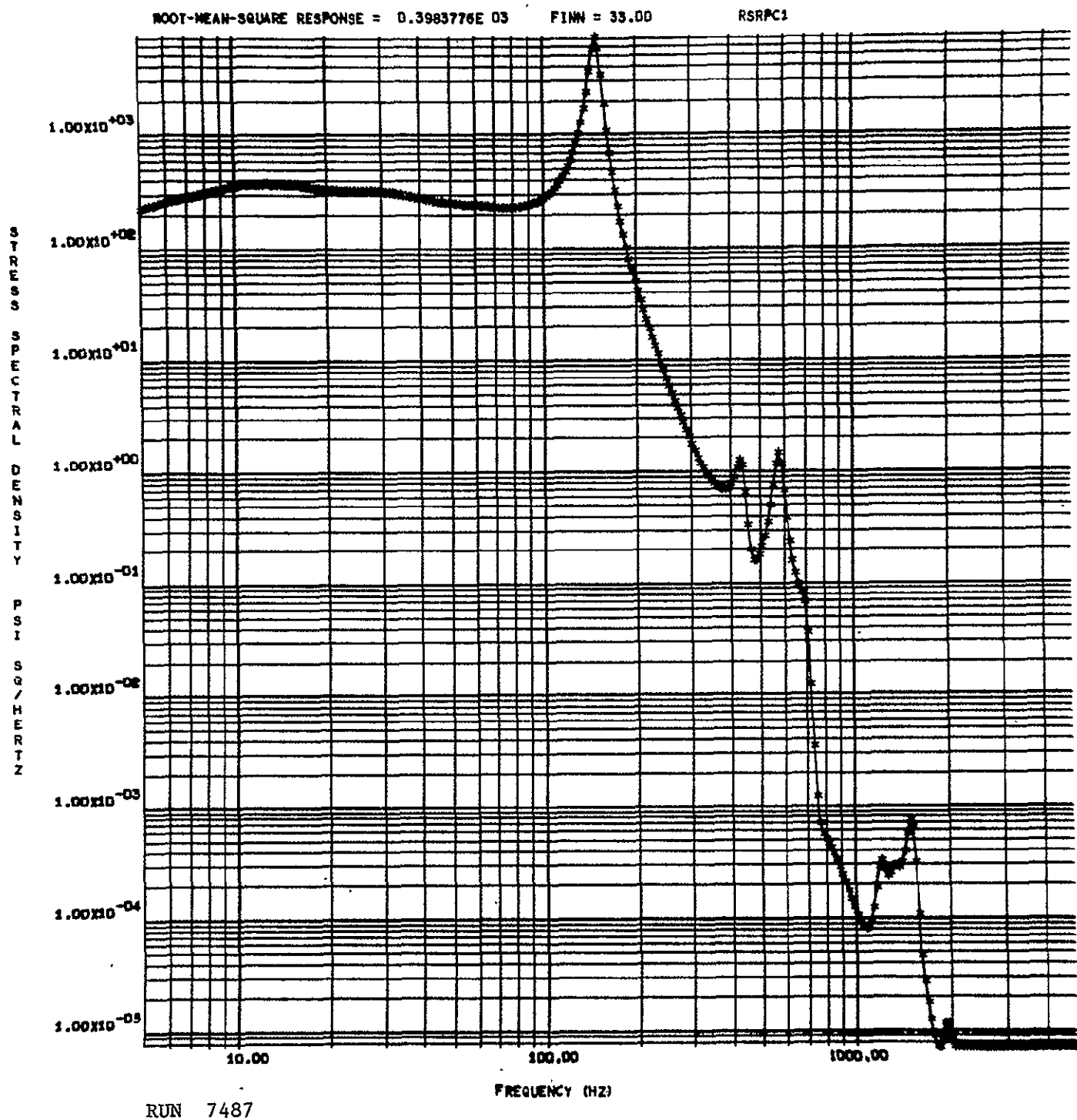
FIGURE 8. STRESS SPECTRAL DENSITY AT CENTER OF FOUR EDGES SIMPLY-
SUPPORTED CURVED RECTANGULAR PANEL CROSS-REINFORCED
WITH STIFFENERS

87

STRESS SPECTRAL DENSITY PSI SQ/HERTZ

1.00x10^{+03}

1.00x10^{+02}

1.00x10^{+01}

1.00x10^{+00}

1.00x10^{-01}

1.00x10^{-02}

1.00x10^{-03}

1.00x10^{-04}

1.00x10^{-05}

10.00   100.00   1000.00

RUN   7487   FREQUENCY (HZ)
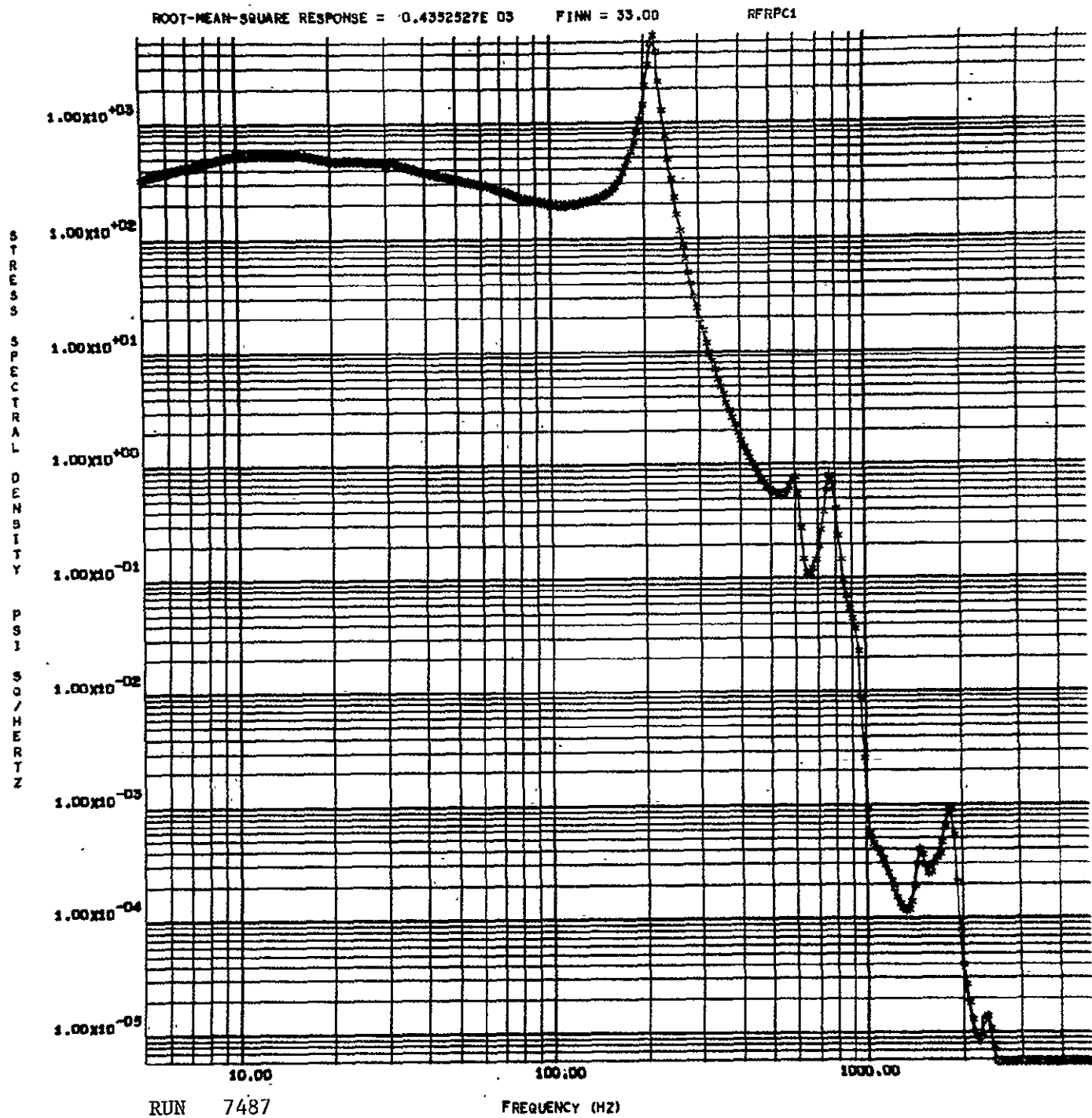
FIGURE 9.   STRESS SPECTRAL DENSITY AT CENTER OF FOUR EDGES CLAMPED
            CURVED RECTANGULAR PANEL CROSS-REINFORCED WITH STIFFENERS
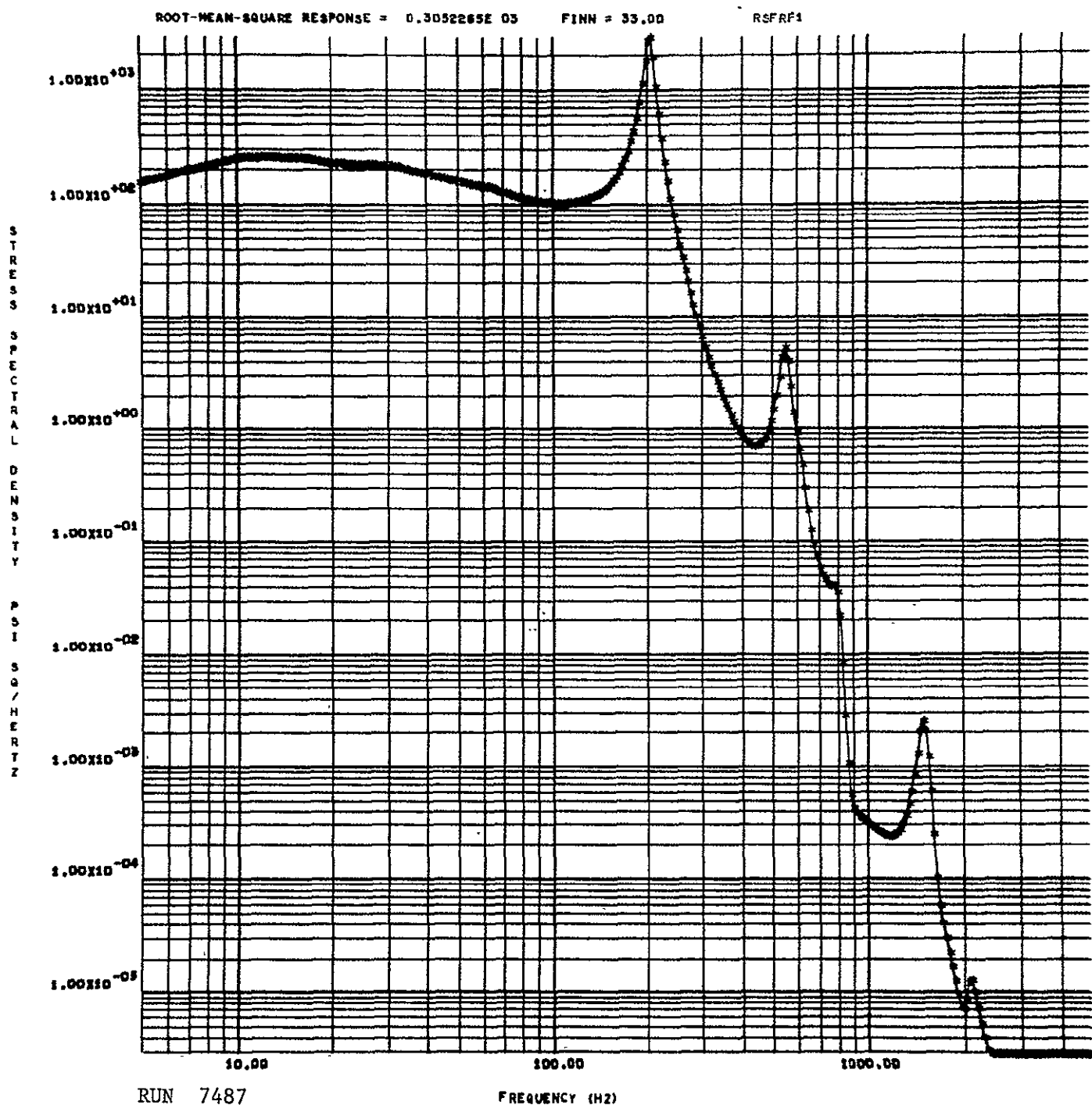
FIGURE 10. STRESS SPECTRAL DENSITY AT CENTER OF TWO OPPOSITE EDGE
SIMPLY-SUPPORTED AND OTHER TWO CLAMPED RECTANGULAR
CURVED PANEL CROSS-REINFORCED WITH STIFFENERS

89
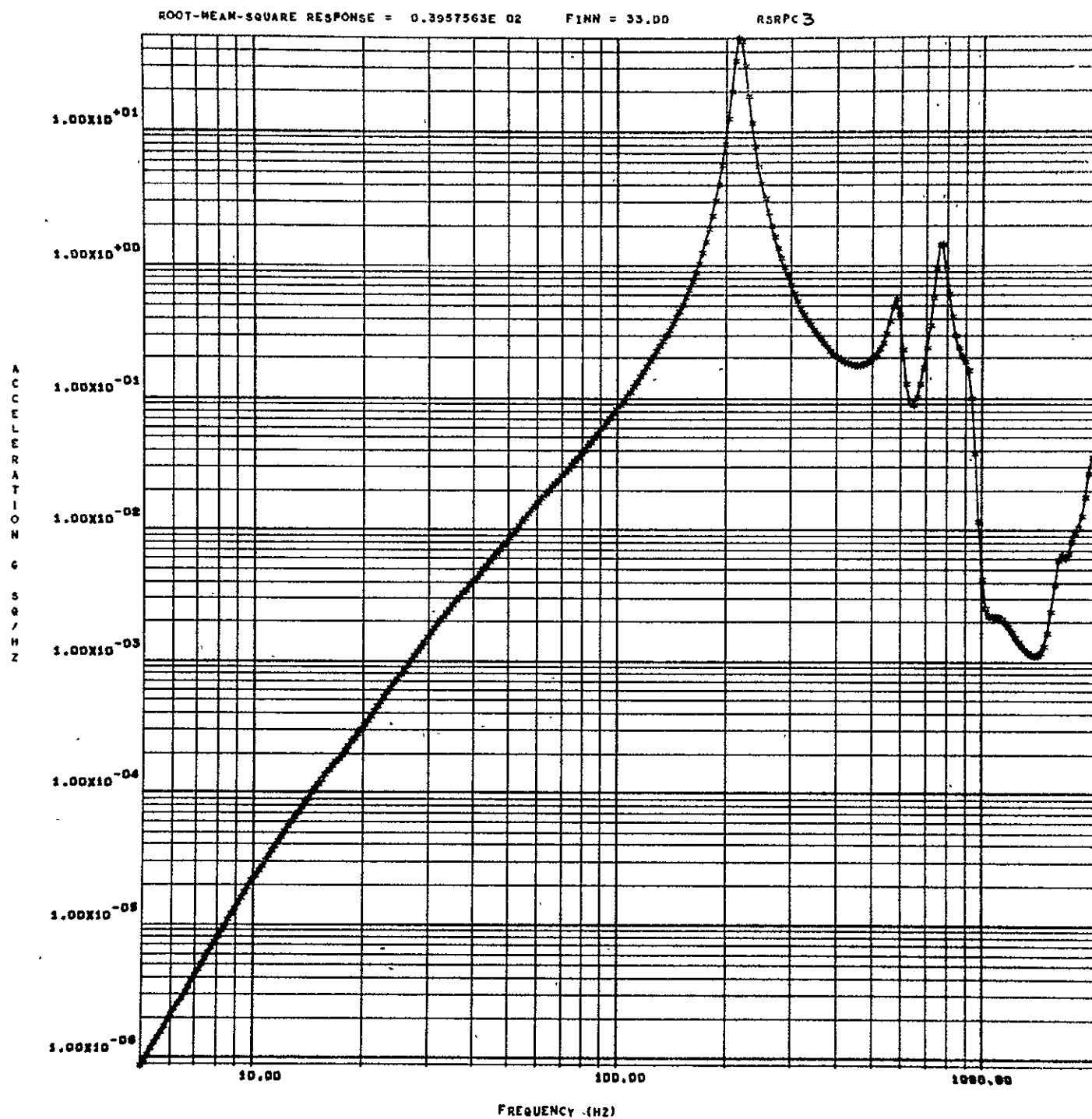
FIGURE 11   ACCELERATION SPECTRAL DENSITY AT CENTER OF PANEL,
ALL TERMS SUMMATION

90

ROOT-MEAN-SQUARE RESPONSE = 0.3958297E 02   FINN = 33.00   RSRPC 3
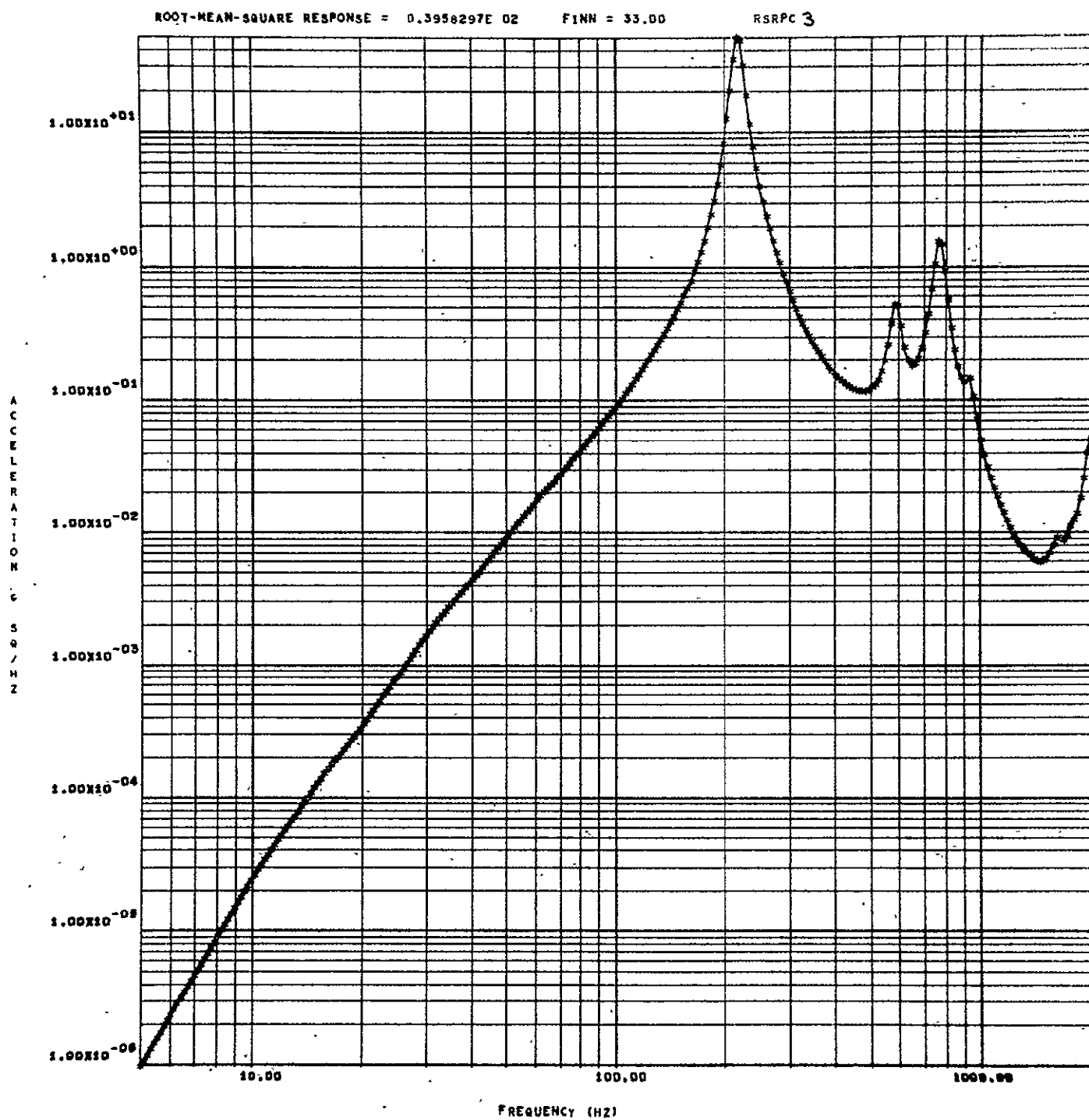
FIGURE 12   ACCELERATION SPECTRAL DENSITY AT CENTER OF PANEL,
CROSS-TERMS NEGLECTED
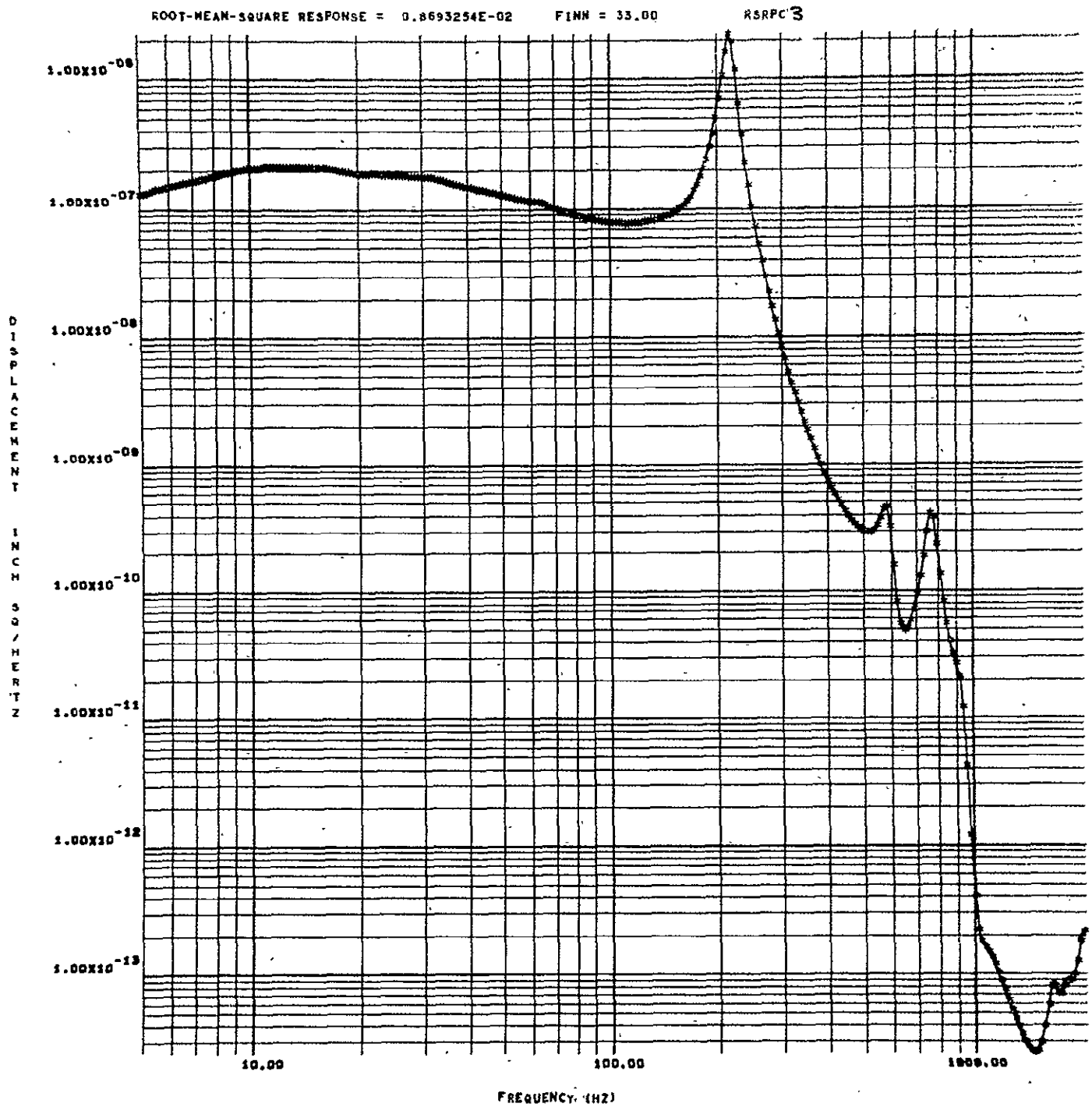
FIGURE 13 DISPLACEMENT SPECTRAL DENSITY AT CENTER OF
PANEL, ALL TERMS SUMMATION
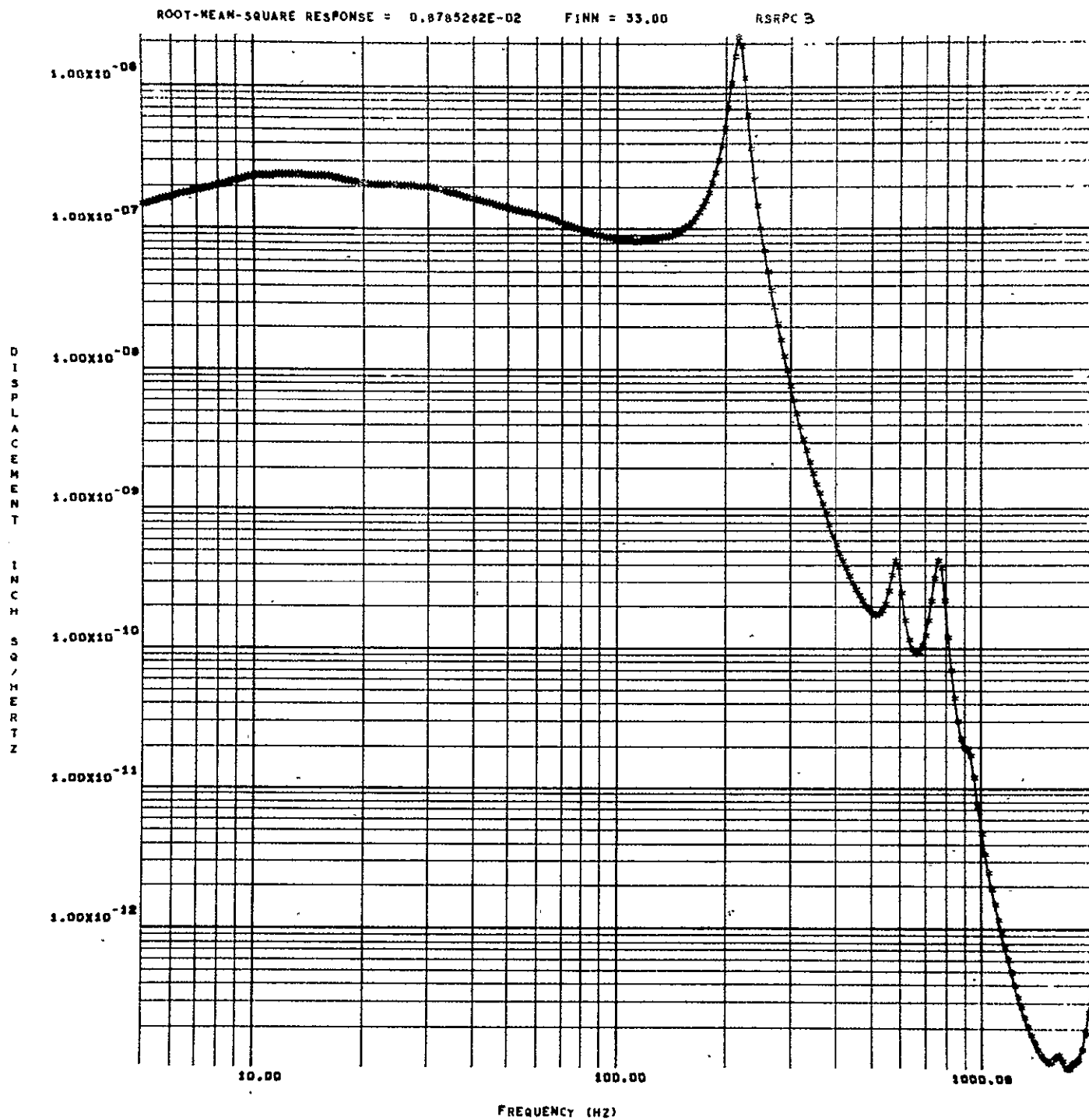
FIGURE 14   DISPLACENT SPECTRAL DENSITY AT CENTER OF PANEL,
CROSS-TERMS NEGLECTED
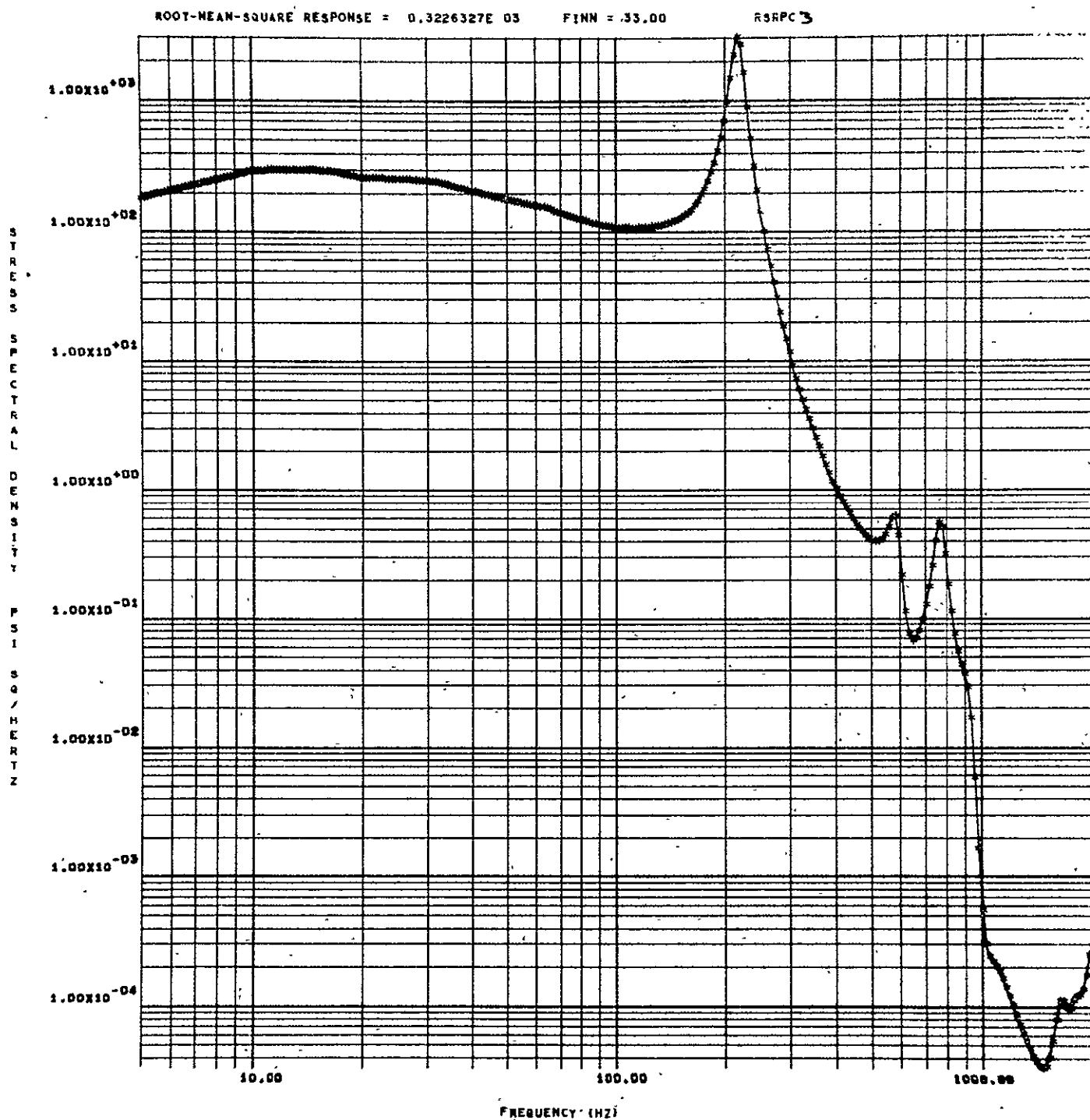
FIGURE 15   STRESS SPECTRAL DENSITY AT CENTER OF PANEL ALL
TERMS SUMMATION
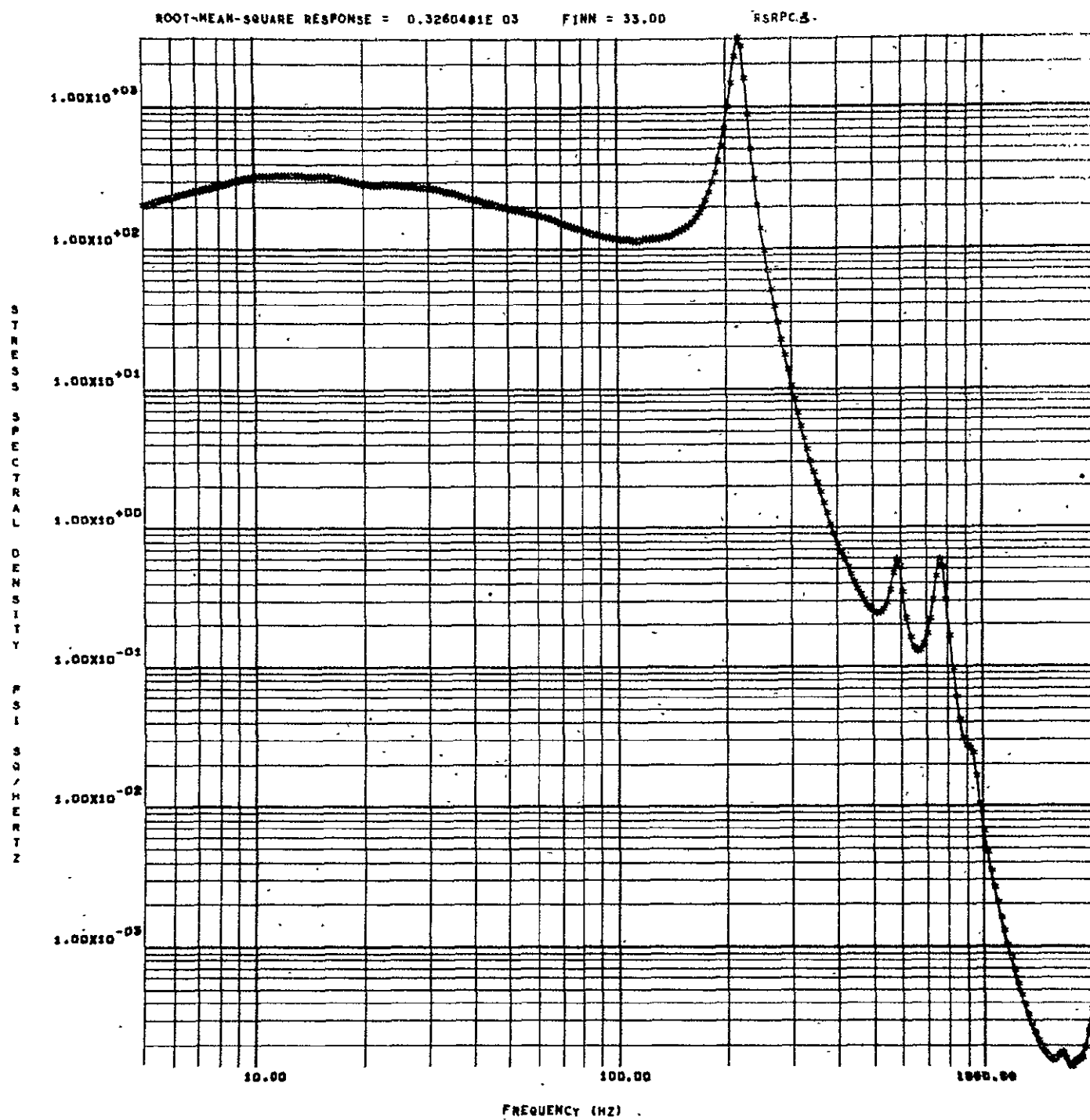
FIGURE 16   STRESS SPECTRAL DENSITY AT CENTER OF PANEL,
CROSS-TERMS NEGLECTED

95

ROOT-MEAN-SQUARE RESPONSE = 0.2554980E 02   FINN = 33.00   RSRPC 3
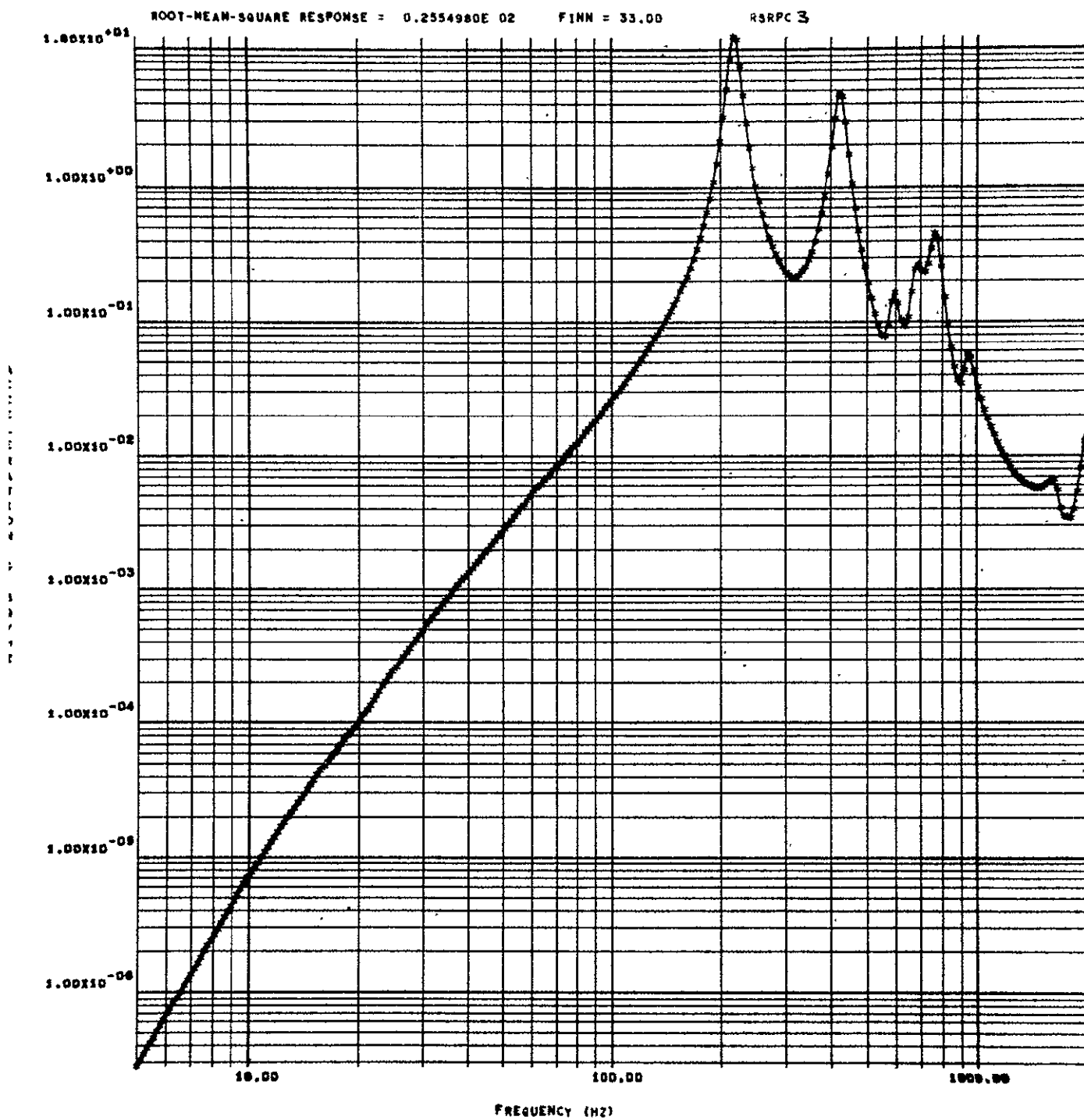
FIGURE 17   ACCELERATION SPECTRAL DENSITY, ALL TERMS SUMMATION,
AT x = ℓ/4 = 11.87 in. y = b/4 = 14.594 in.
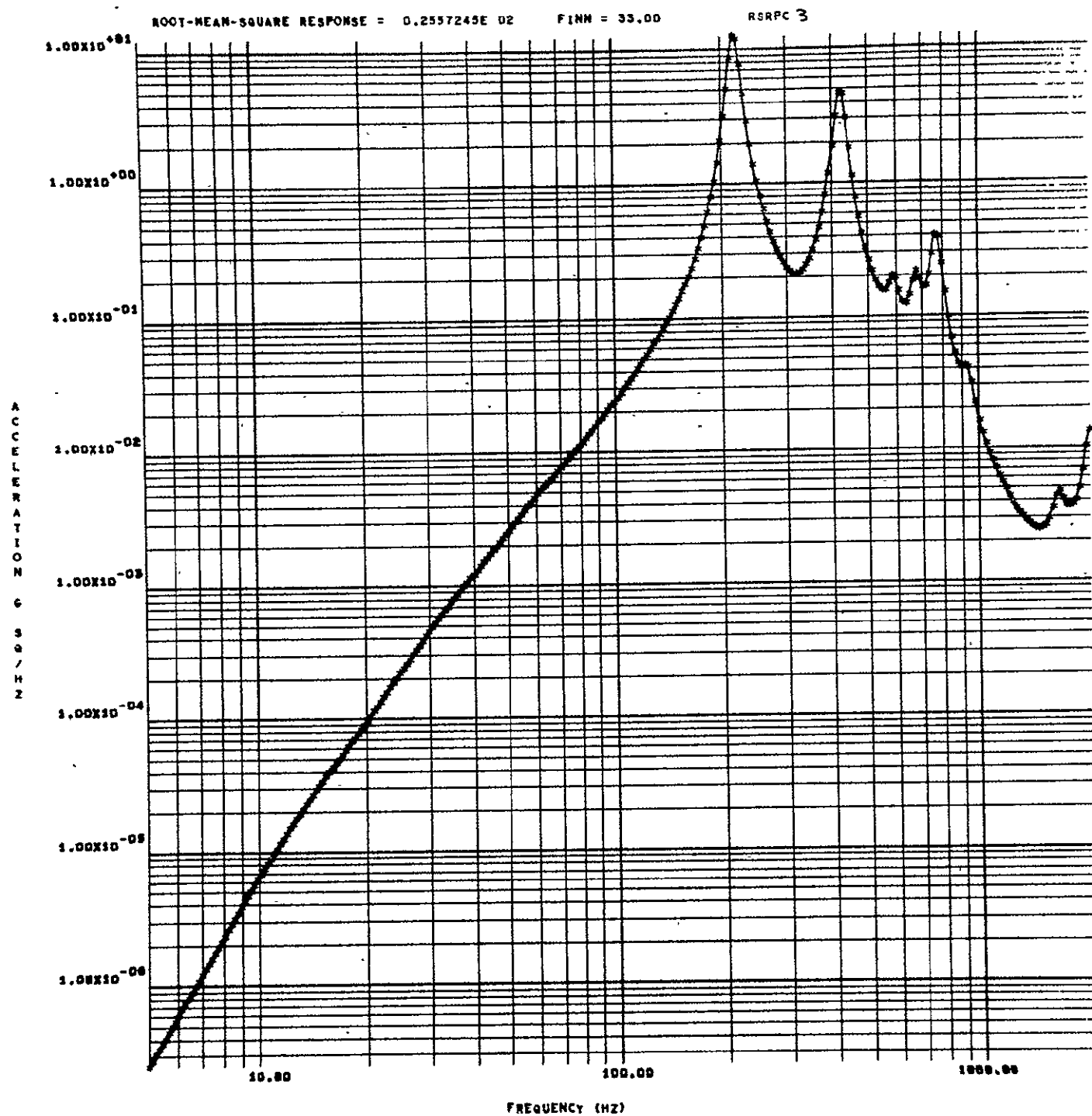
FIGURE 18   ACCELERATION SPECTRAL DENSITY, CROSS-TERMS NEGLECTED,
              AT x = ℓ/4 = 11.87 in. y = b/4 = 14.594 in.

97

FIGURE 19   DISPLACEMENT SPECTRAL DENSITY, ALL TERMS SUMMATION,
AT x = ℓ/4 = 11.87 in. y = b/4 = 14.594 in.
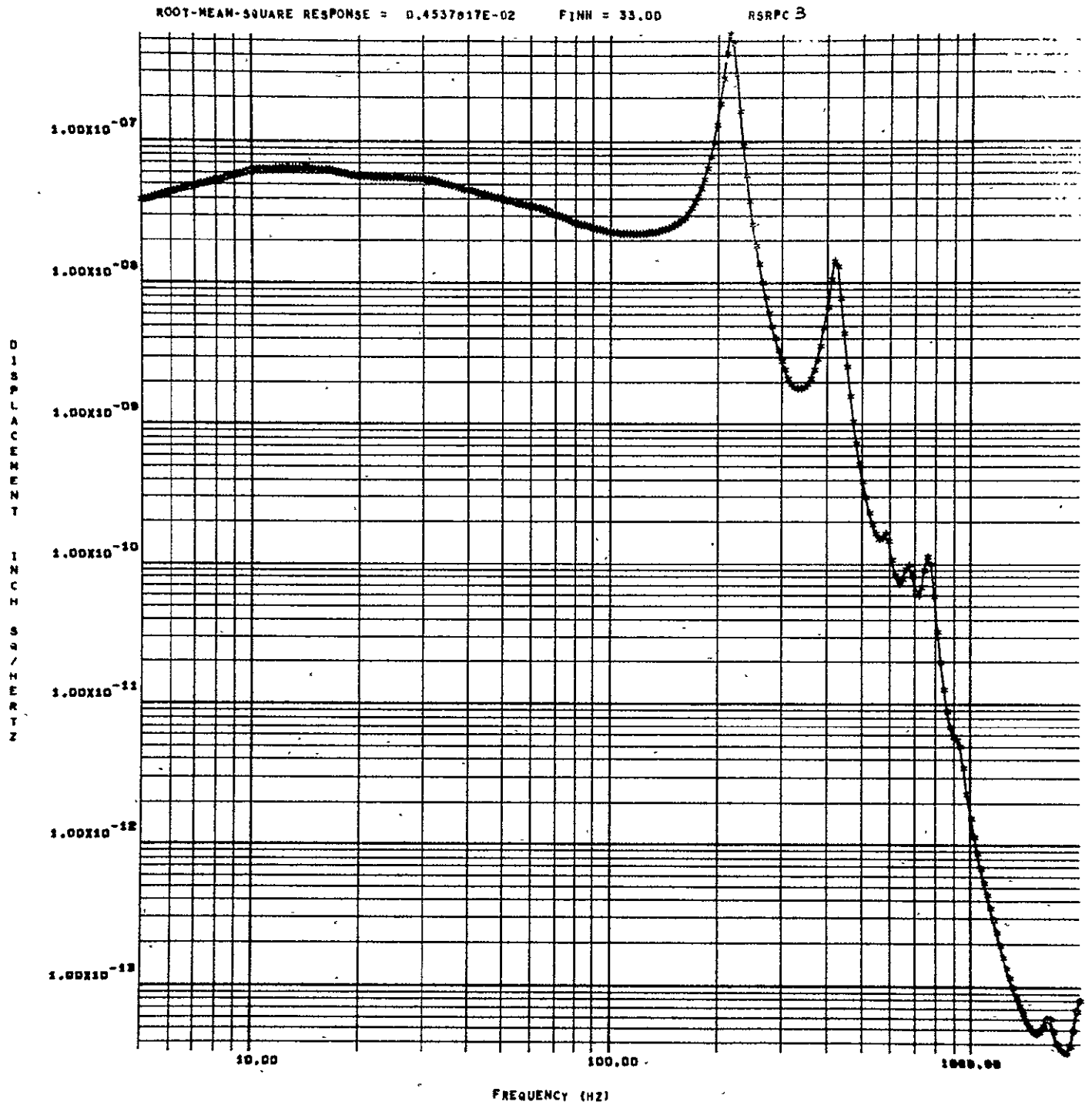
FIGURE 20   DISPLACEMENT SPECTRAL DENSITY, CROSS-TERMS NEGLECTED,
              AT x = $\ell/4$ = 11.87 in.   y = b/4 = 14.594 in.

99
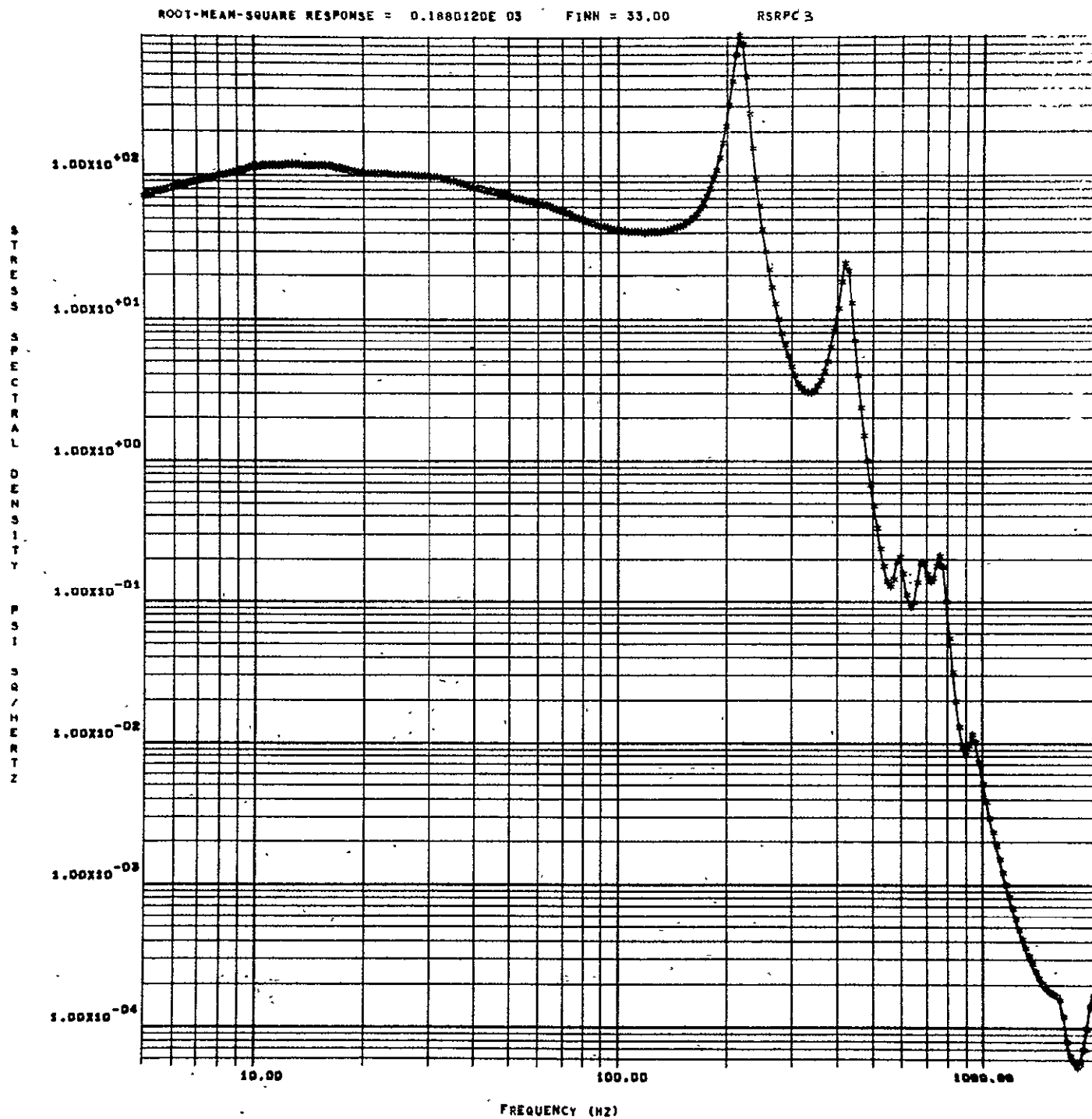
FIGURE 21   STRESS SPECTRAL DENSITY, ALL TERMS SUMMATION,
             AT x = ℓ/4 = 11.87 in. y = b/4 = 14.594 in.
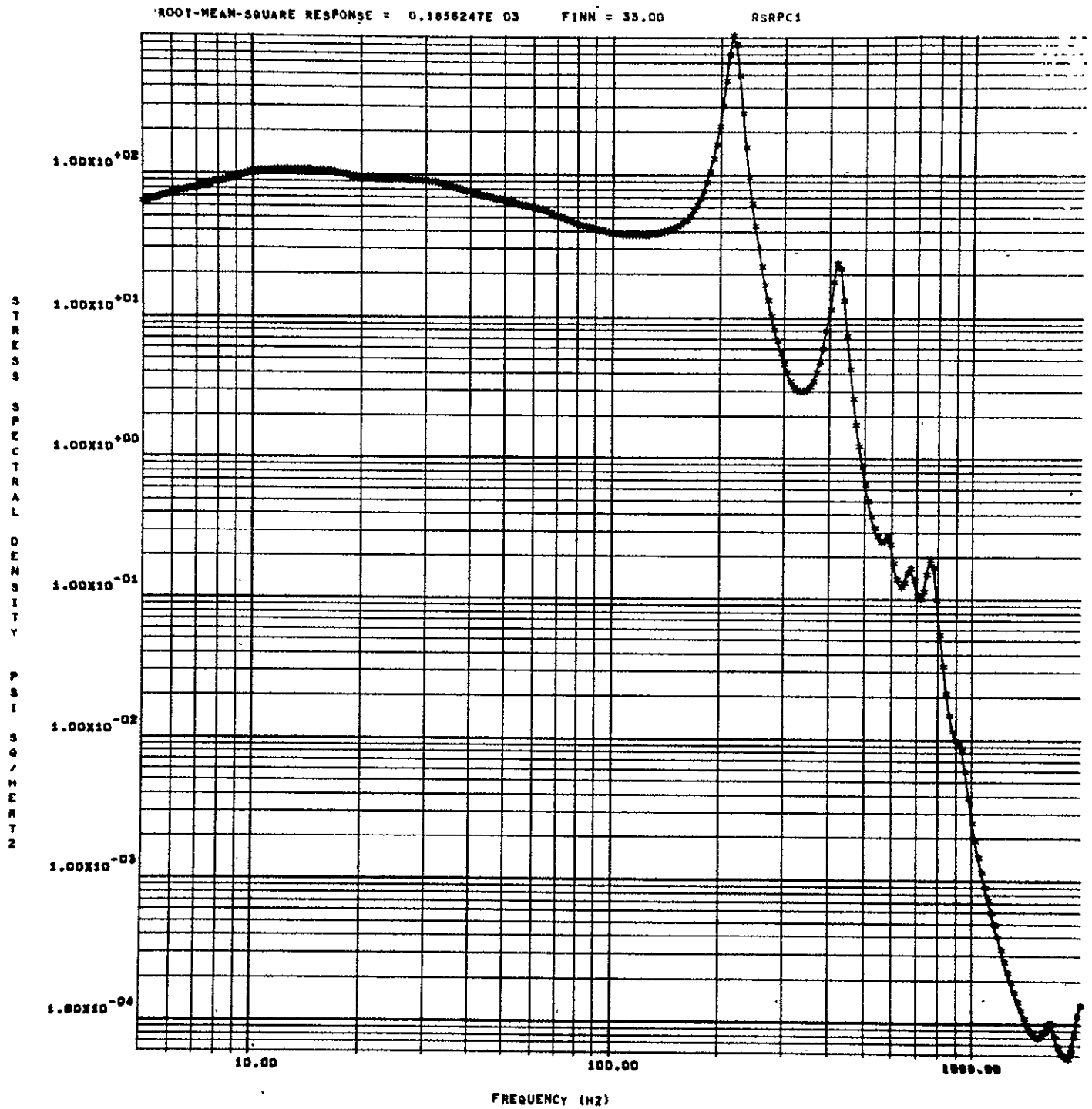
FIGURE 22   STRESS SPECTRAL DENSITY, CROSS-TERMS NEGLECTED,
AT x = ℓ/4 = 11.87 in. y = b/4 = 14.594 in.
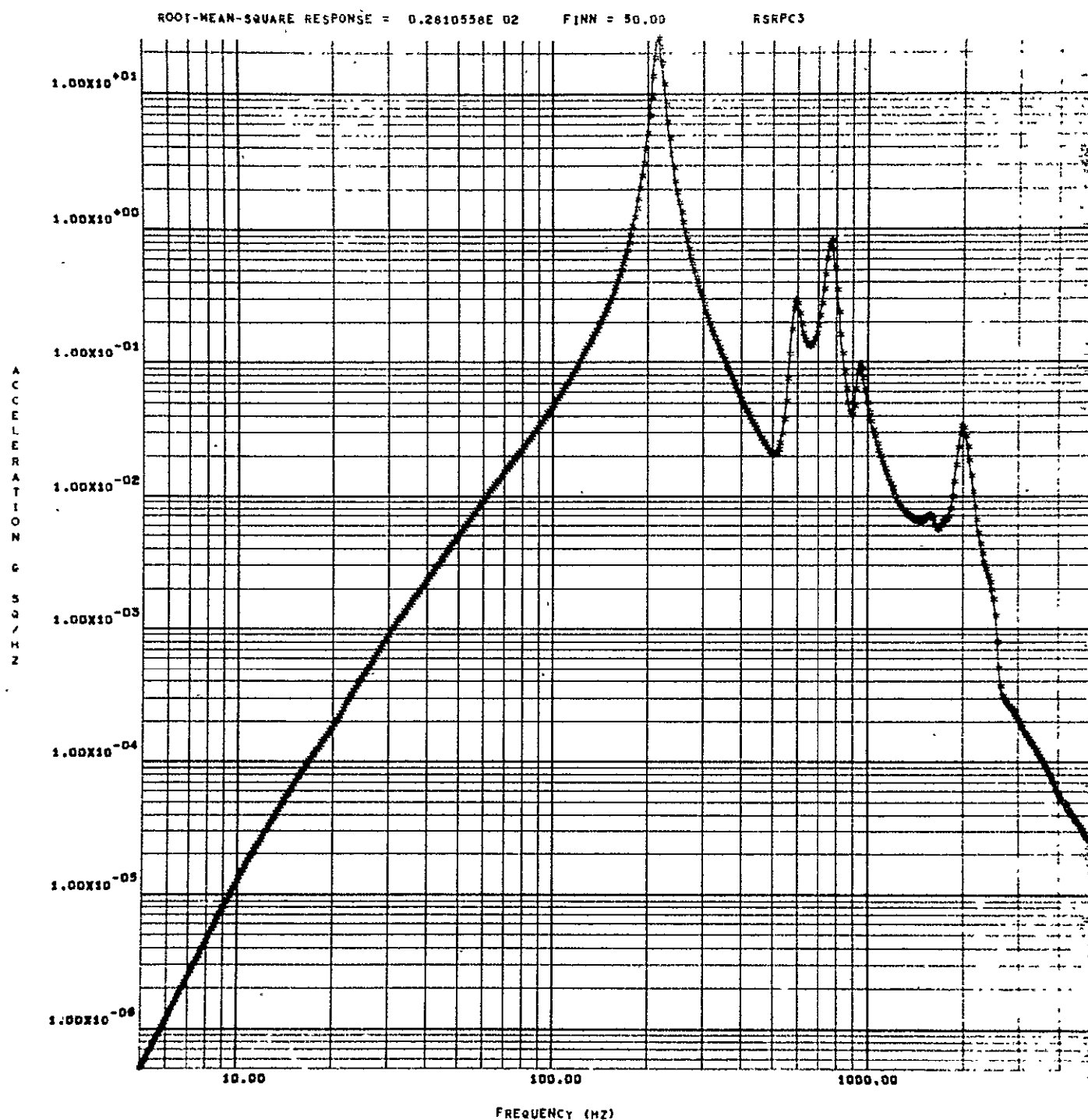
FIGURE 23   ACCELERATION SPECTRAL DENSITY, ALL TERMS SUMMATION

AT $x = \frac{\ell}{2}$ = 23.75 INCHES, $y = \frac{b}{4}$ = 14.594 INCHES
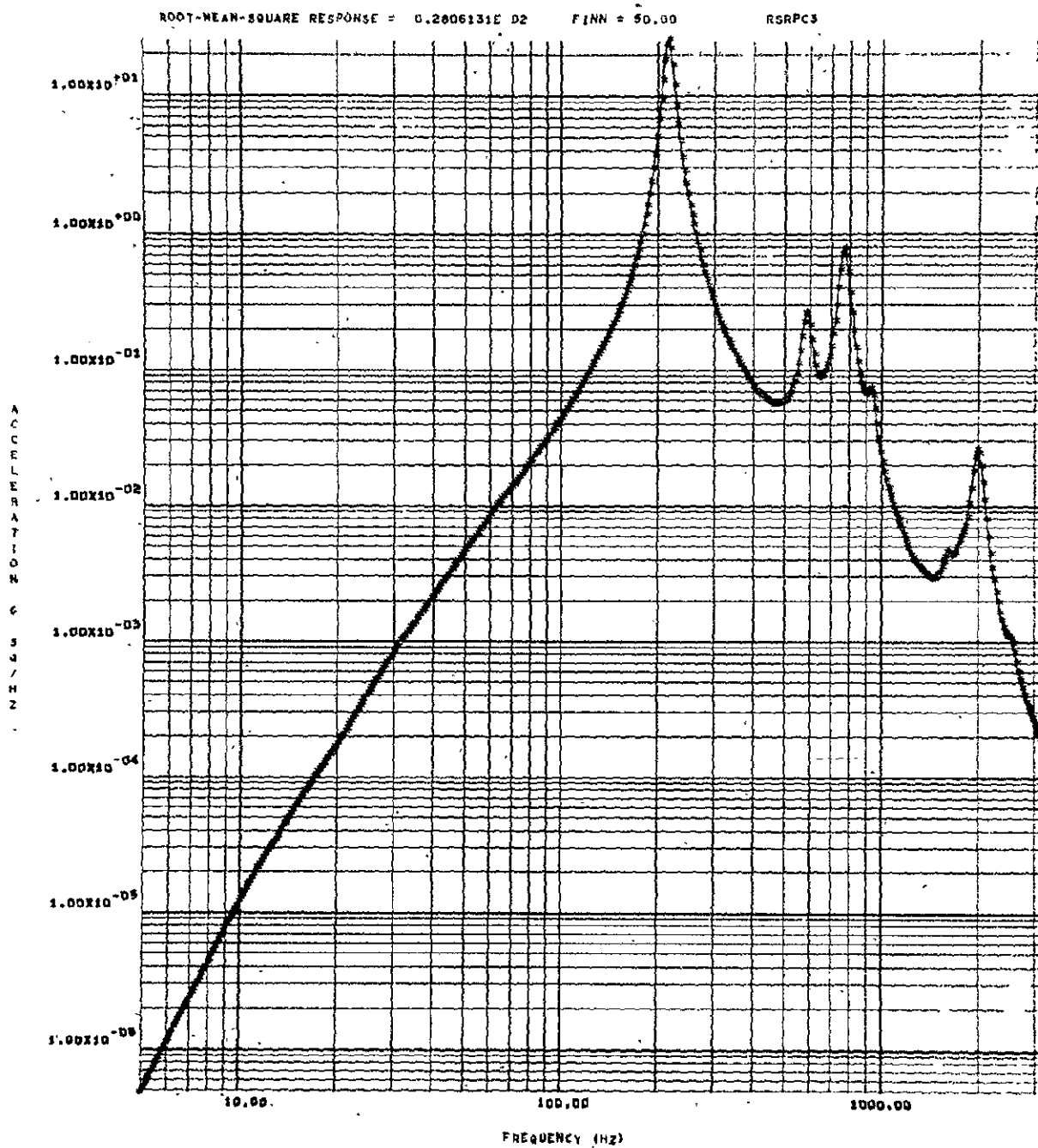
FIGURE 24   ACCELERATION SPECTRAL DENSITY, CROSS-TERMS NEGLECTED

AT $x = \dfrac{\ell}{2}$ = 23.75 INCHES, $y = \dfrac{b}{4}$ = 14.594 INCHES
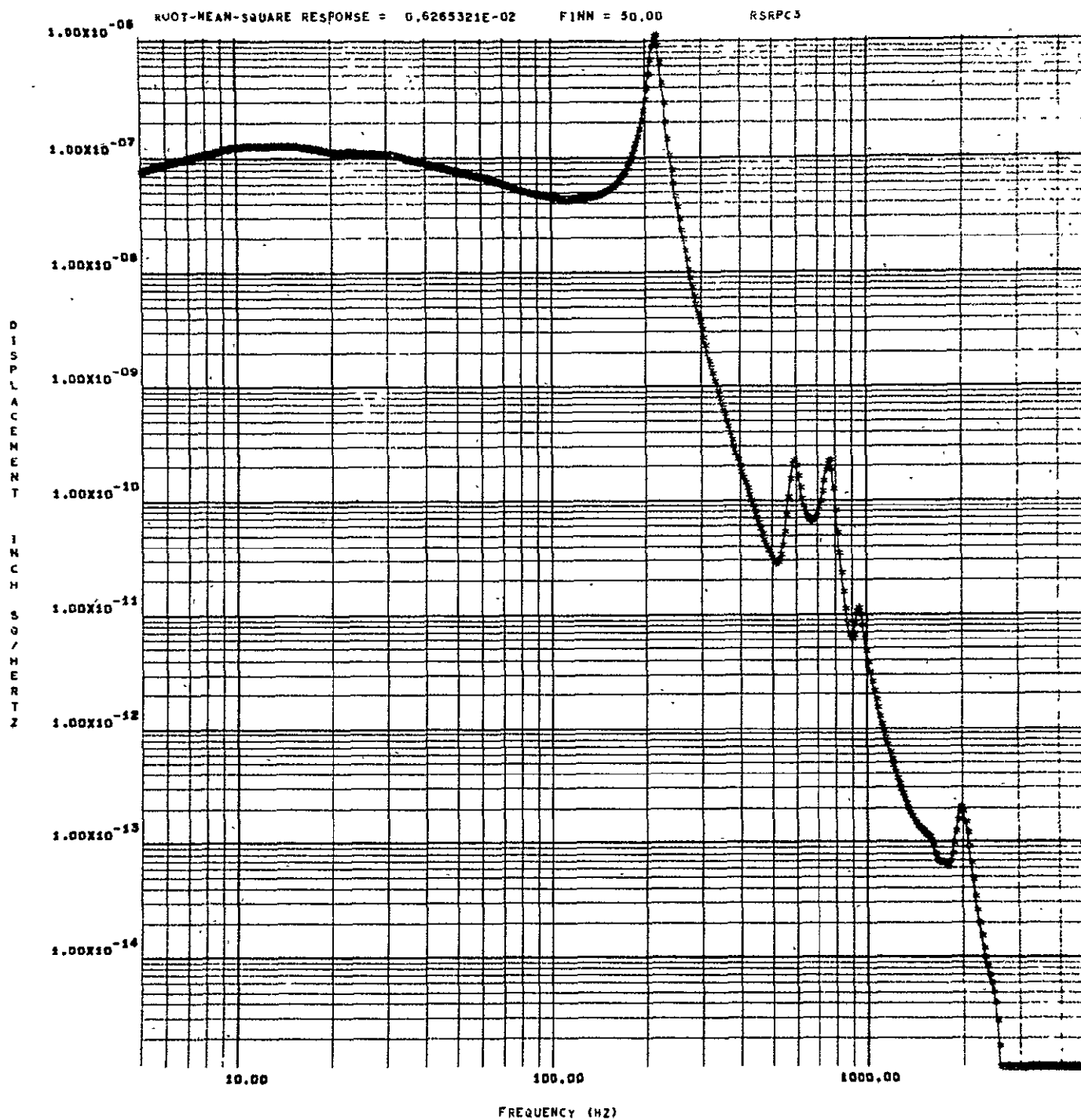
FIGURE 25 DISPLACEMENT SPECTRAL DENSITY, ALL TERMS SUMMATION,

AT $x = \frac{\ell}{2}$ = 23.75 INCHES, $y = \frac{b}{4}$ = 14.594 INCHES
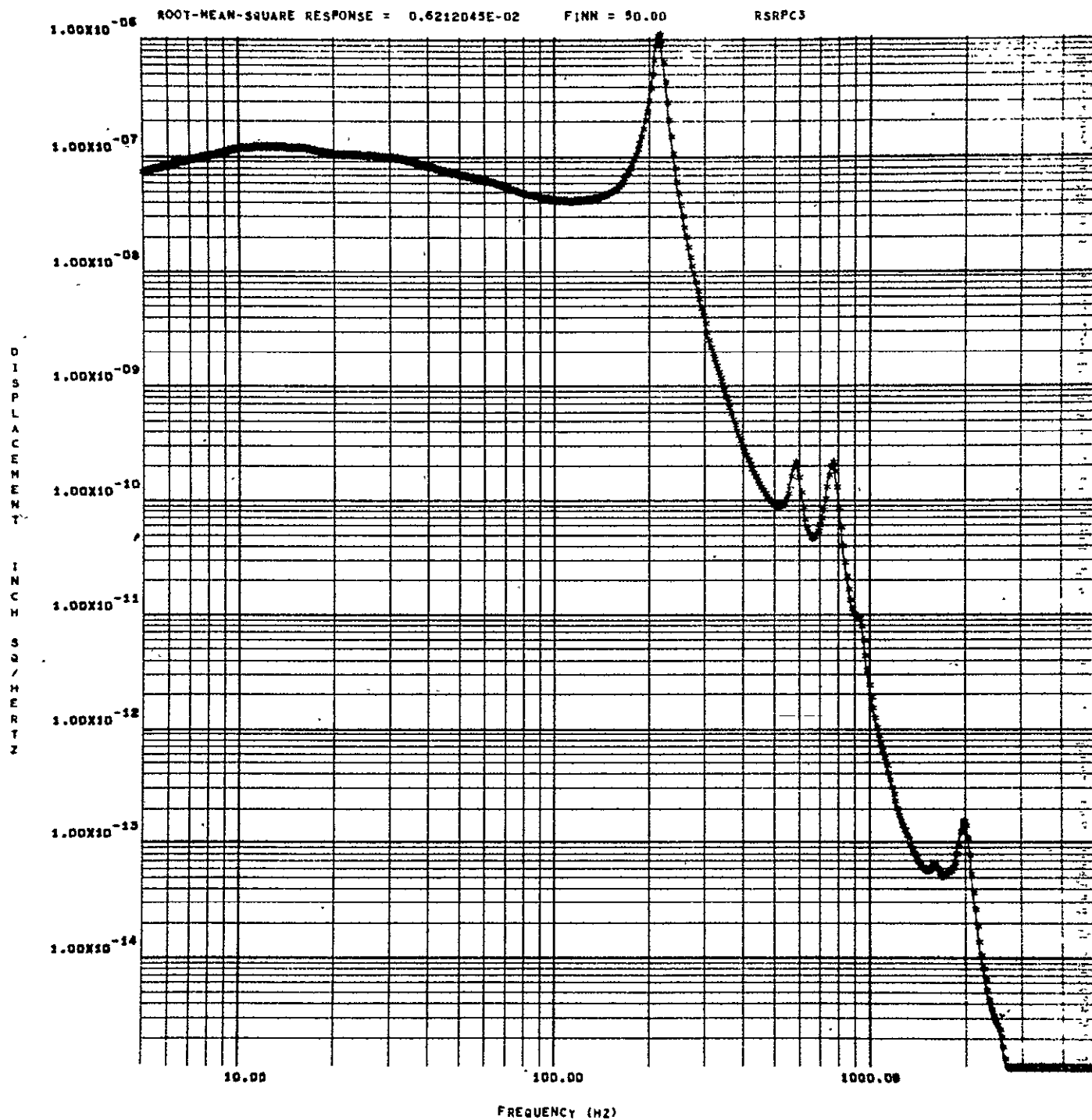
FIGURE 26   DISPLACEMENT SPECTRAL DENSITY, CROSS-TERM NEGLECTED,

AT $x = \dfrac{\ell}{2}$ = 23.75 INCHES, $y = \dfrac{b}{4}$ = 14.594 INCHES
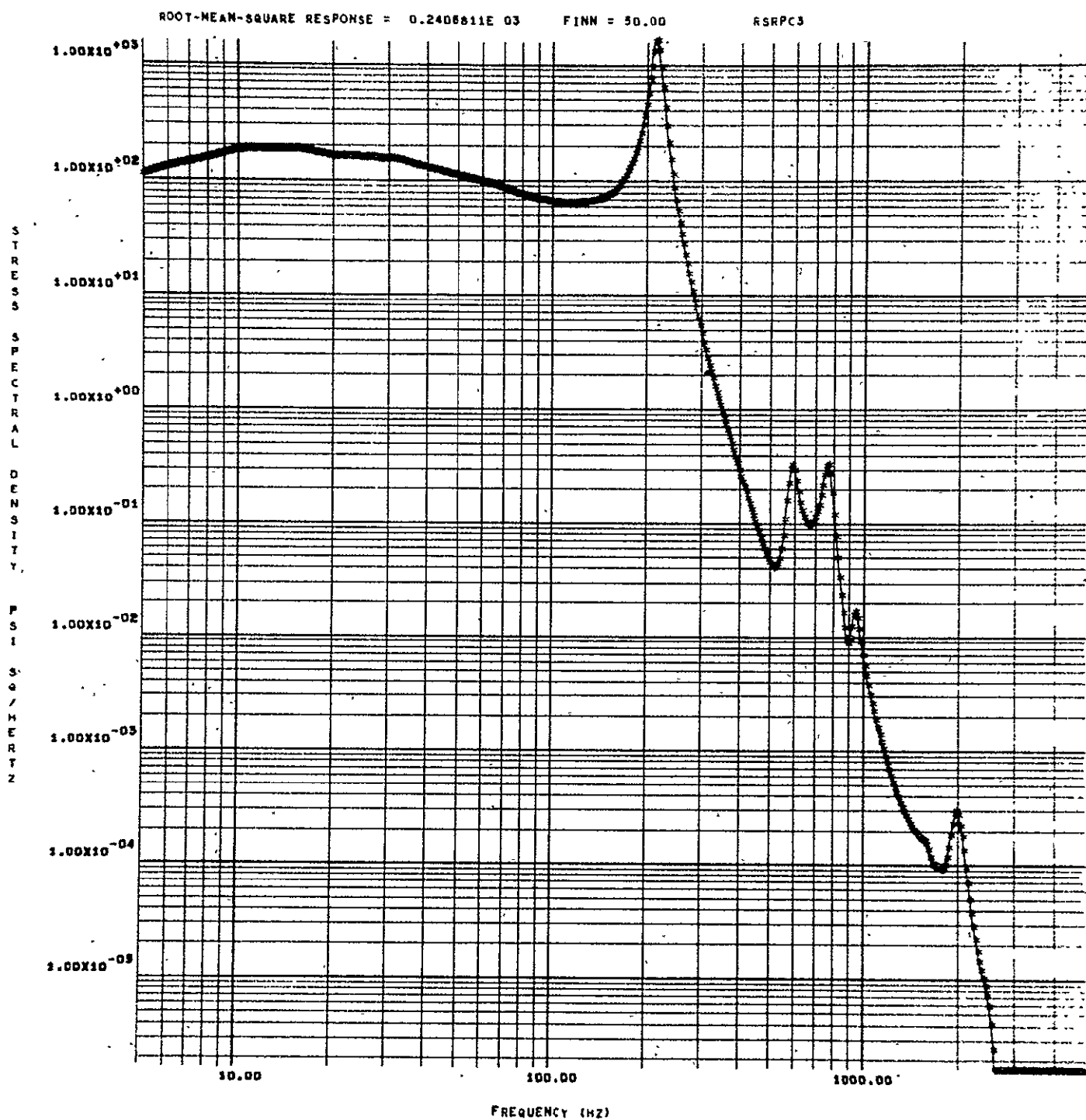
FIGURE 27   STRESS SPECTRAL DENSITY, ALL TERMS SUMMATION,
AT $x = \frac{\ell}{2} = 23.75$ INCHES, $y = \frac{b}{4} = 14.594$ INCHES
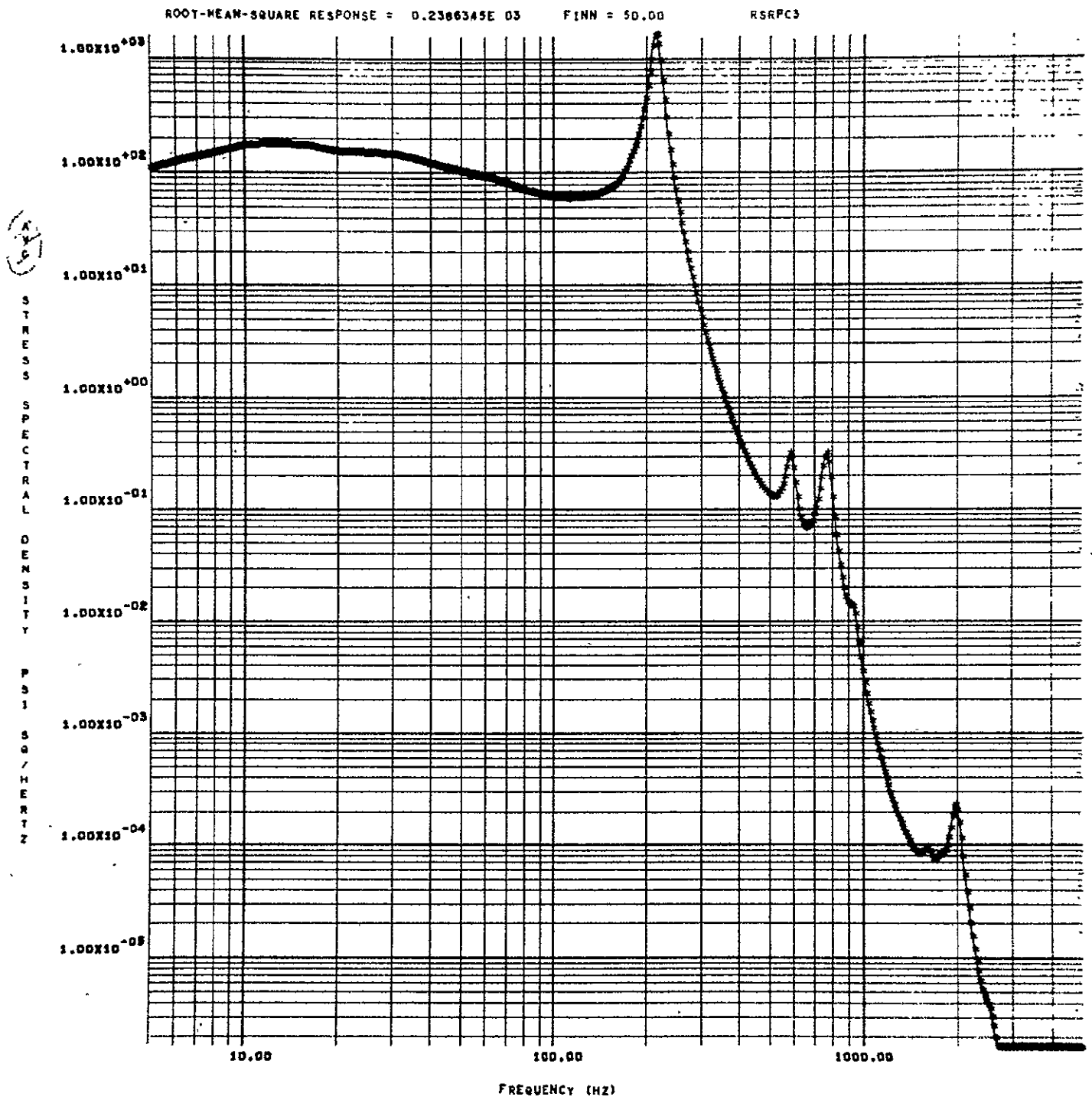
FIGURE 28 STRESS SPECTRAL DENSITY, CROSS-TERM NEGLECTED,

AT $x = \frac{\ell}{2} = 23.75$ INCHES, $y = \frac{b}{4} = 14.594$ INCHES

107

ROOT-MEAN-SQUARE RESPONSE = 0.3623868E 02   FINN = 50.00   RSRPC3

RUN 7412
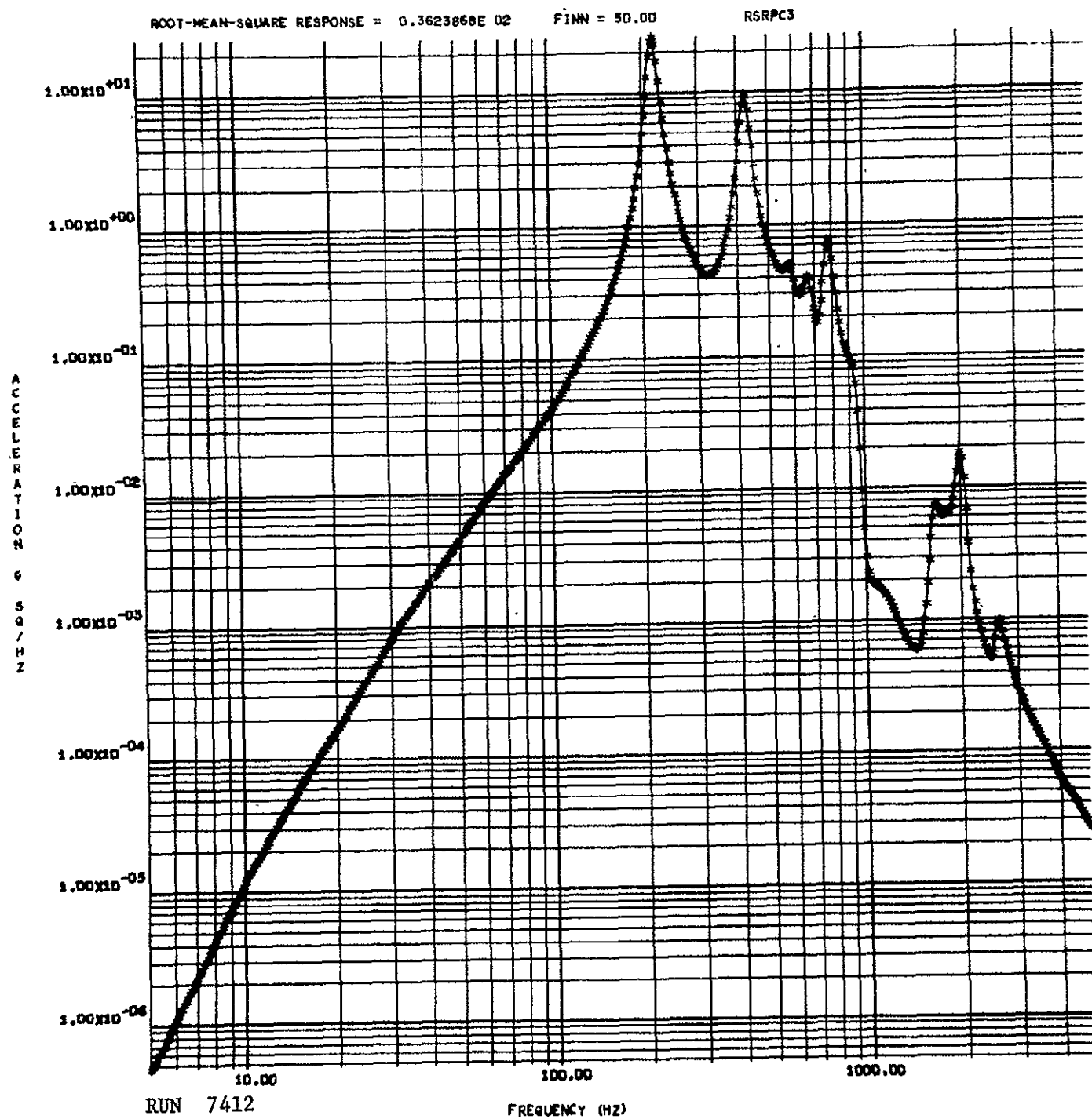
FIGURE 29   ACCELERATION SPECTRAL DENSITY, ALL TERMS SUMMATION,
AT x = $\ell/4$ = 11.87 in., y = b/2 = 29.187 in.
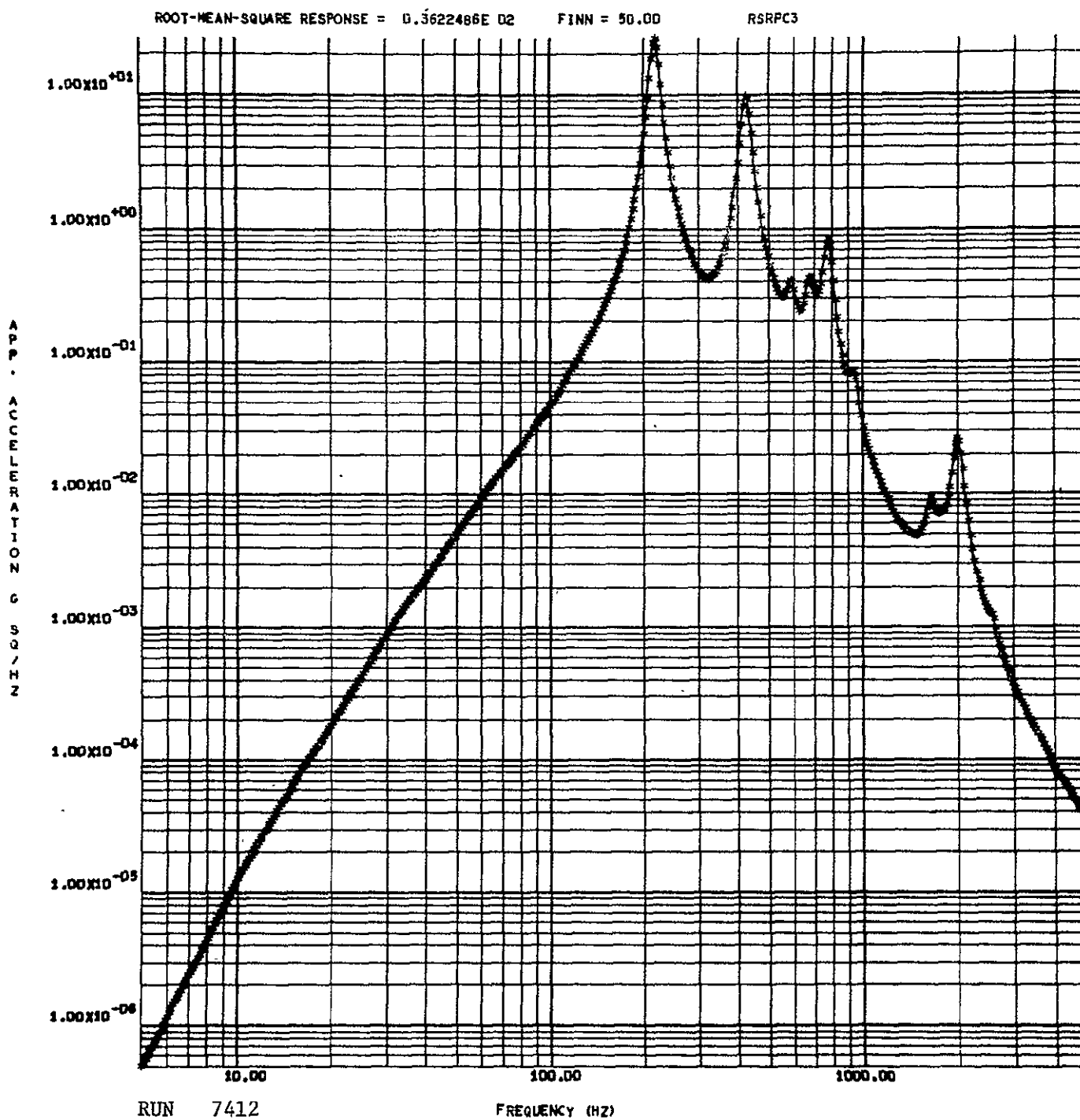
FIGURE 30   ACCELERATION SPECTRAL DENSITY, CROSS TERMS NEGLECTED,
AT x = ℓ/4 = 11.87 in., y = b/2 = 29.187 in.

FIGURE 31   DISPLACEMENT SPECTRAL DENSITY, ALL TERMS SUMMATION,
AT x = ℓ /4 = 11.87 in. , y = b/2 = 29.187 in.

ROOT-MEAN-SQUARE RESPONSE = 0.6417355E-02   FINN = 50.00   RSRPC3

RUN 7412

FREQUENCY (HZ)
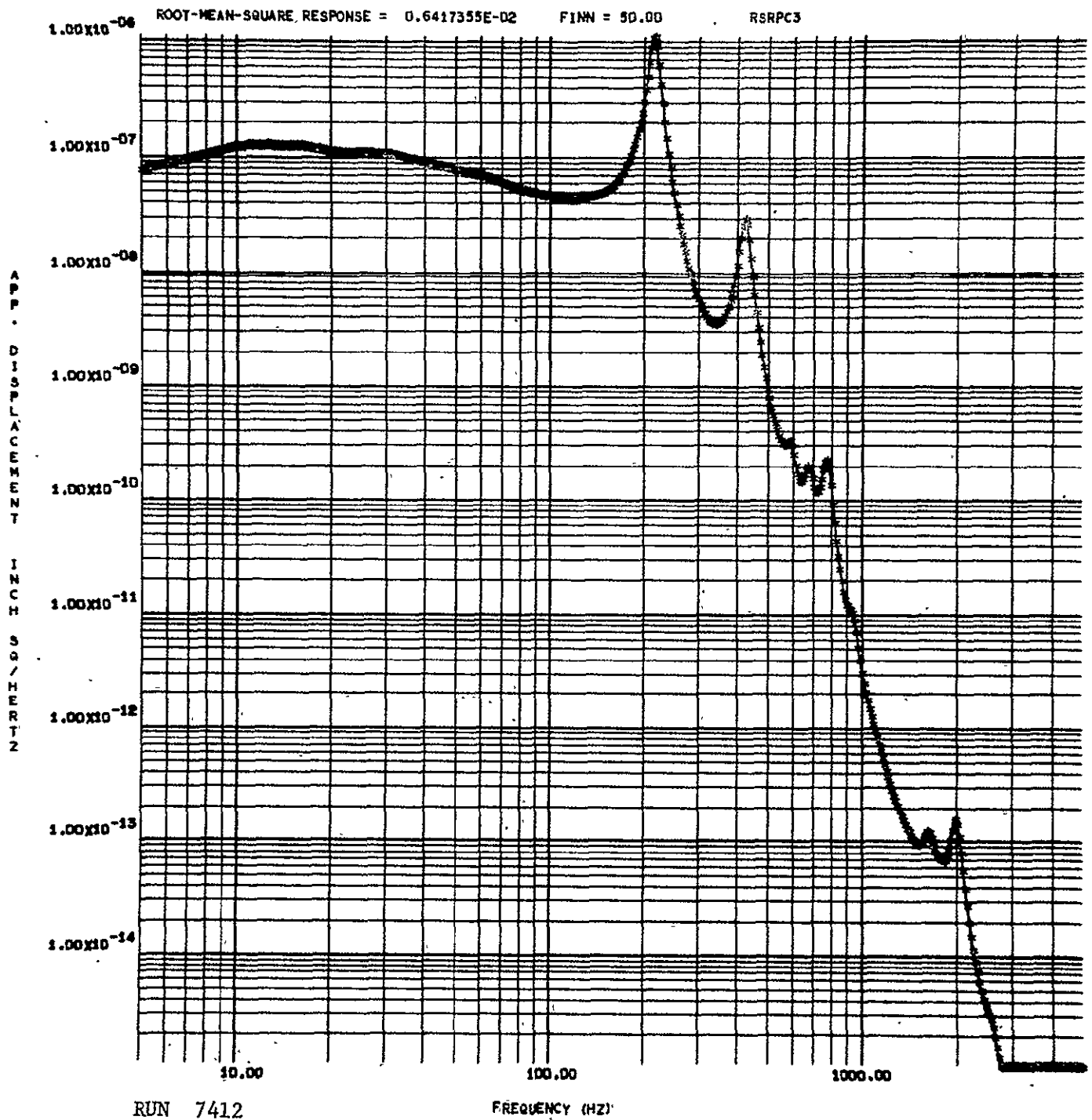
FIGURE 32   DISPLACEMENT SPECTRAL DENSITY, CROSS TERM NEGLECTED,
AT x = ℓ/4 = 11.87 in., y = b/2 = 29.187 in.

FIGURE 33 STRESS SPECTRAL DENSITY, ALL TERMS SUMMATION,
AT x = $\ell/4$ = 11.87 in. , y = b/2 = 29.187 in.

ROOT-MEAN-SQUARE RESPONSE = 0.2482881E 03 · FINN = 50.00 RSRPC3

RUN 7412
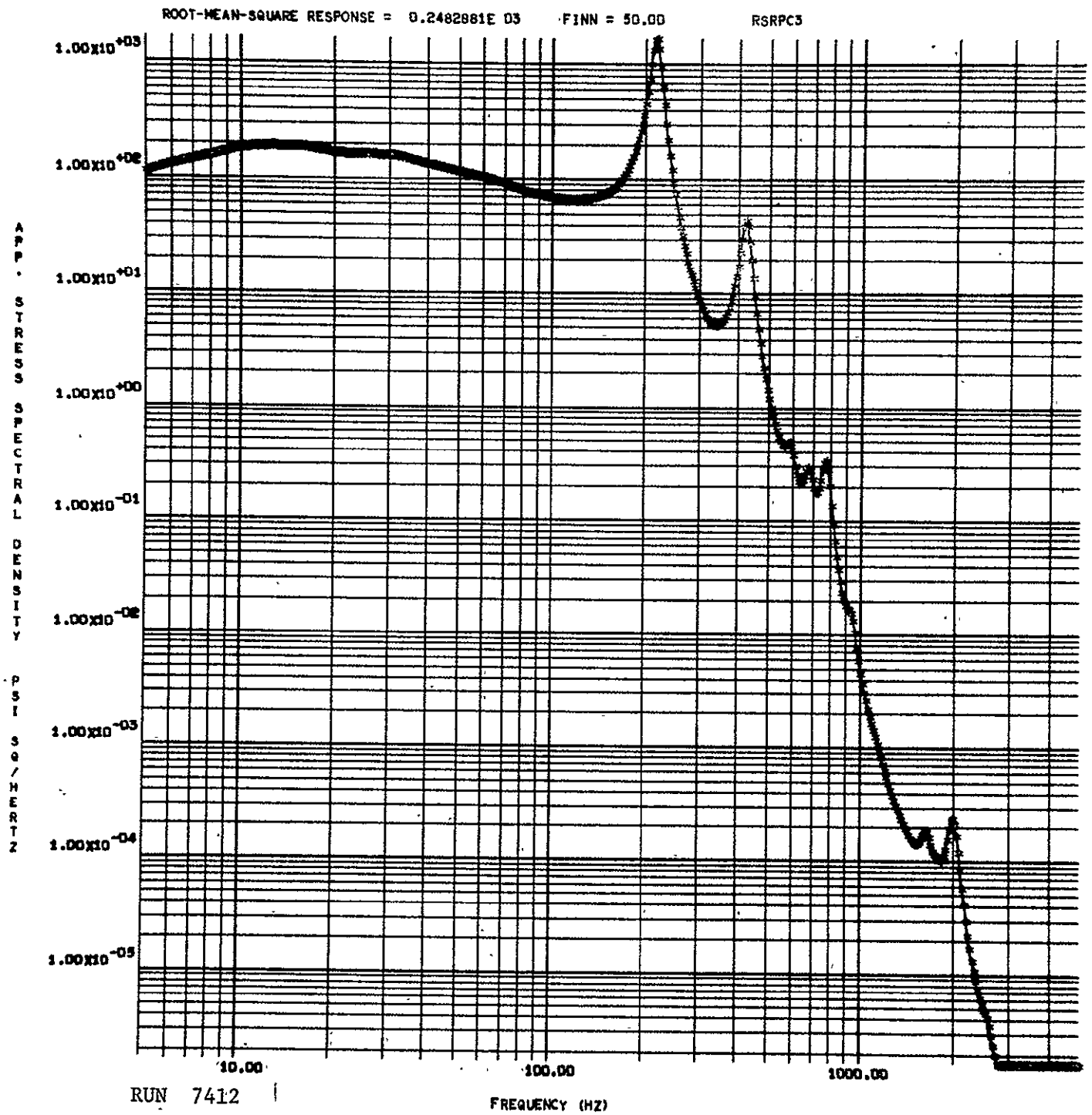
FIGURE 34 STRESS SPECTRAL DENSITY, CROSS TERMS NEGLECTED, AT x = · ℓ/4 = 11. 87 in. , y = b/2 = 29. 187 in.

113

ROOT-MEAN-SQUARE RESPONSE = 0.4319305E 02   FINN = 33.00   RSRPC4

RUN 8009
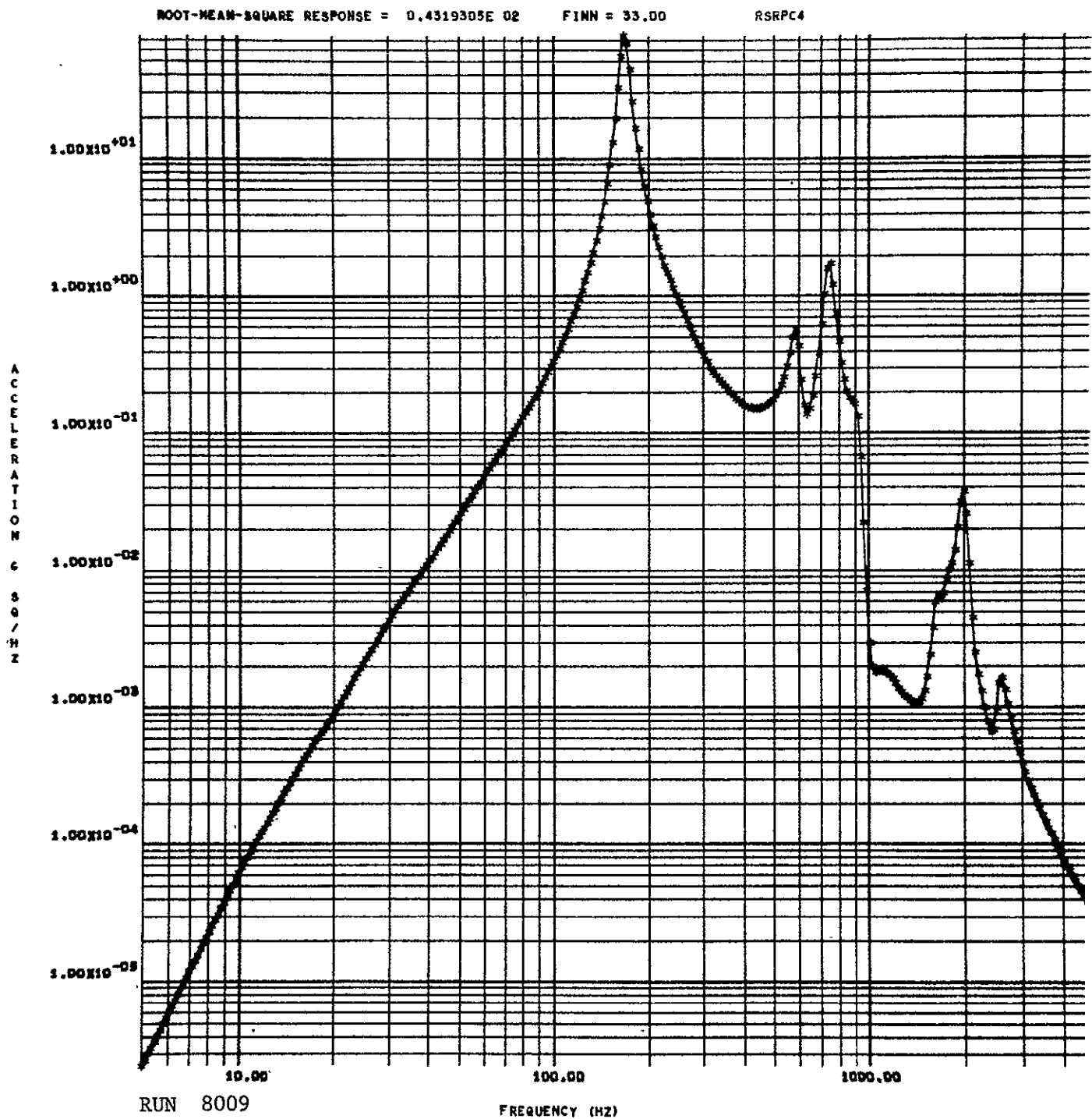
FIGURE 35   ACCELERATION SPECTRAL DENSITY AT CENTER OF PANEL,
             RADIUS OF CURVATURE a = 100 INCHES

114
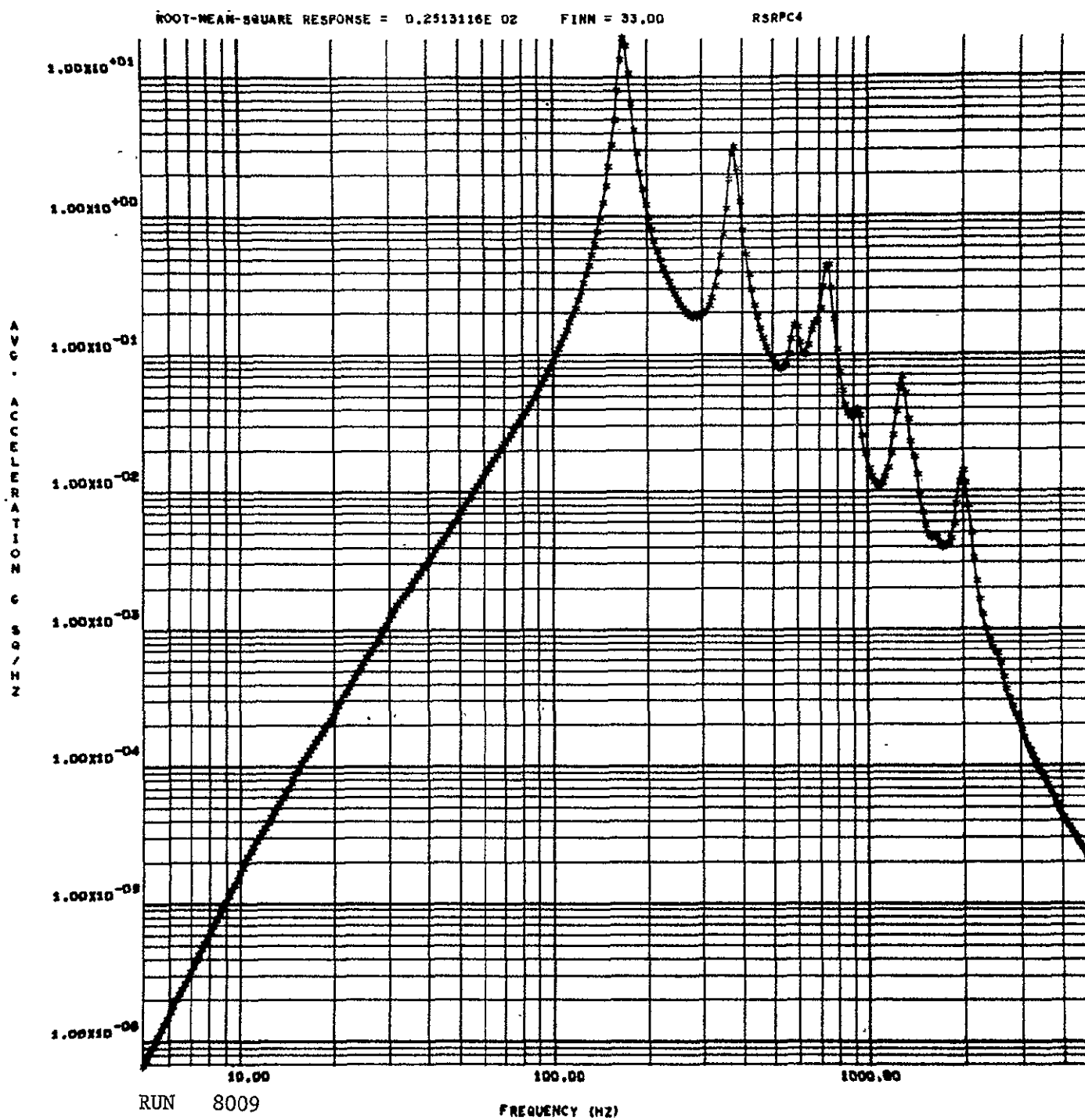
RUN   8009

FIGURE 36   AVERAGE ACCELERATION SPECTRAL DENSITY OVER WHOLE
PANEL, RADIUS OF CURVATURE a = 100 INCHES
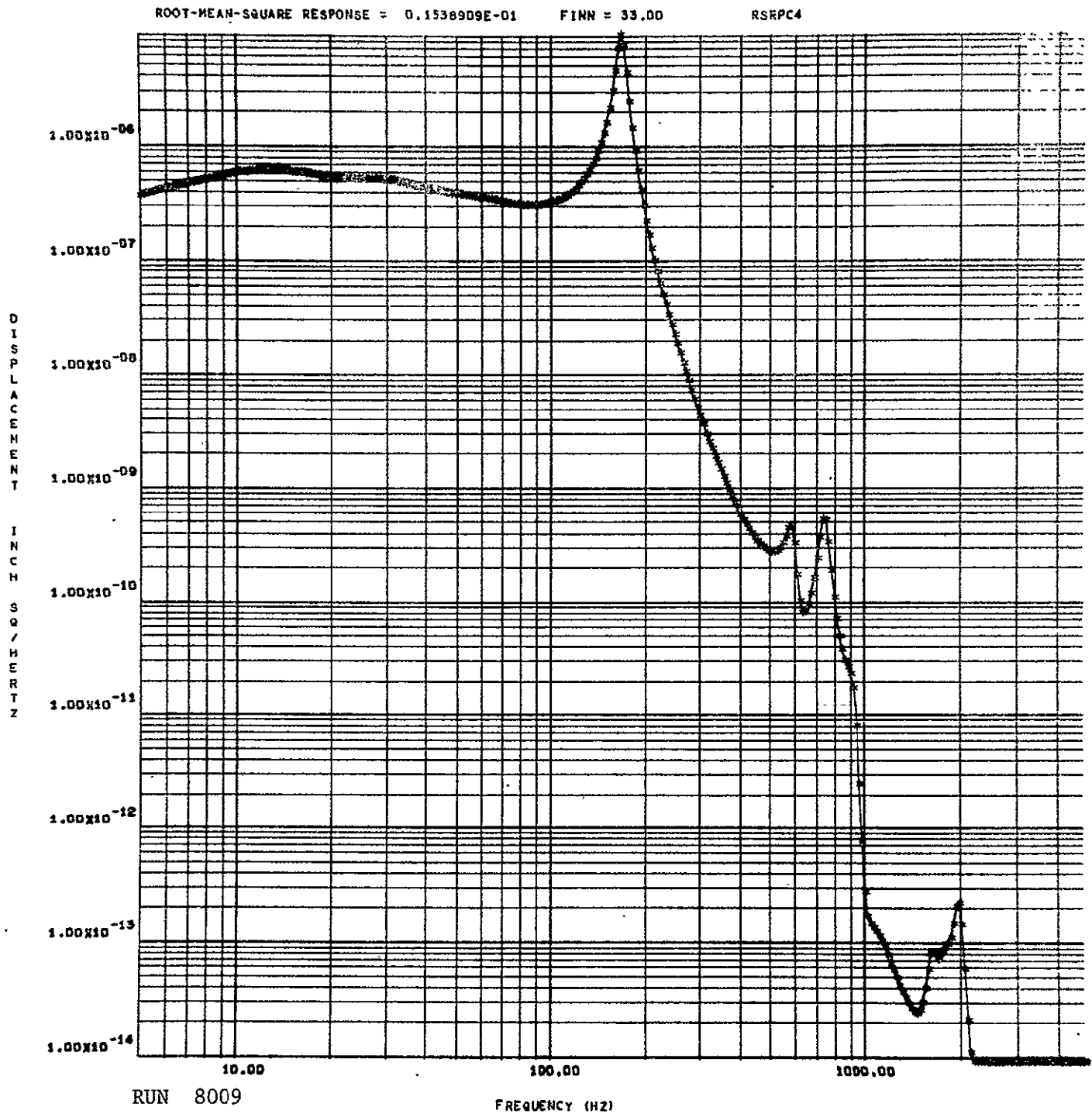
FIGURE 37   DISPLACEMENT SPECTRAL DENSITY AT CENTER OF PANEL,
RADIUS OF CURVATURE   a = 100 INCHES

ROOT-MEAN-SQUARE RESPONSE = 0.7809841E-02   FINN = 33.00   RSRPC4
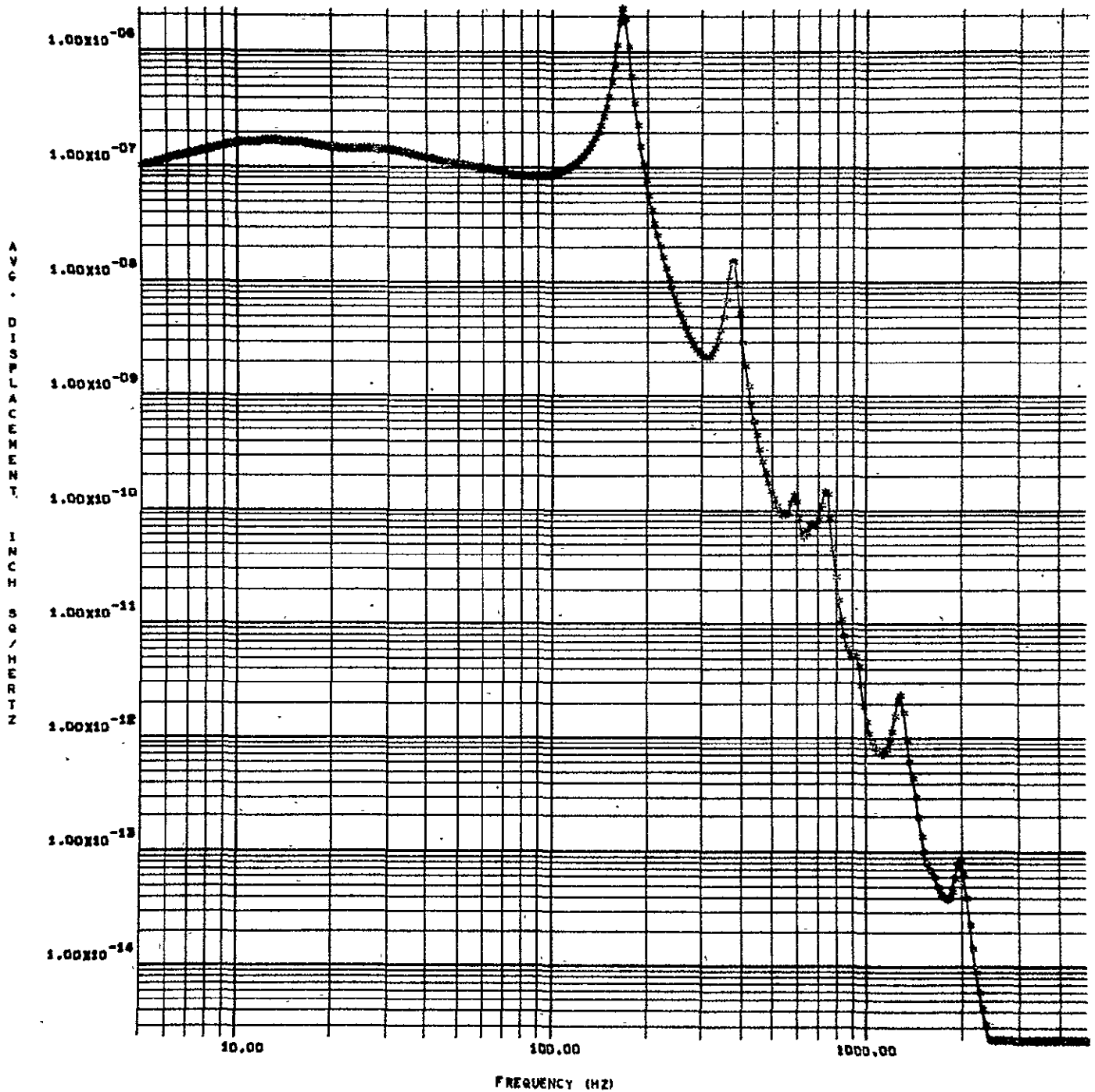
FIGURE 38   AVERAGE DISPLACEMENT SPECTRAL DENSITY OVER WHOLE
PANEL, RADIUS OF CURVATURE a = 100 INCHES

RUN 8009
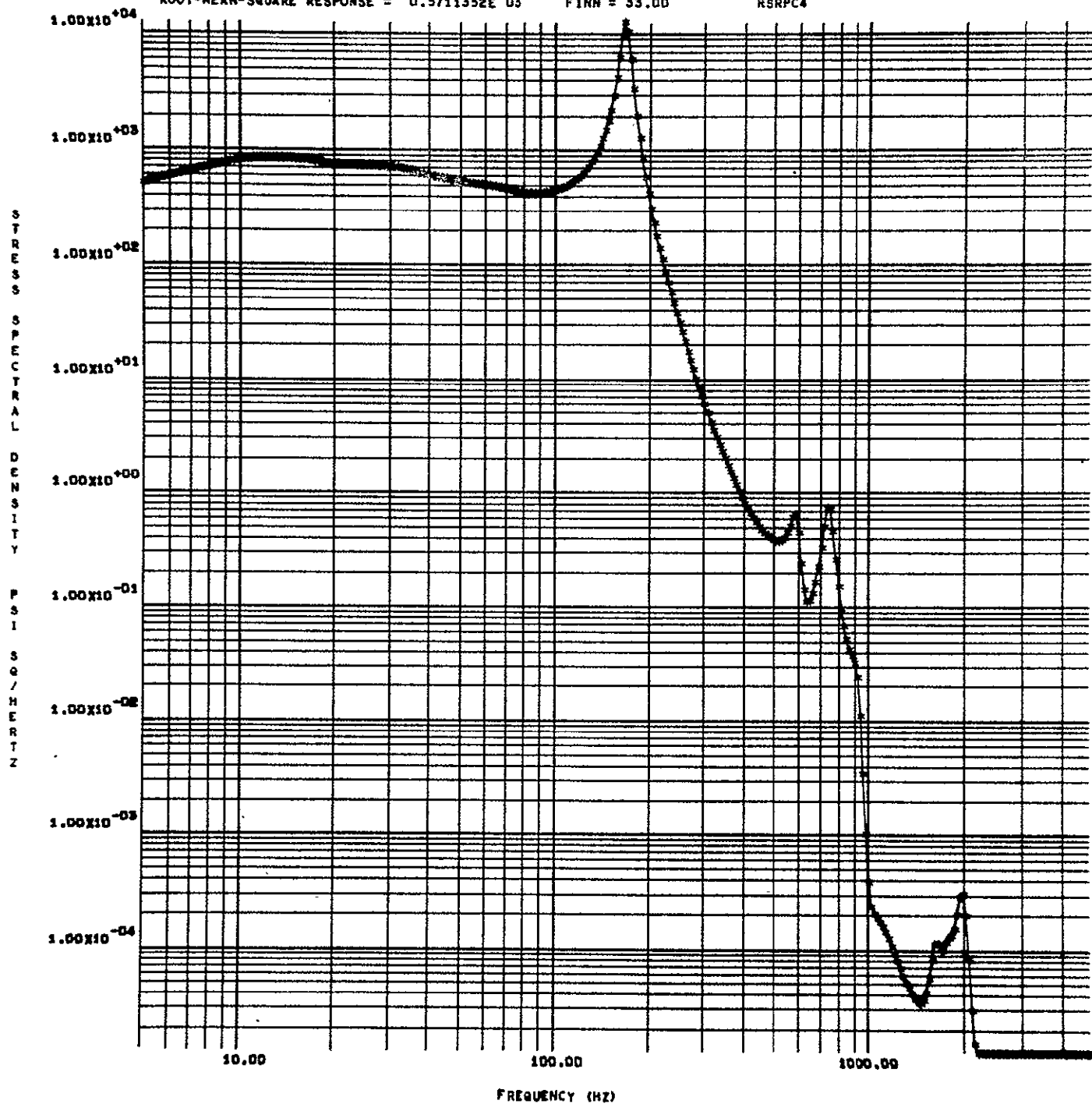
FIGURE 39   STRESS SPECTRAL DENSITY AT CENTER OF PANEL,
RADIUS OF CURVATURE a = 100 INCHES

118
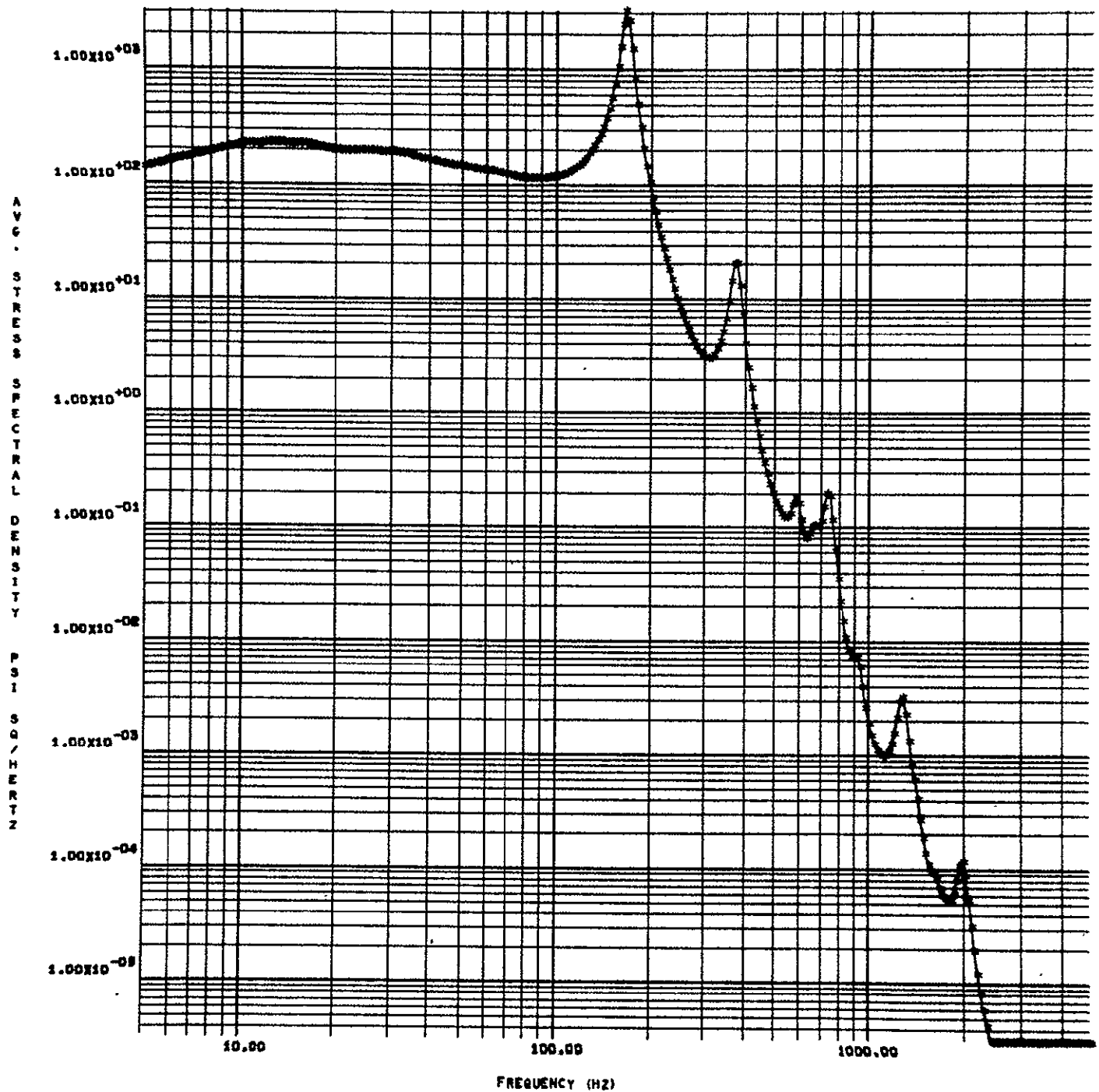
FIGURE 40   AVERAGE STRESS SPECTRAL DENSITY OVER WHOLE PANEL,
RADIUS OF CURVATURE a = 100 INCHES

PANEL DATA: LENGTH = 47.5 INCHES
WIDTH = 58.4 INCHES
THICKNESS = 0.75 INCH
YOUNG'S MODULUS = 10 X 10^6 lbf/in^2
POISSON'S RATIO = 0.287
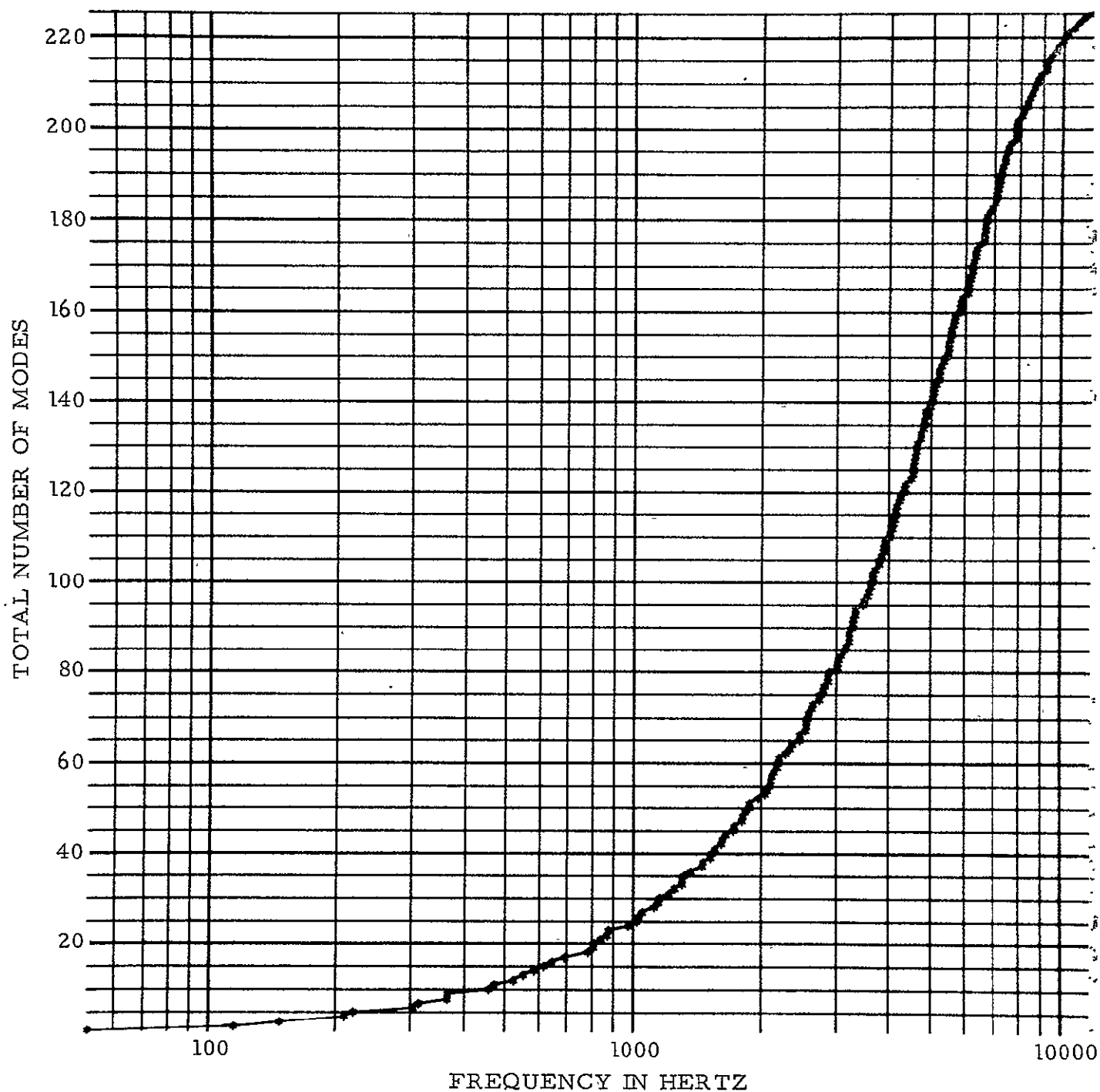
FIGURE 41   NUMBER OF MODES AS A FUNCTION OF FREQUENCY OF A SIMPLY
SUPPORTED UNIFORM RECTANGULAR PANEL
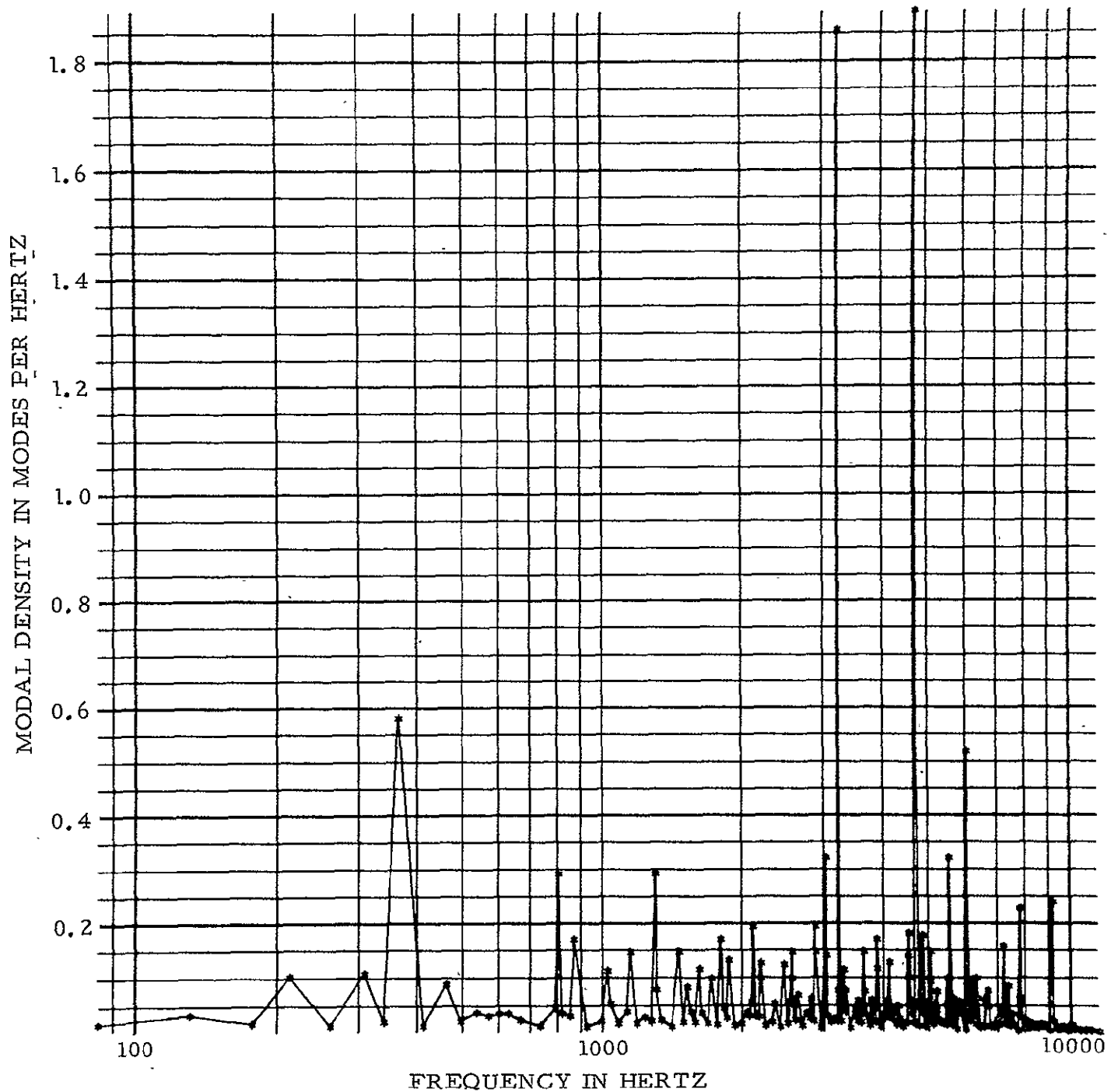
FIGURE 42   MODAL DENSITY OF A SIMPLY SUPPORTED
UNIFORM RECTANGULAR PANEL

c = 13500 in/sec.

f = 100 Hertz
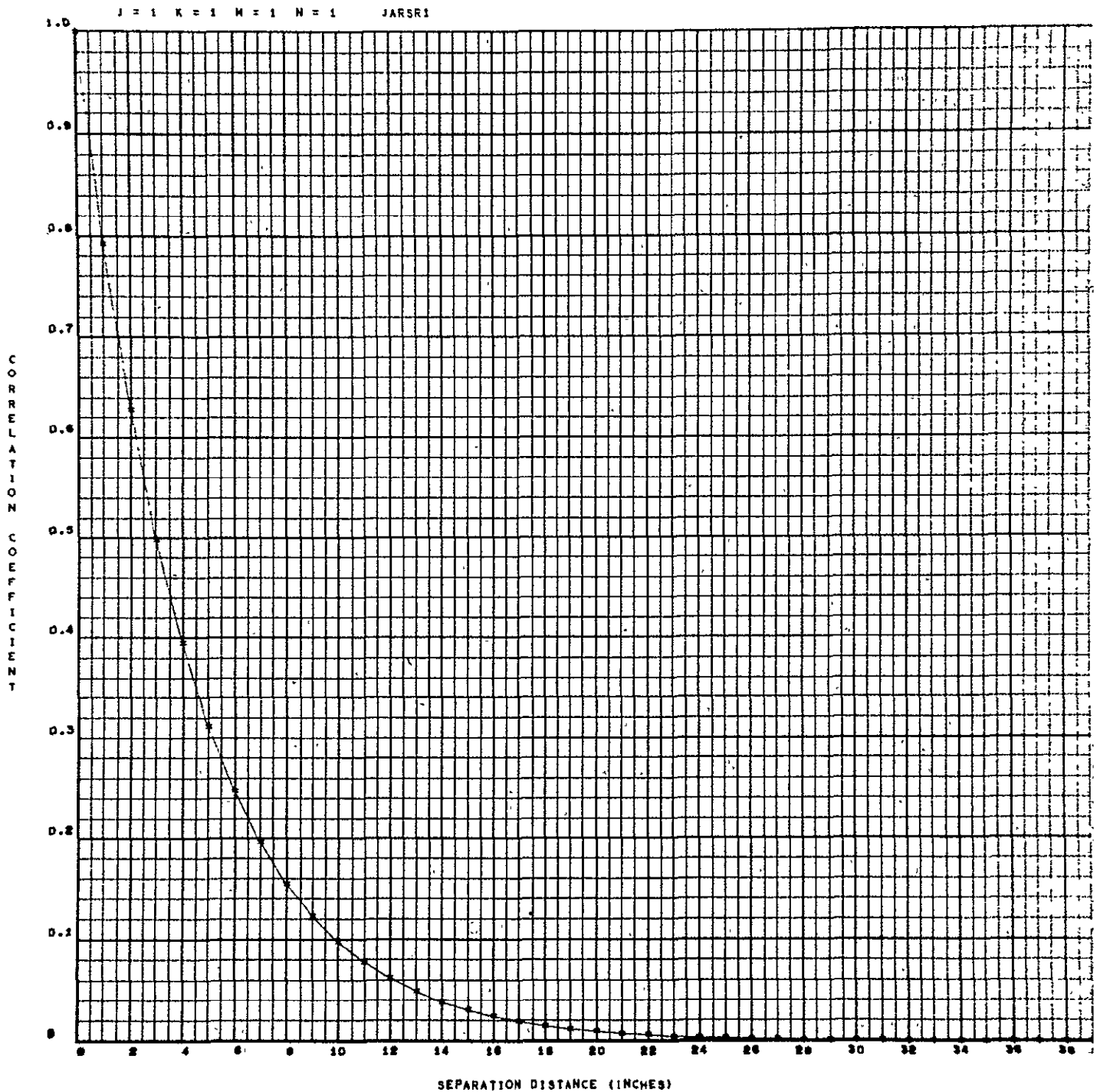
FIGURE 43. PLOT OF EXPONENTIALLY DECAYING CORRELATION FUNCTION WITH
DECAY CONSTANT A = 5

c = 13500 in./sec.
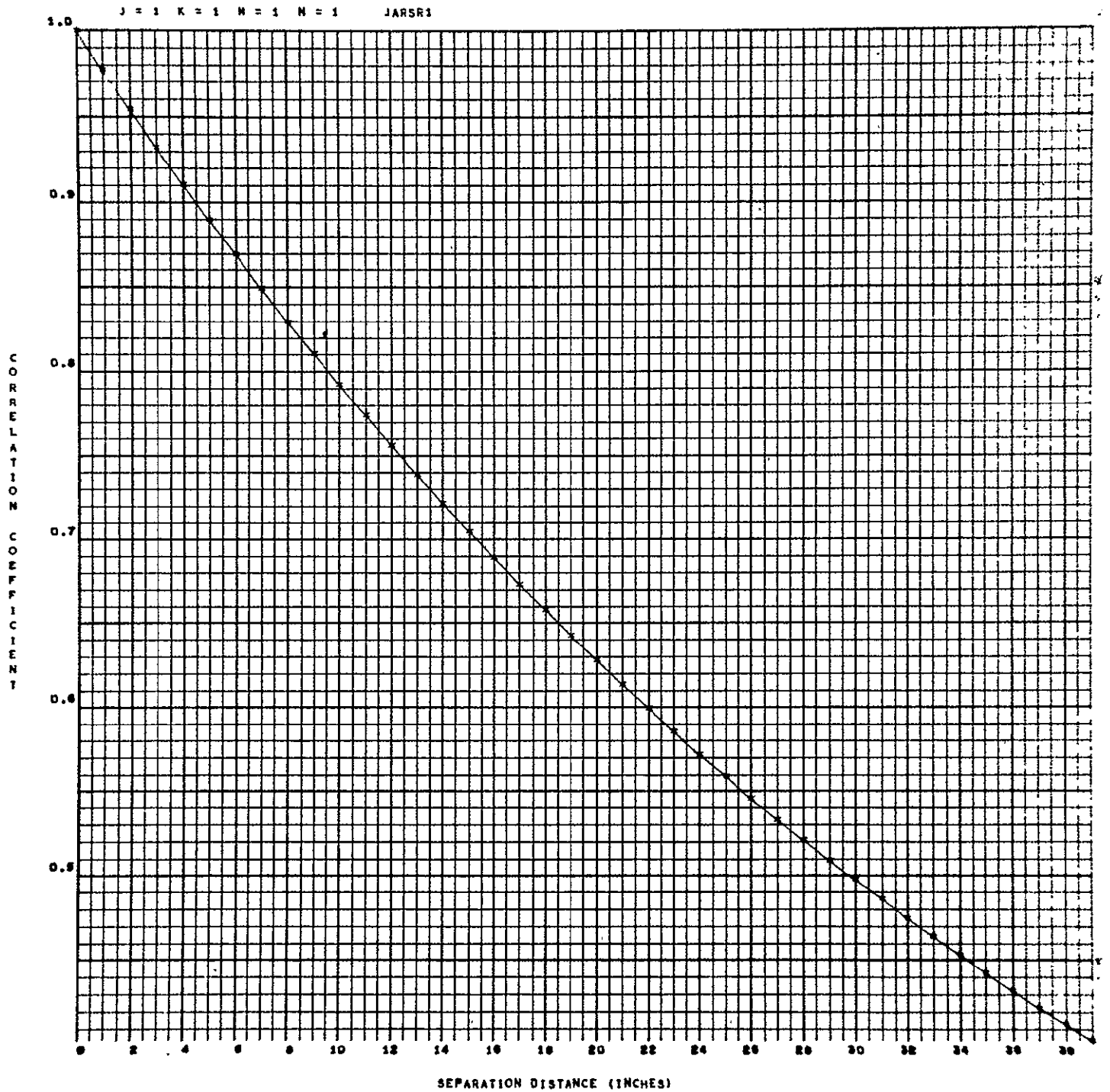
f = 100 Hertz

FIGURE 44. PLOT OF EXPONENTIALLY DECAYING CORRELATION FUNCTION WITH
DECAY CONSTANT A = 0.5

c = 13500 in./sec.

f = 100 Hertz
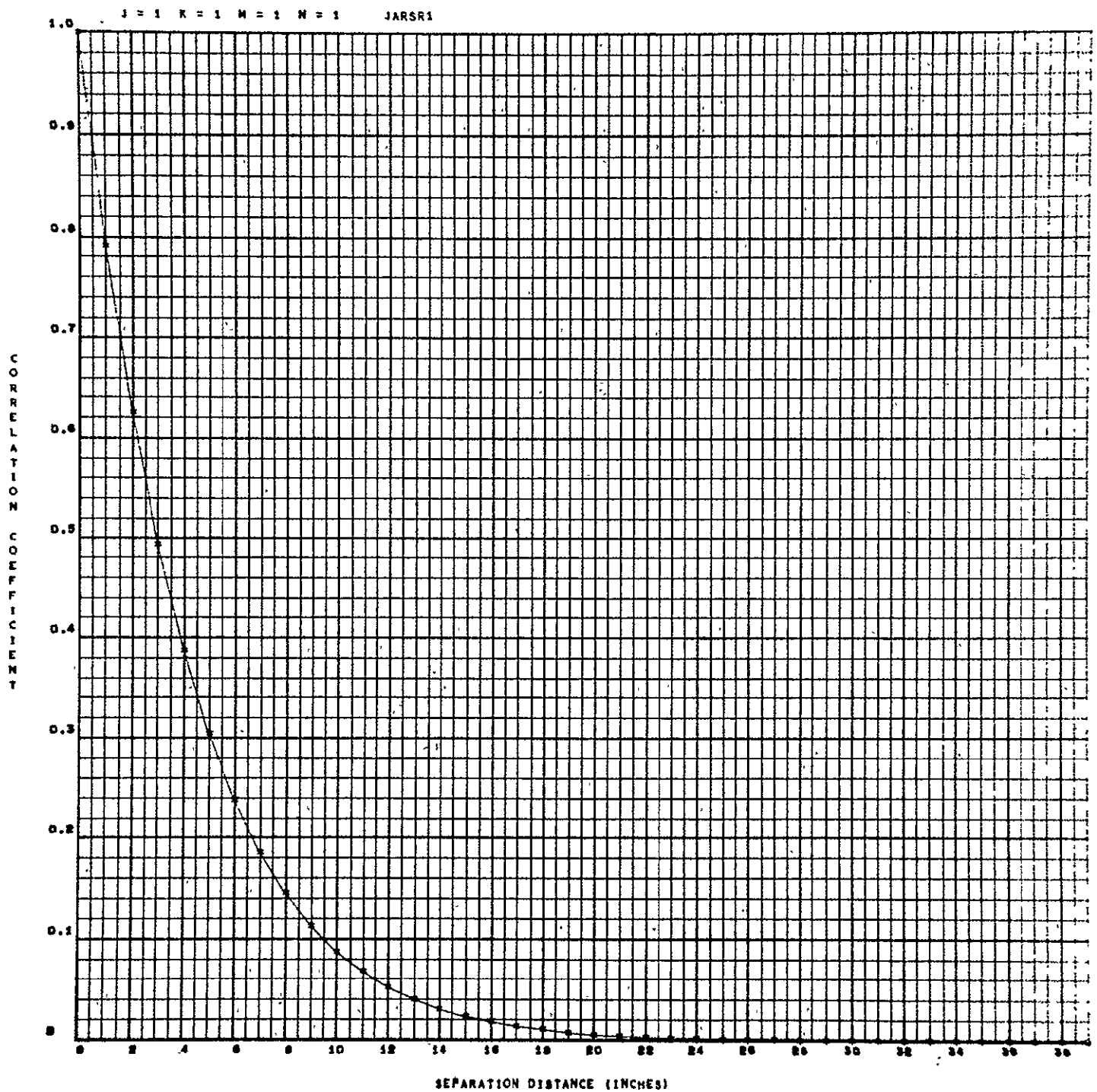
FIGURE 45.   PLOT OF SINUSOIDAL DECAYING CORRELATION FUNCTION WITH DECAY
              CONSTANT A = 5

c = 13500 in./sec.

f = 100 Hertz
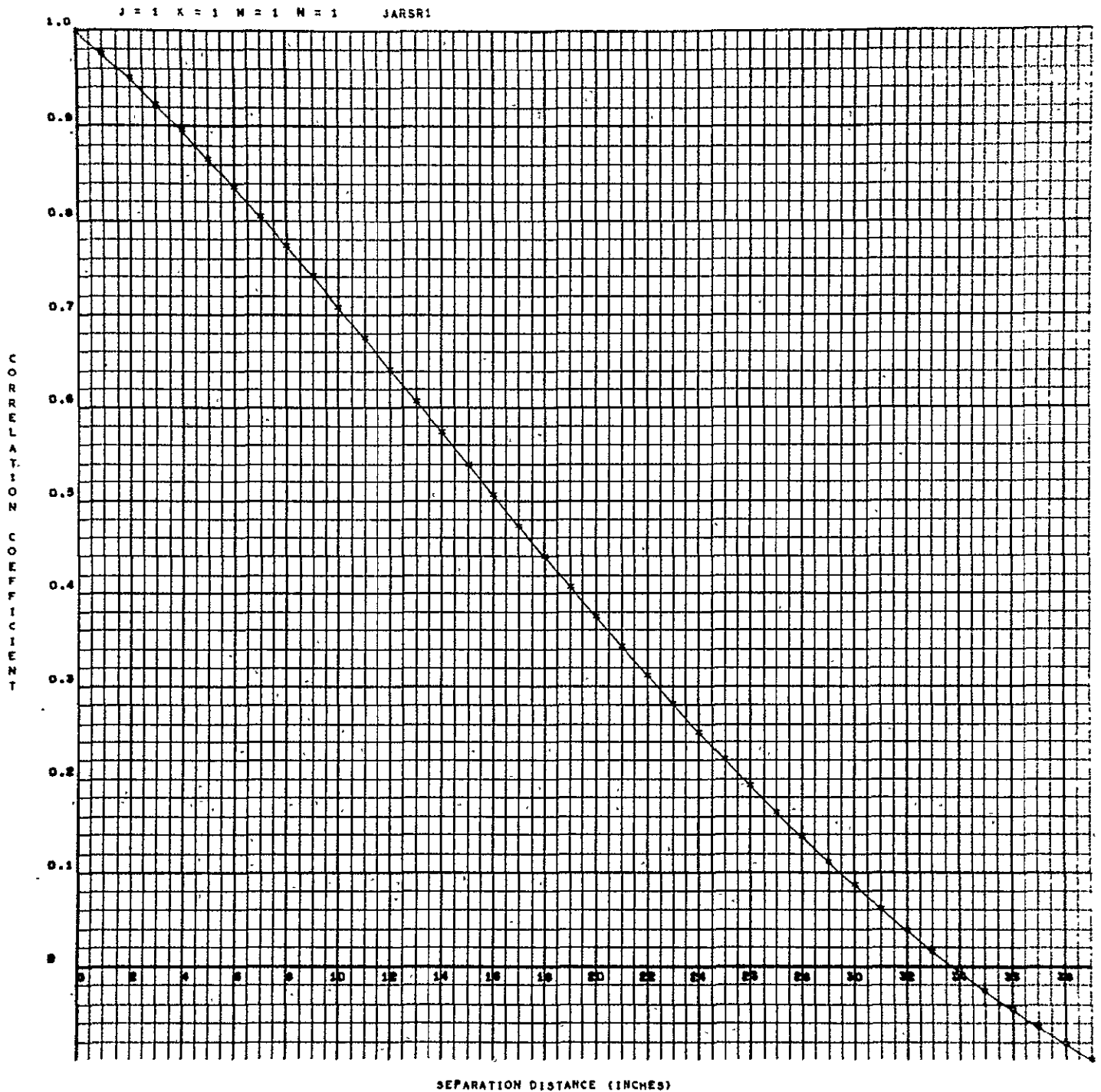
FIGURE 46.   PLOT OF SINUSOIDAL DECAYING CORRELATION FUNCTION WITH DECAY
             CONSTANT A = 0.5

125
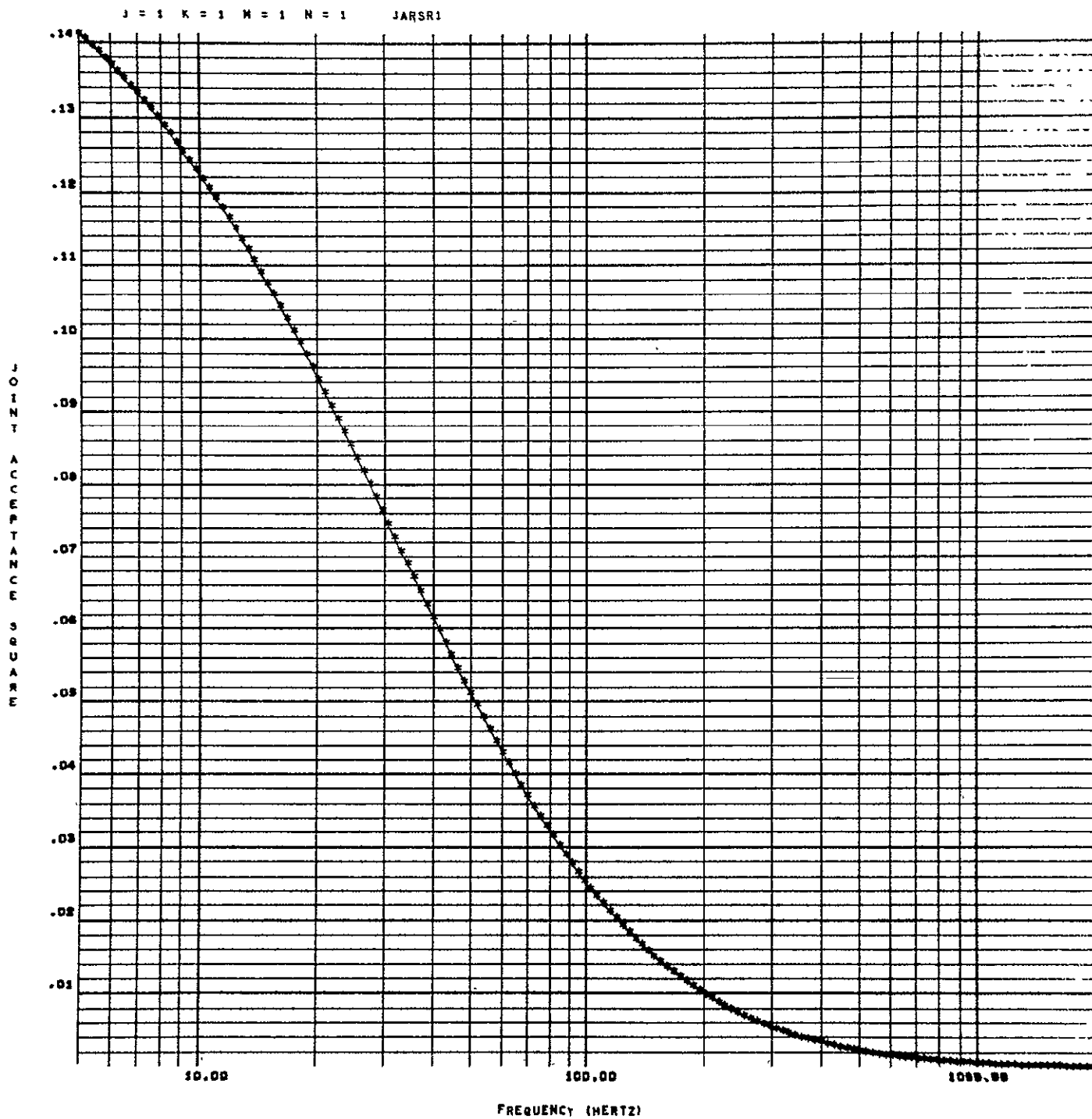
FIGURE 47.   JOINT ACCEPTANCE, EXPONENTIALLY DECAYING CORRELATION FUNCTION
MODE INDICES: j = 1, k - 1, m - 1, n = 1
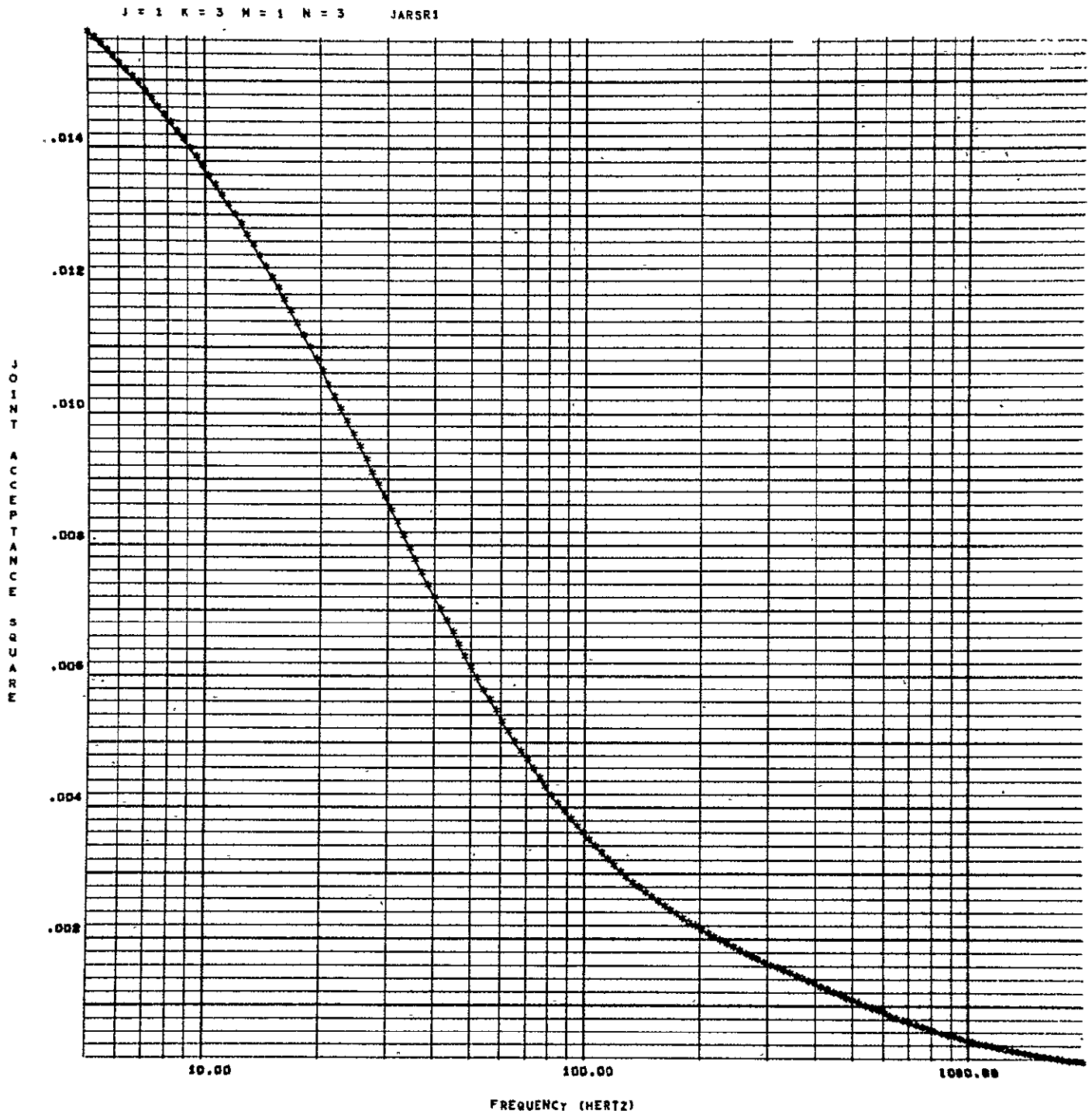
FIGURE 48.   JOINT ACCEPTANCE, EXPONENTIAL DECAYING CORRELATION FUNCTION,
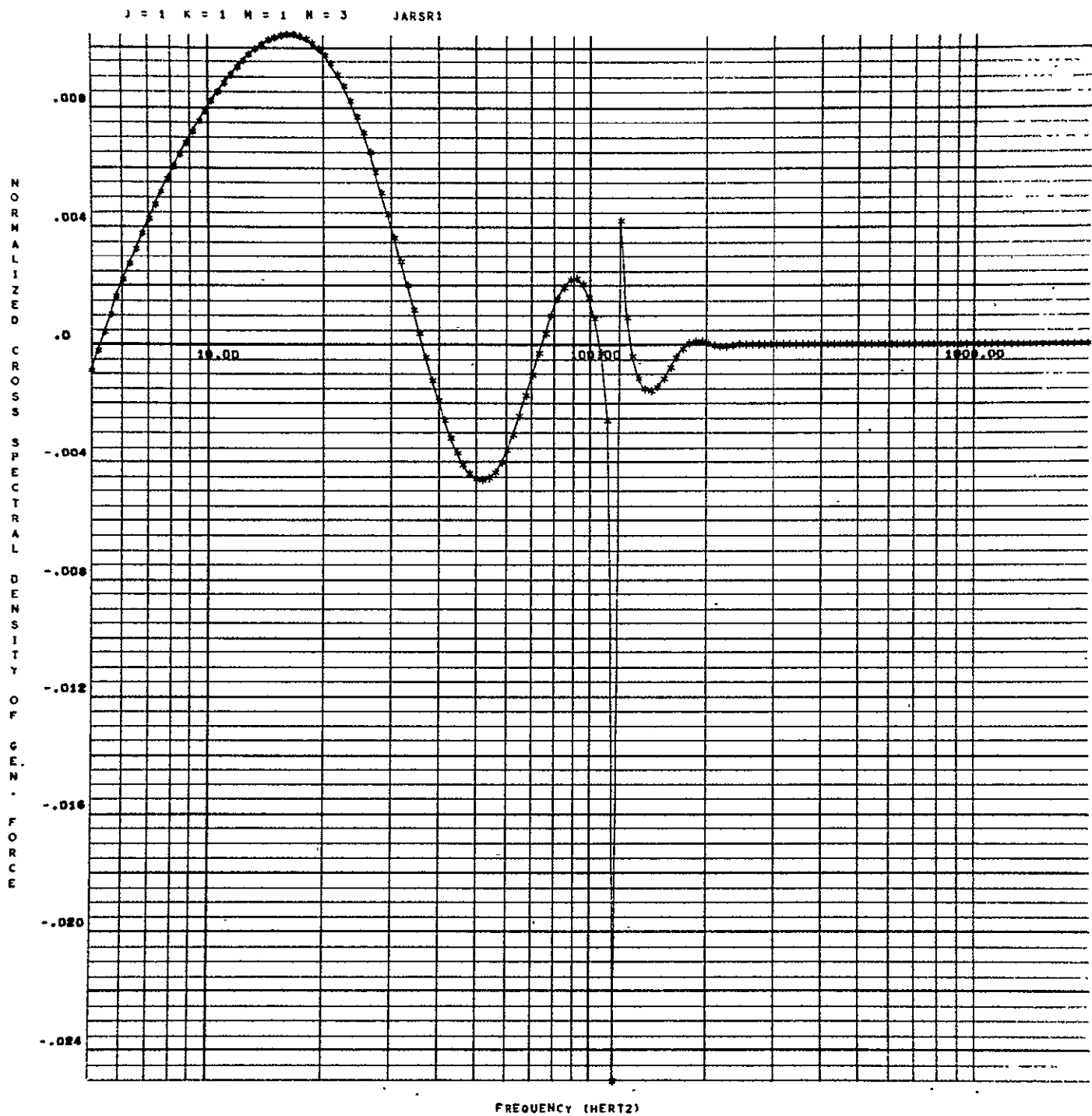MODE INDICES: j = 1, k = 3, m = 1, n = 3

127

FIGURE 49. JOINT ACCEPTANCE, EXPONENTIALLY DECAYING CORRELATION FUNCTION, MODE INDICES: j = 1, k = 1, m = 1, n = 3

128
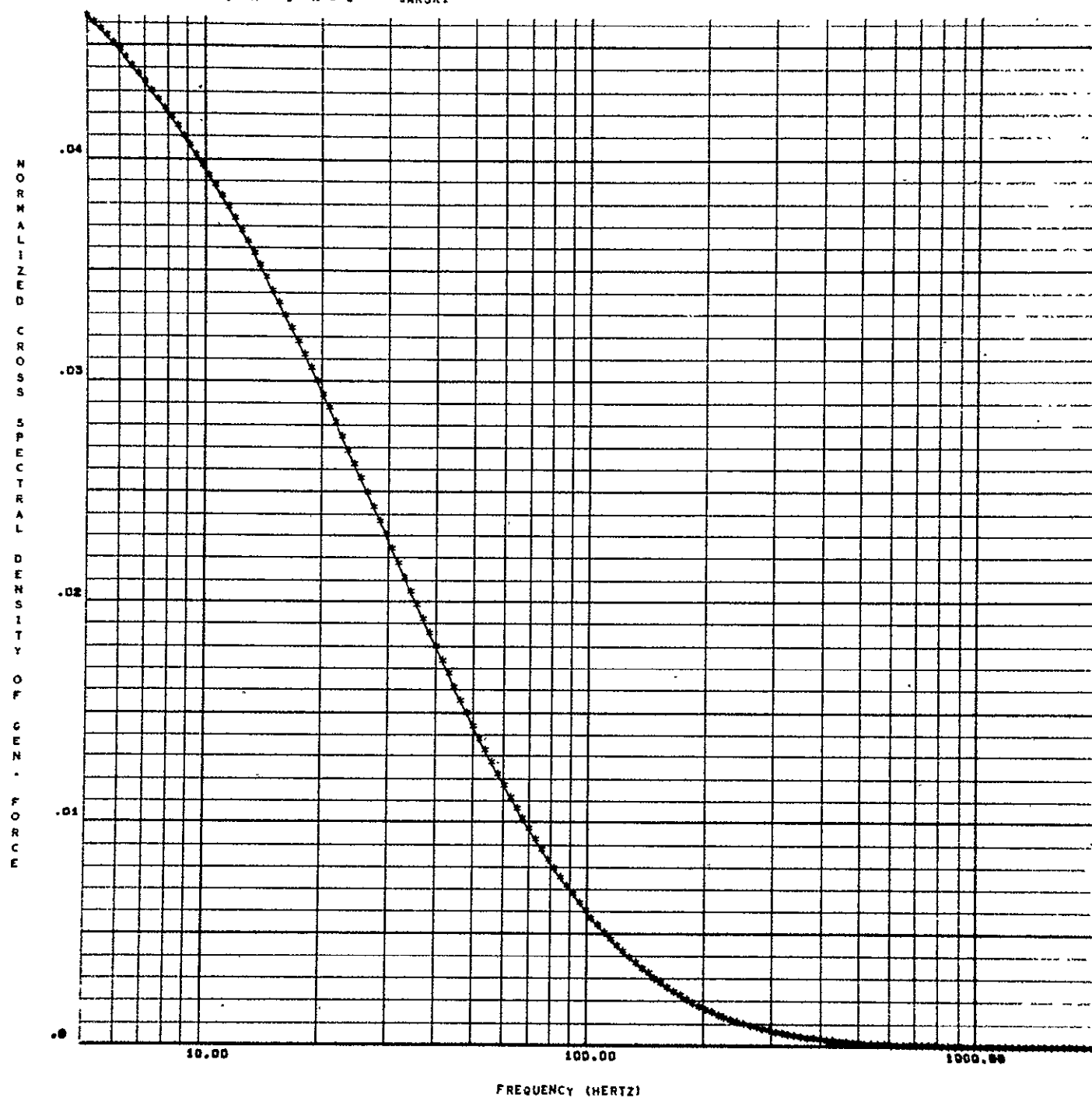
FIGURE 50. NORMALIZED SPECTRAL DENSITY OF GENERALIZED FORCE, EXPONENTIALLY DECAYING CORRELATION FUNCTION, MODE INDICES: 1, 1, 1, 3
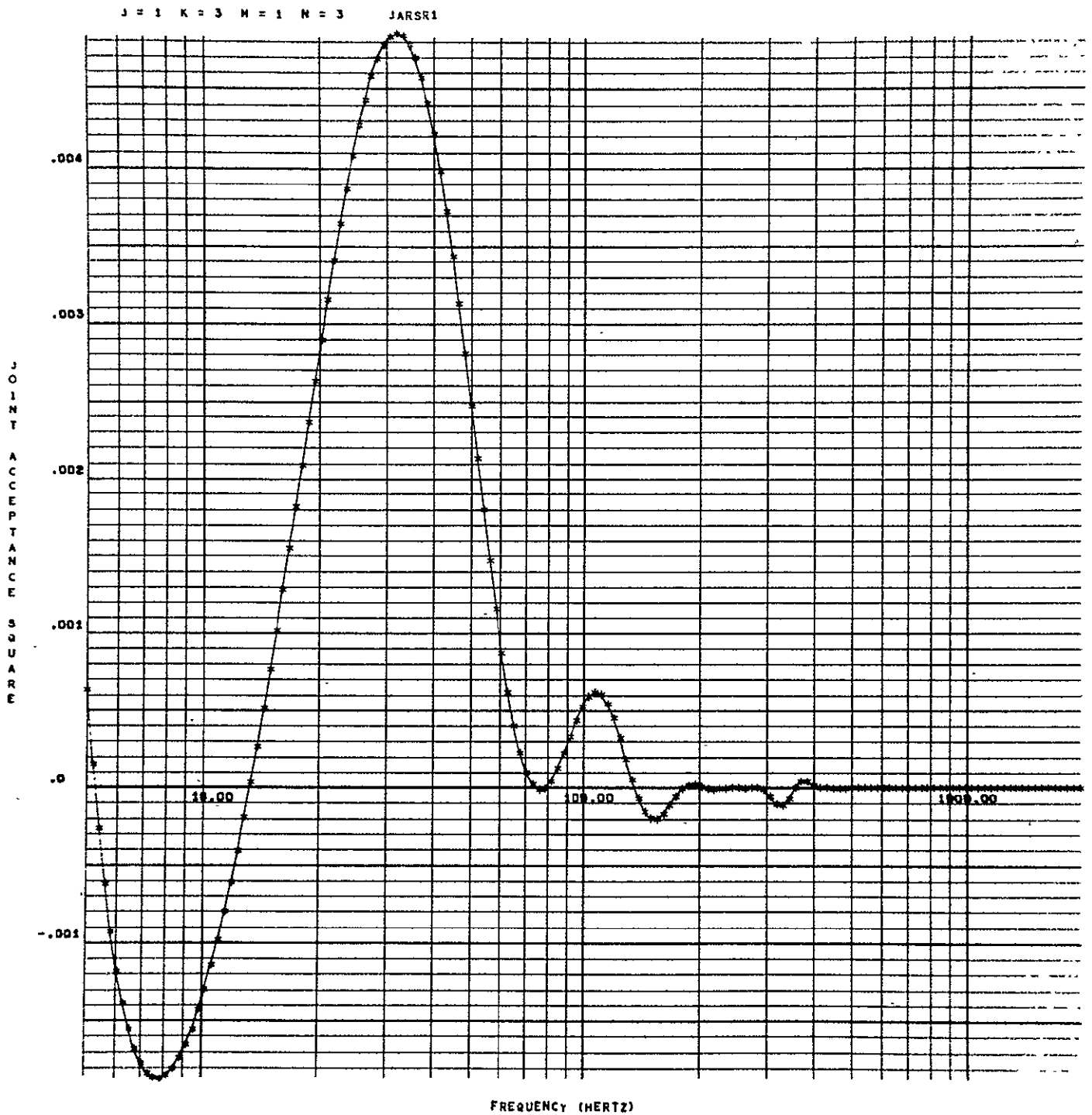
129

$A_1 = 5$
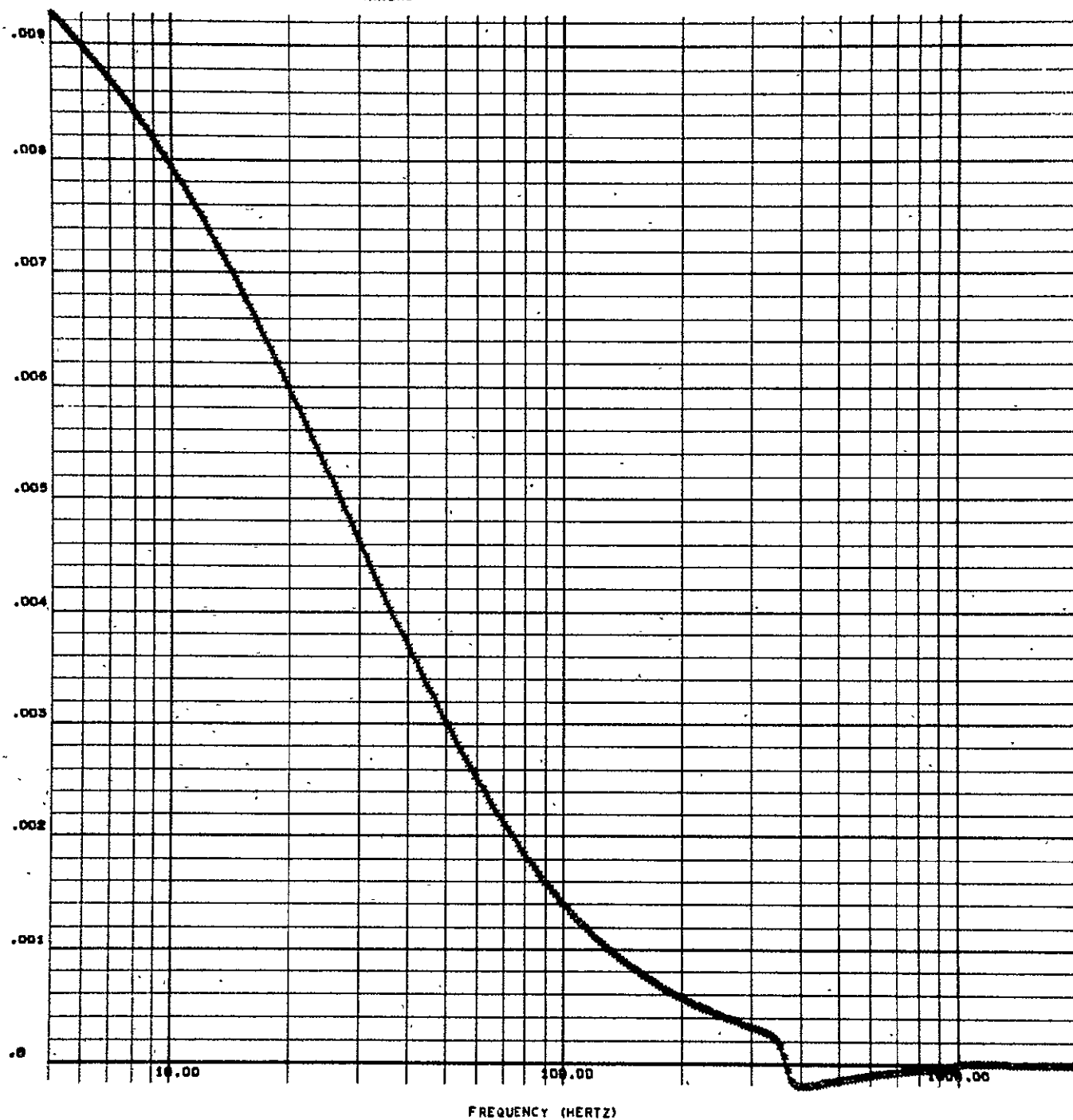
$A_2 = 0.5$ RUN 8208

FIGURE 51.   JOINT ACCEPTANCE, EXPONENTIALLY DECAYING CORRELATION FUNCTION
MODE INDICES: j = 1, k = 3, m = 1, n = 5

130

$A_1 = 5$

$A_2 = 0.5$

RUN 8208

J = 1 K = 3 M = 1 N = 5   JARSR1
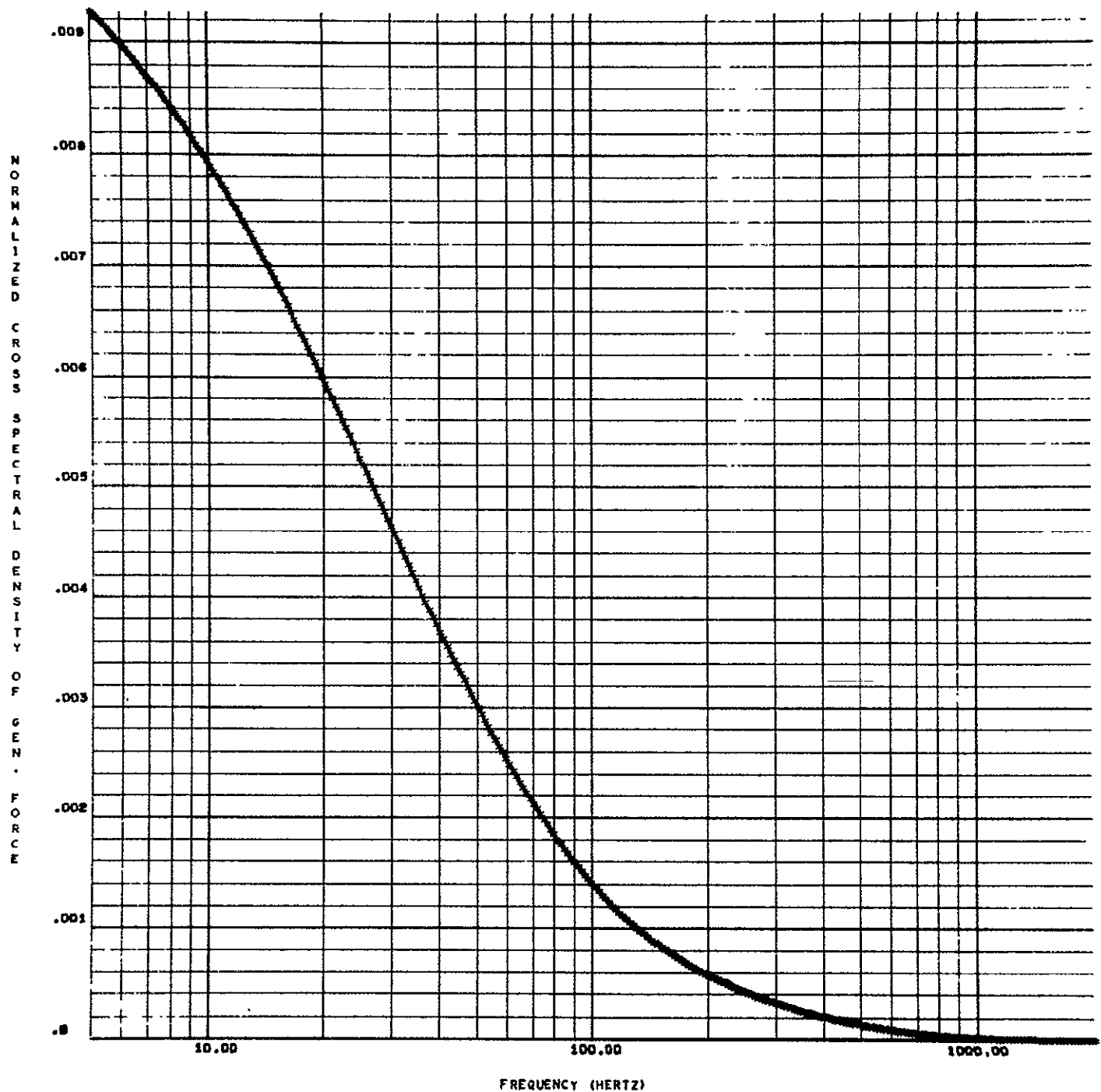
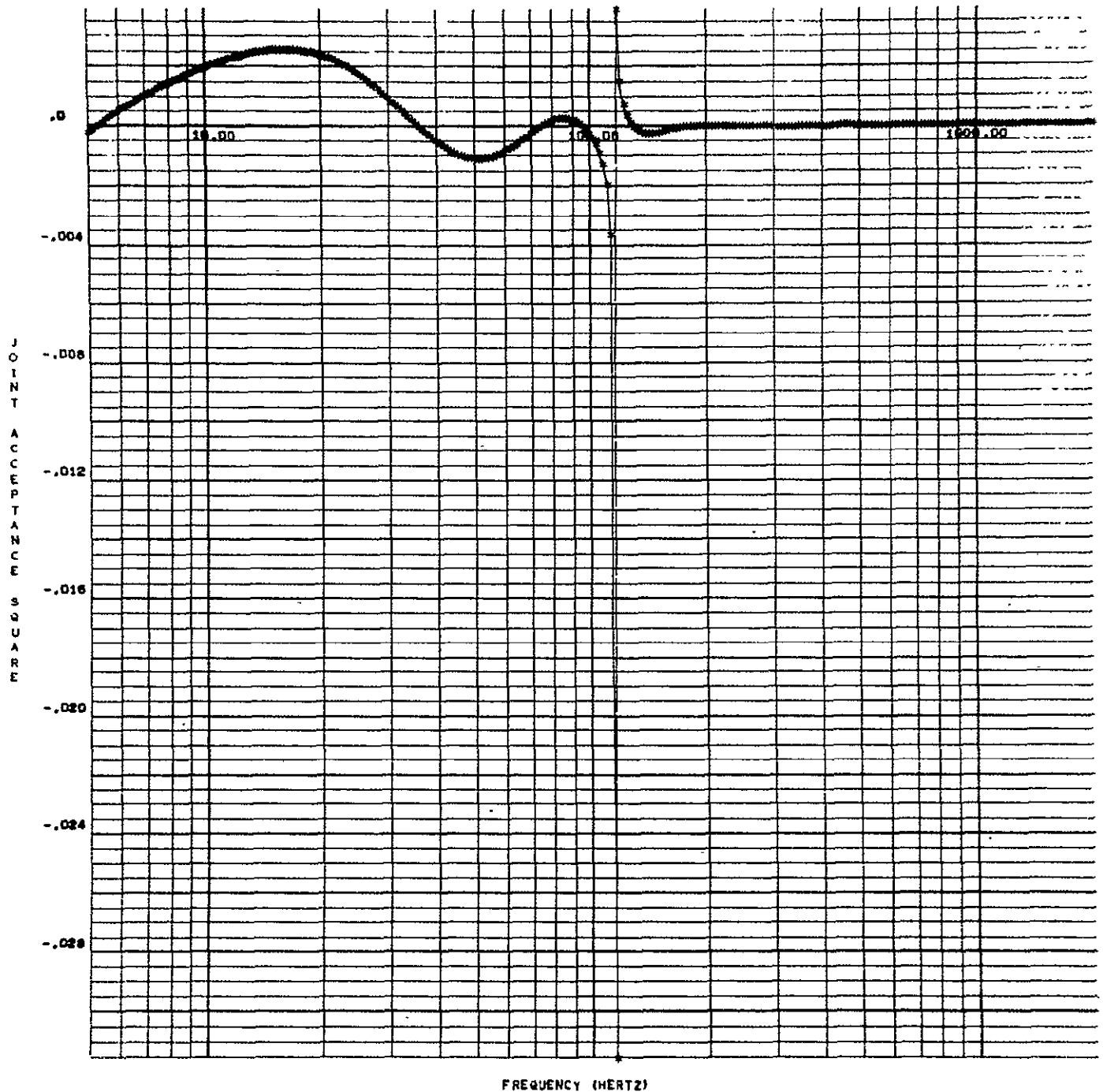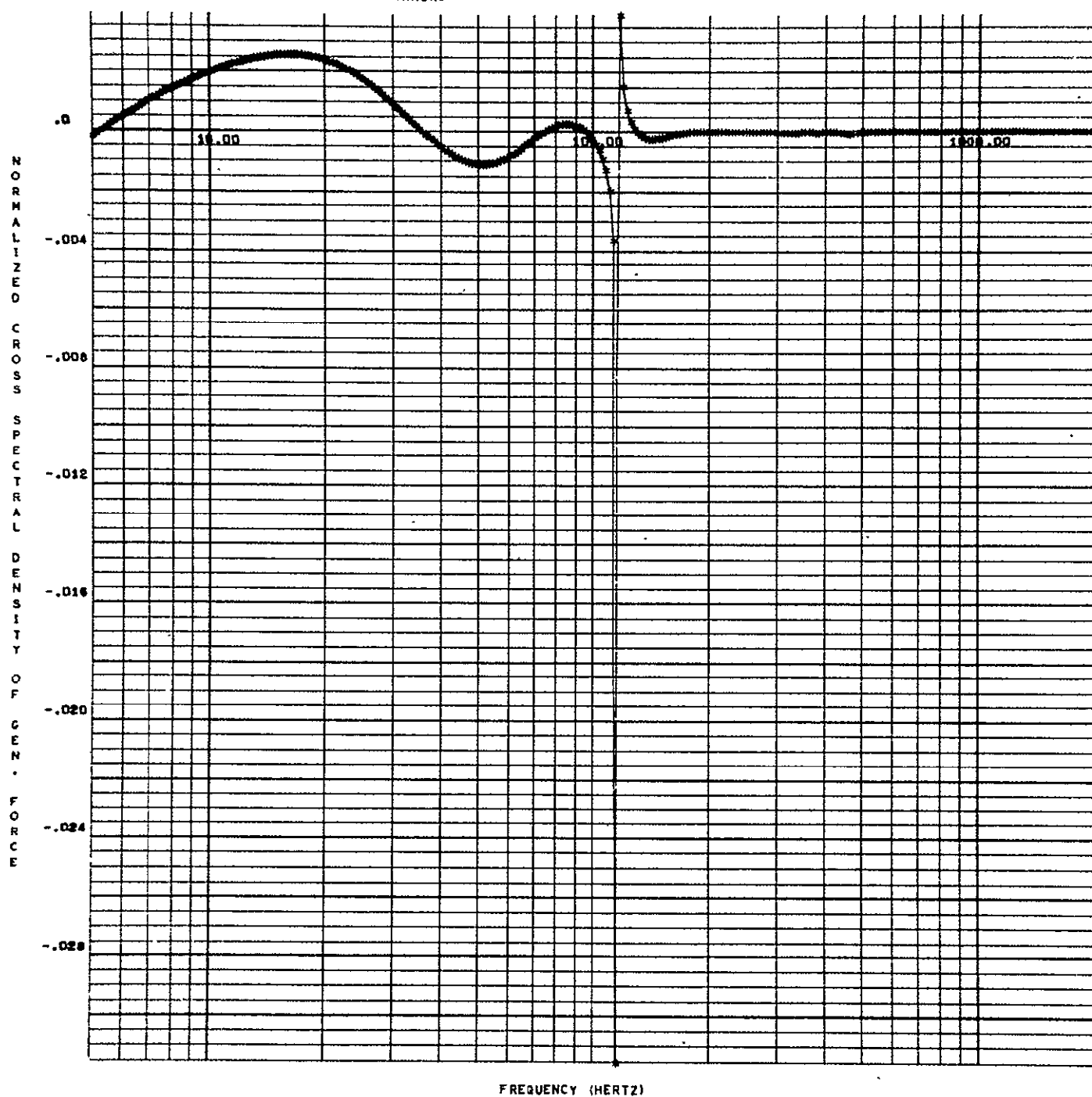FIGURE 52.   NORMALIZED SPECTRAL DENSITY OF GENERALIZED FORCE, EXPONENTIALLY
DECAYING CORRELATION FUNCTION, MODE INDICES: 1, 3, 1, 5

131
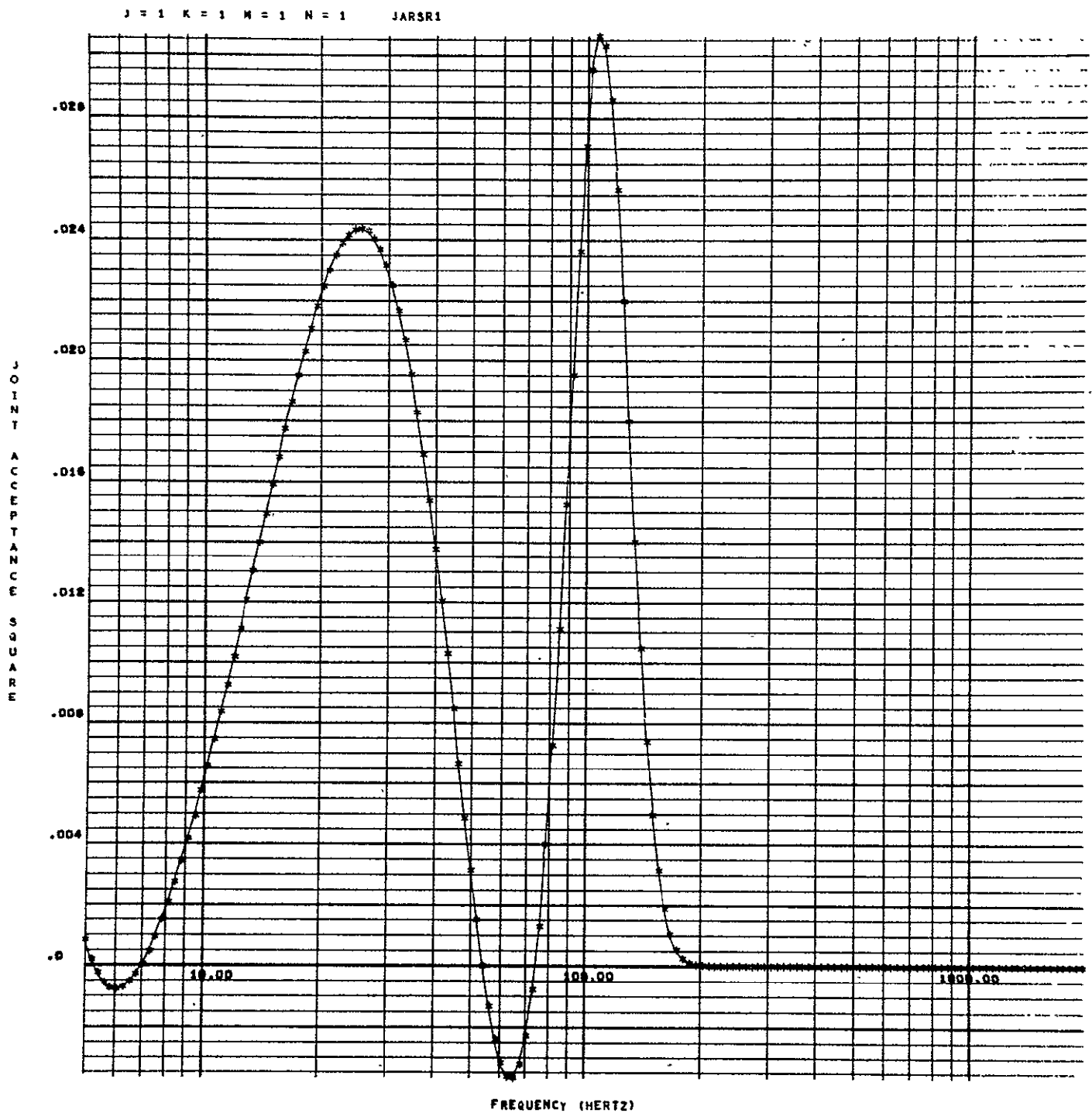
FIGURE 53. JOINT ACCEPTANCE, SINUSOIDAL DECAYING CORRELATION FUNCTION,
MODE INDICES: j = 1, k = 1, m = 1, n = 1

132
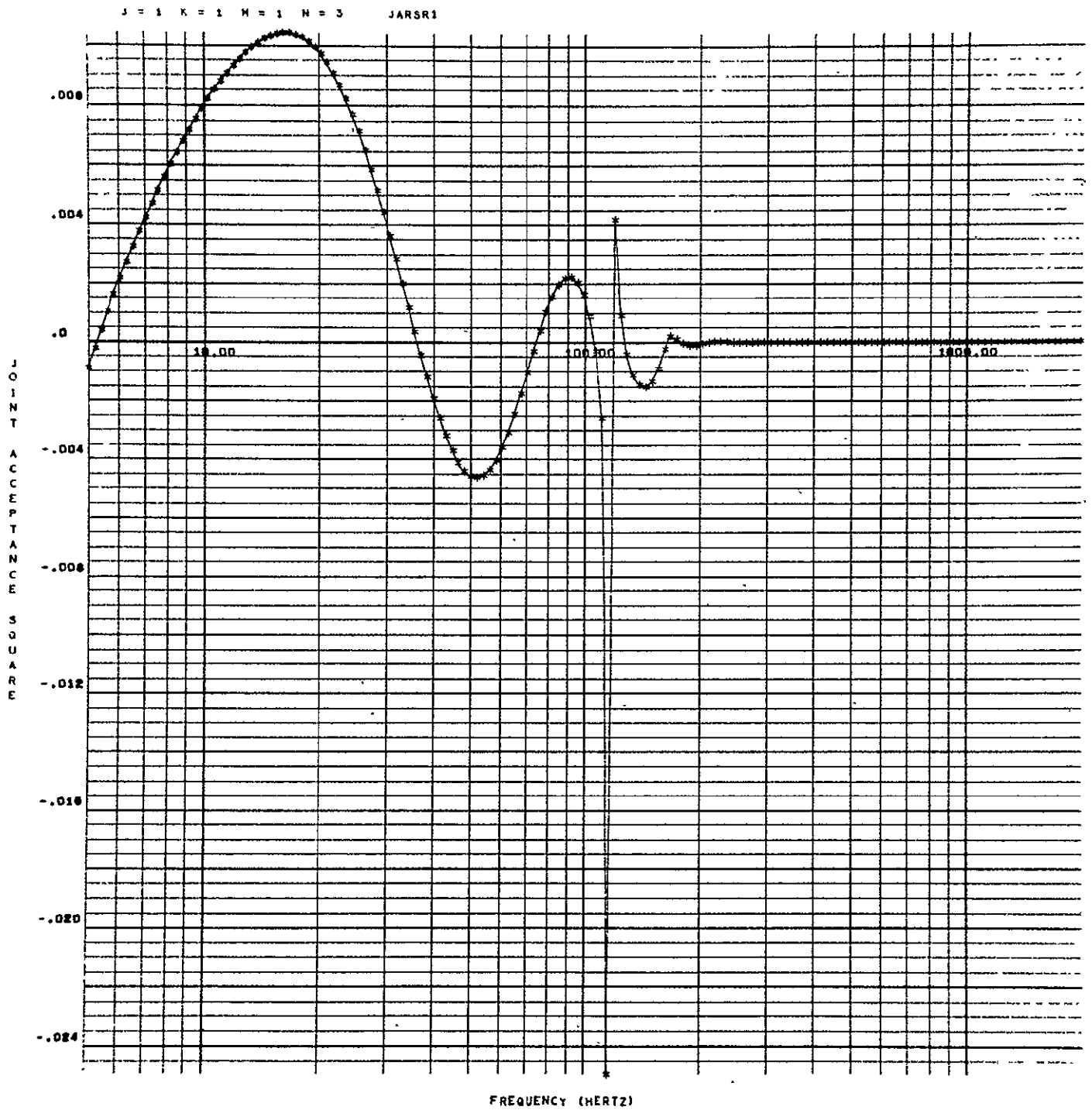
FIGURE 54. JOINT ACCEPTANCE, SINUSOIDAL DECAYING CORRELATION FUNCTION,
MODE INDICES: j = 1, k = 1, m= 1, n = 3

FIGURE 55.   NORMALIZED CROSS SPECTRAL DENSITY OF GENERALIZED FORCE,
SINUSOIDAL DECAYING CORRELATION FUNCTION, MODE INDICES:
1, 1, 1, 3

134

FIGURE 56. JOINT ACCEPTANCE, SINUSOIDAL DECAYING CORRELATION FUNCTION,
MODE INDICES: j = 1, k= 3, m = 1, n = 3

$A_1 = 5$

$A_2 = 0.5$ RUN 8208

J = 1   K = 3   M = 1   N = 5   JARSR1

FIGURE 57.   JOINT ACCEPTANCE, SINUSOIDAL DECAYING CORRELATION FUNCTION,
MODE INDICES: j = 1, k = 3, m = 1, n = 5

136

$A_1 = 5$ RUN 8208

$A_2 = 0.5$

J = 1 K = 3 M = 1 N = 3   JARSR1

FIGURE 58. NORMALIZED CROSS SPECTRAL DENSITY OF GENERALIZED FORCE, SINUSOIDAL DECAYING CORRELATION FUNCTION, MODE INDICES: 1, 3, 1, 5
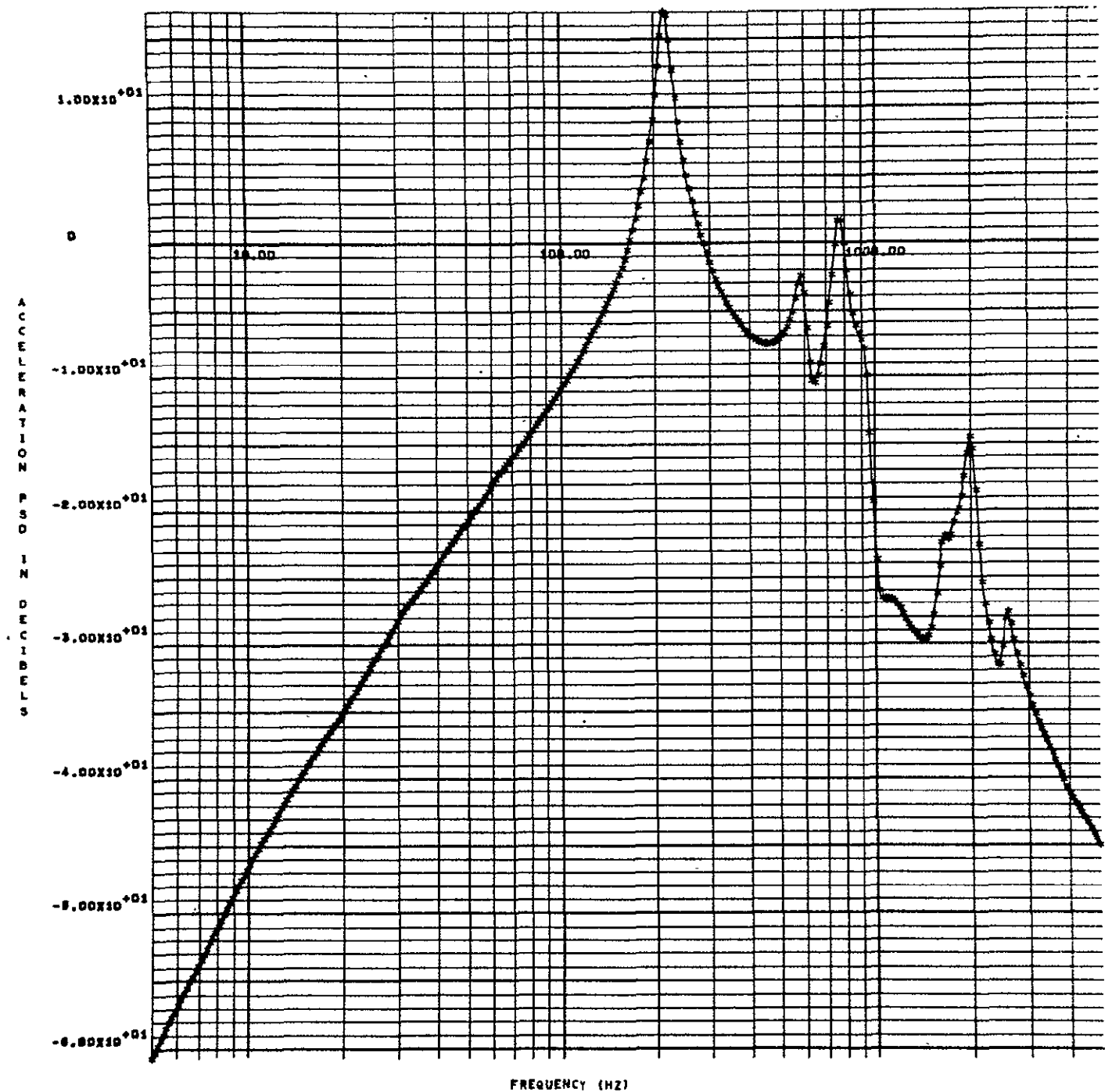
FIGURE 59. DECIBEL SCALE ACCELERATION SPECTRAL DENSITY AT CENTER OF
SIMPLY-SUPPORTED CURVED RECTANGULAR PANEL CROSS-REINFORCED
WITH STIFFENERS

138

RUN 3468
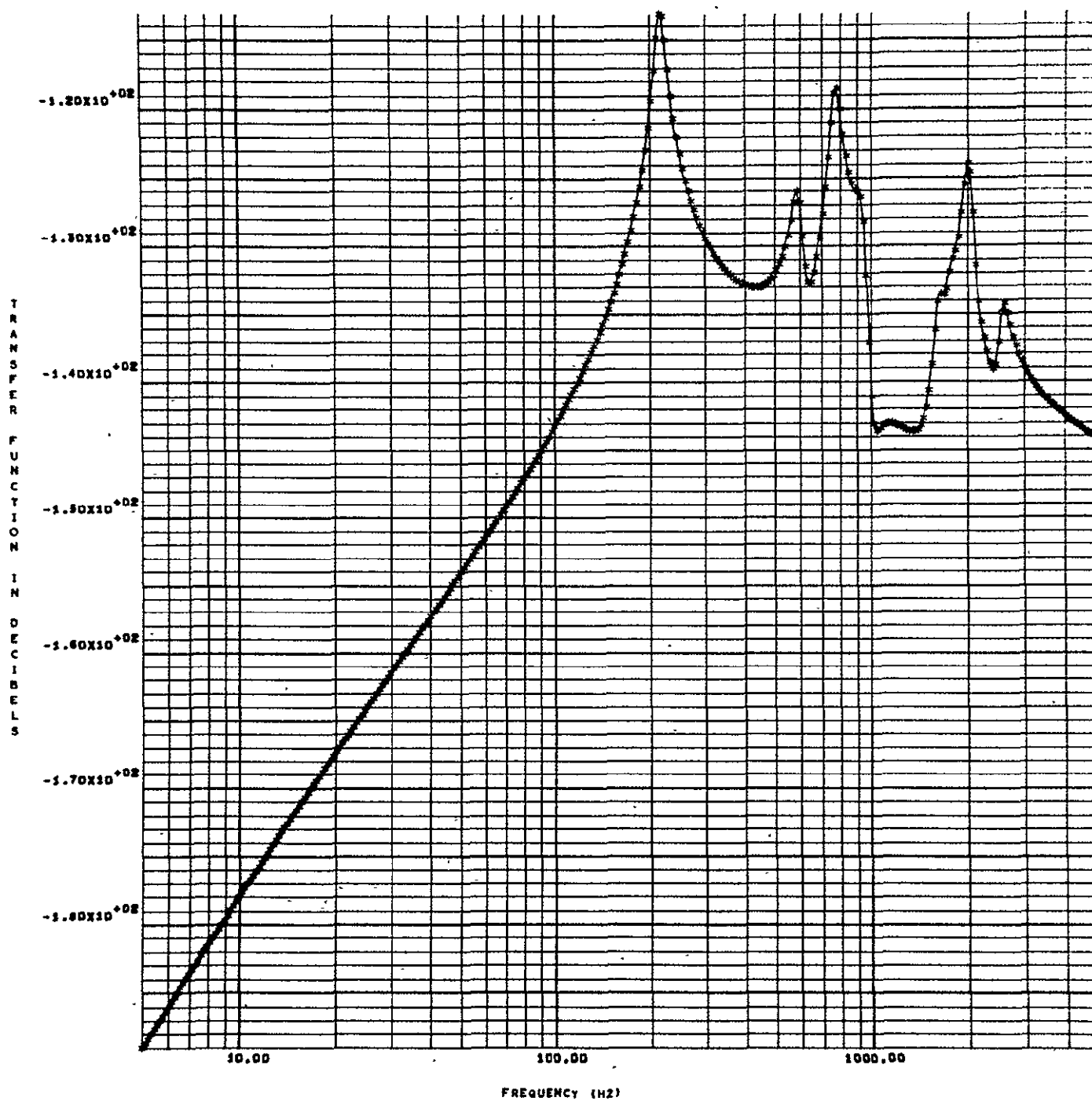
FIGURE 60 VIBRO-ACOUSTIC TRANSFER FUNCTION AT CENTER OF SIMPLY-
SUPPORTED CURVED RECTANGULAR PANEL CROSS-REINFORCED
WITH STIFFENERS

139
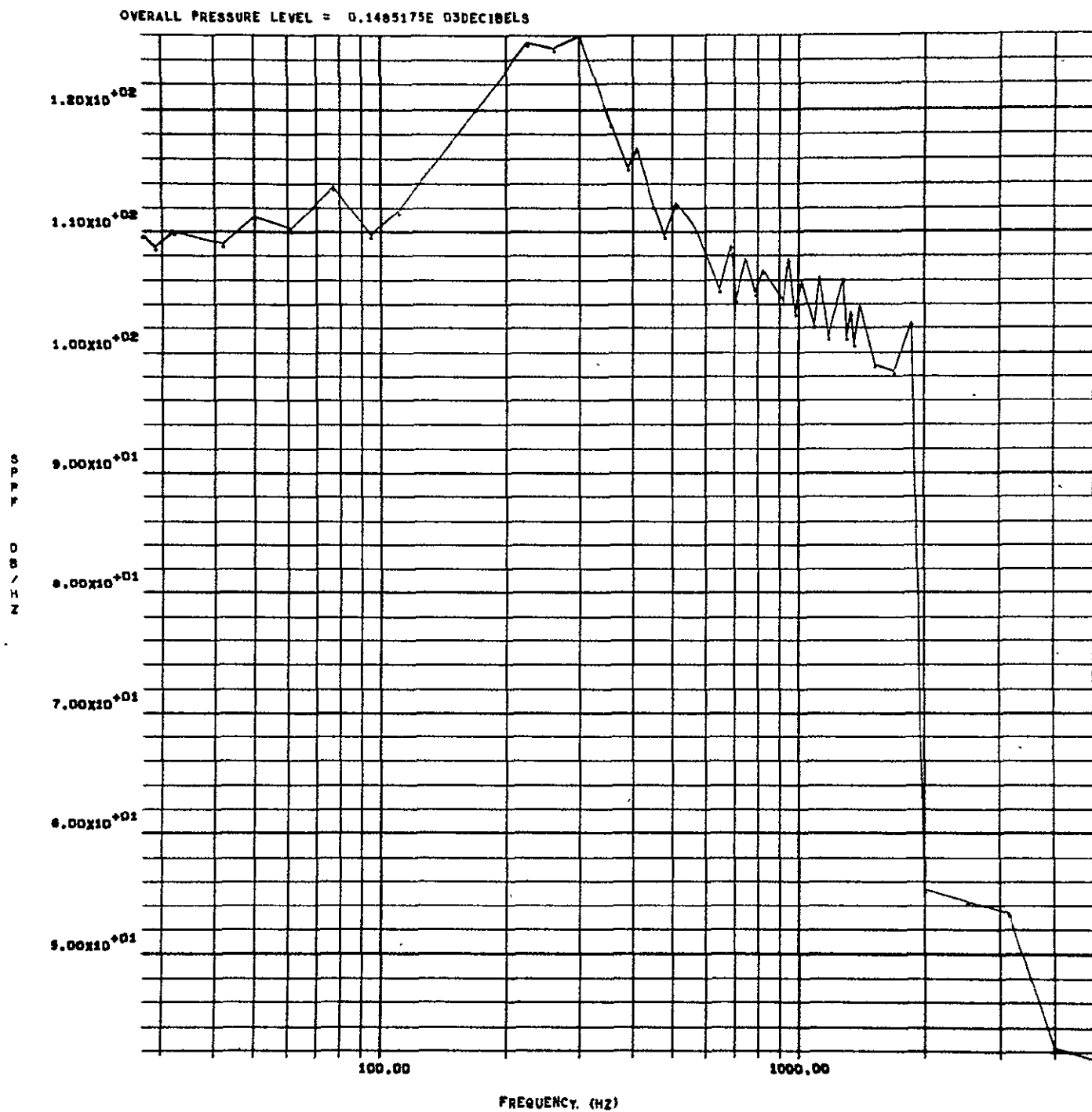
FIGURE 61. ACOUSTIC PRESSURE SPECTRAL DENSITY IN DECIBELS FOR FATIGUE
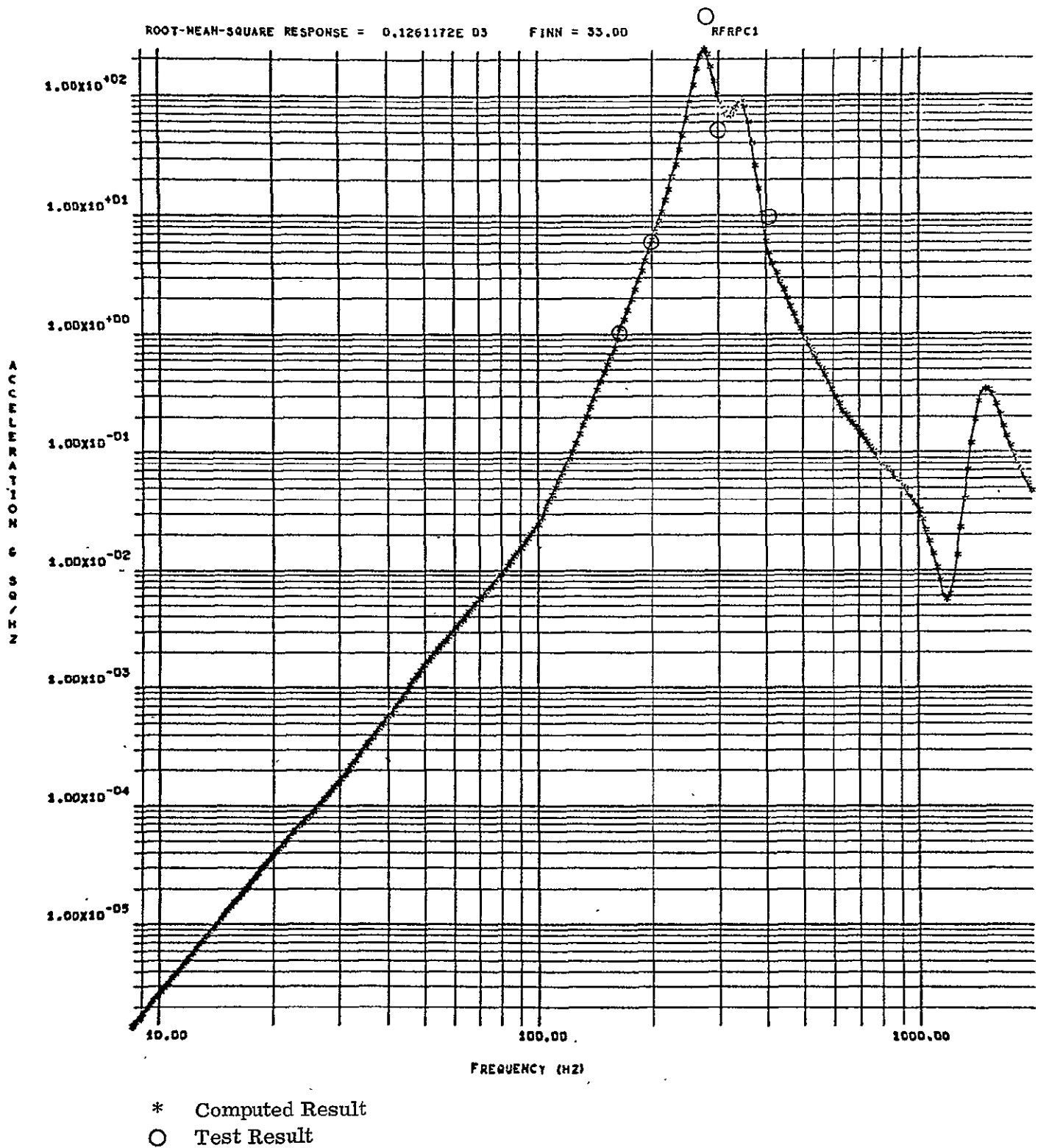TEST IN PROJECT NAS8-21425

140

ROOT-MEAN-SQUARE RESPONSE = 0.1261172E 03   FINN = 33.00   RFRPC1

FIGURE 62.   COMPARISON OF CALCULATED RESULT WITH
TEST RESULT, LOCATION NO. 9

141
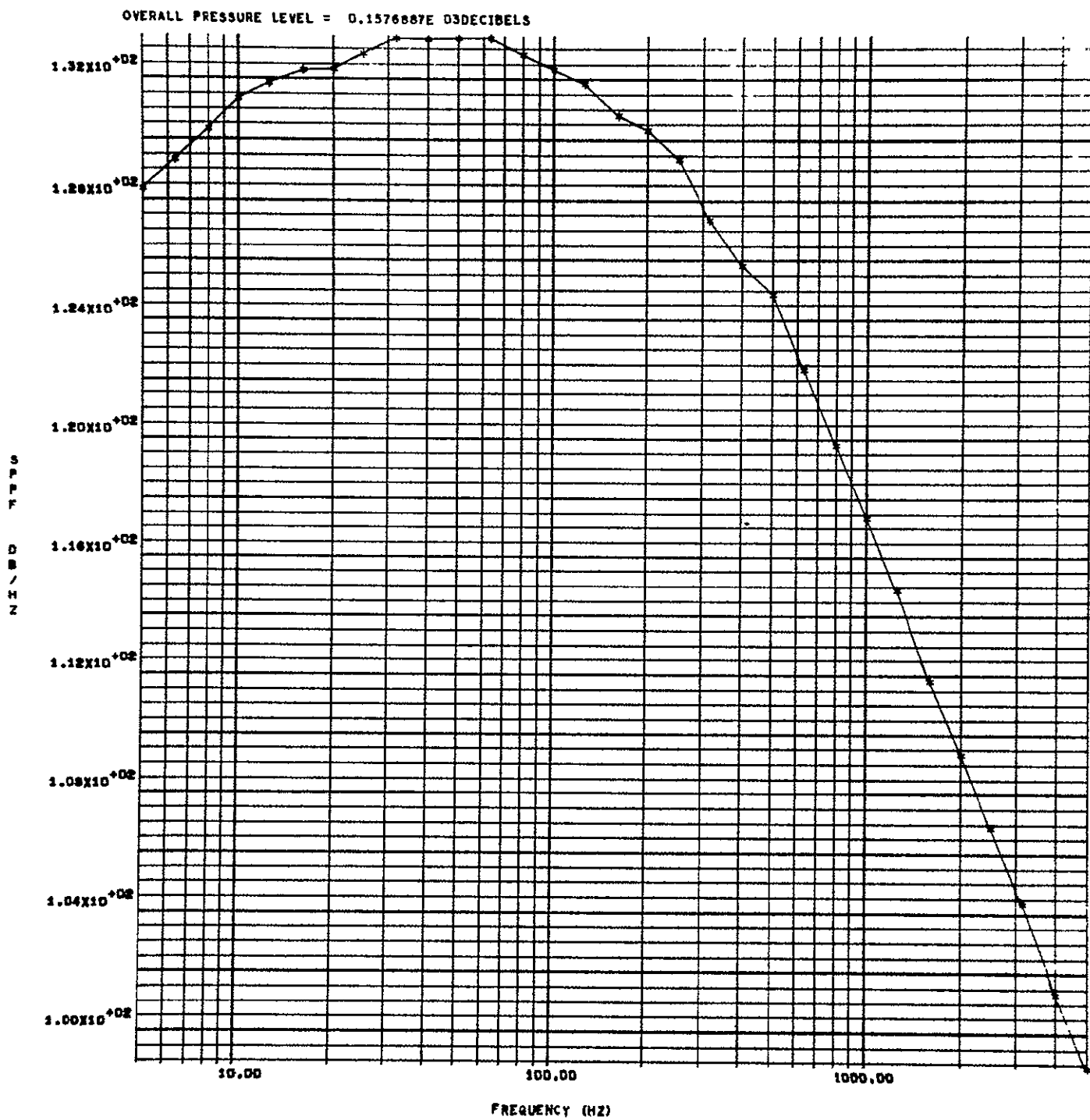
FIGURE 63   EXCITATION PRESSURE SPECTRAL DENSITY IN DECIBELS
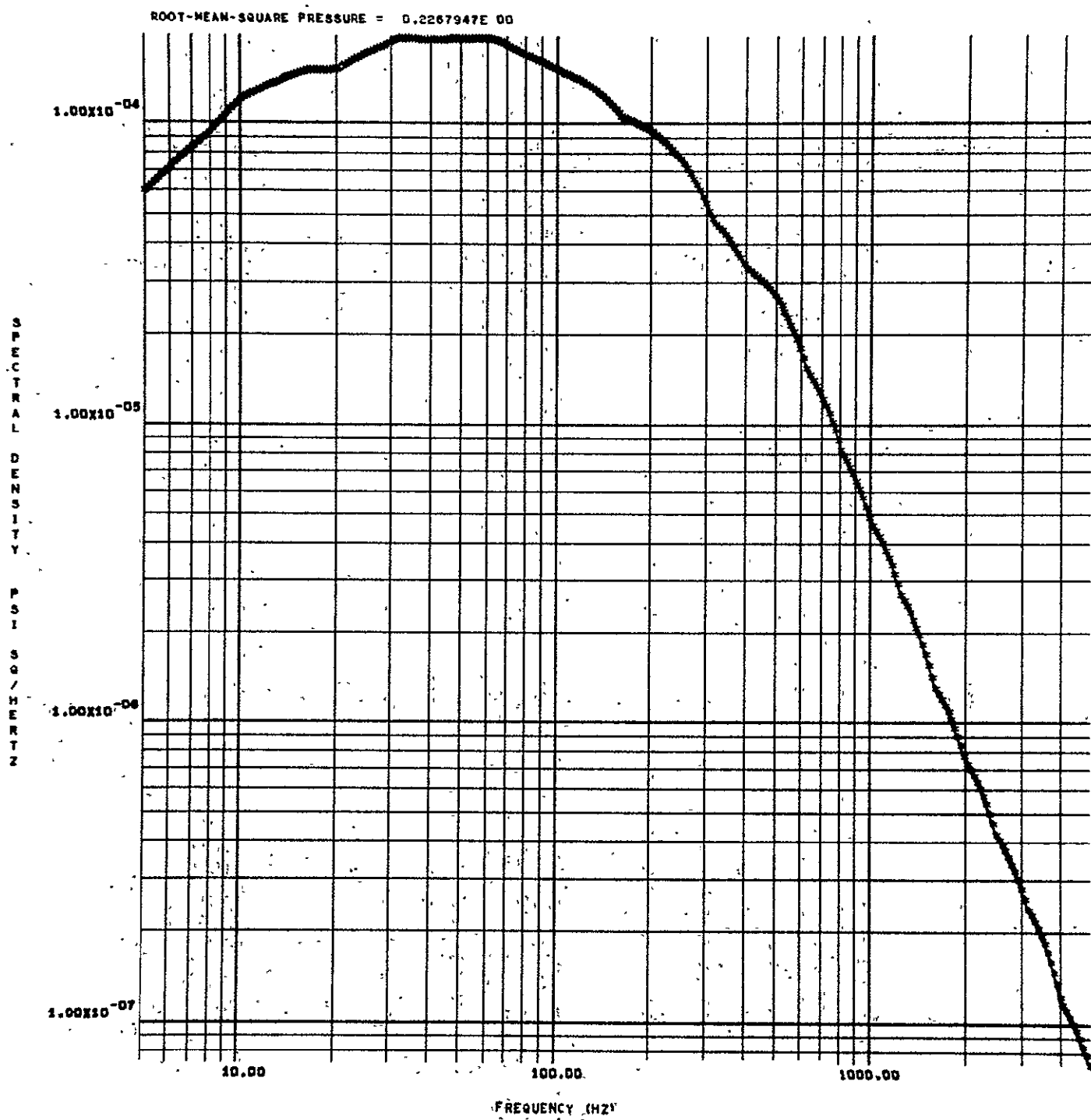AS FUNCTION OF FREQUENCY IN HERTZ

142

FIGURE. 64. EXCITATION PRESSURE SPECTRAL DENSITY IN (PSI)^2
PER HERTZ

143

FINAL REPORT

COMPUTER PROGRAMS FOR PREDICTION OF STRUCTURAL
VIBRATIONS DUE TO FLUCTUATING PRESSURE ENVIRONMENTS.

VOLUME ONE

THEORETICAL ANALYSIS
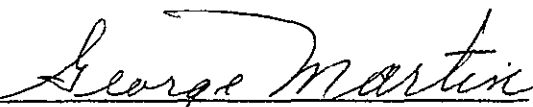
By   *Tsin Nien Lee* (signature)
Tsin Nien Lee
Vibration and Acoustics Group

and   *Wayne L. Swanson* (signature)
Wayne L. Swanson, Supervisor
Vibration and Acoustics Group

Approved: *George Martin* (signature)
George Martin, Manager
Structural Engineering Branch

144

DISTRIBUTION

This report is to be distributed as follows:

PR-SC	1
MS-IL	1
MS-T	1
MS-I	1
R-P&VE-RI	12, plus reproducible master